NEURAL CODING AND TIMING OF VISUAL TARGET SELECTION IN THE FRONTAL EYE FIELD

By

Jeremiah Y. Cohen

Dissertation

Submitted to the Faculty of the

Graduate School of Vanderbilt University

in partial fulfillment of the requirements

for the degree of

DOCTOR OF PHILOSOPHY

in

Neuroscience

December, 2009

Nashville, Tennessee

Approved:

Professor Jeffrey D. Schall, advisor

Professor Mark T. Wallace, chair of committee

Professor René Marois

Professor Martin Paré

PREFACE

> ...the anatomy of the nerves provides more pleasant and profitable speculations than the theory concerning any other part of the animal body: for by means of it, are revealed the true and genuine reasons for very many of the actions and passions that take place in our body.
>
> —Thomas Willis, 1664 in Clarke and Jacyna (1987)

I can attest to the first part of Willis's claim, that neuroscience provides the most pleasant study in biology. The road to this thesis has been, above all, a joy. As to his second claim, the reader can decide whether the work in this thesis is profitable.

> No man is an island entire of itself...
>
> —John Donne, Devotions upon Emergent Occasions, 1624; XVII. nunc lento sonitu dicunt, morieris, meditation

I wish to thank several people for their support: My advisor and mentor, Jeff Schall, who has taught me to be a scientist; Members of Jeff Schall's laboratory for guidance and stimulating discussion, in particular Rich Heitz, Geoff Woodman, Erik Emeric and Pierre Pouget; My dissertation committee, Mark Wallace, René Marois, Martin Paré and Jeff Schall; Leadership of the Vanderbilt Neuroscience Graduate Program; My family, who has given me a life of love and support.

This work was supported by National Institutes of Health Grants T32-MH-064913, R01-EY-08890, P30-EY-08126, and P30-HD-015052, and Robin and Richard Patton through the E. Bronson Ingram Chair in Neuroscience.

TABLE OF CONTENTS

LIST OF TABLES

LIST OF FIGURES

CHAPTER I

INTRODUCTION: SACCADE TARGET SELECTION AND DECISION MAKING IN THE BRAIN

1.1 Introduction

> It would be an important subject of pedagogical methodology to provide firm and necessary rules for the perceptual activity of the eye.
>
> —Purkinje 1819, in Wade and Brožek (2001).

Primate visual behavior is organized around a fovea which provides high acuity vision over a limited range of the central visual field. Consequently, to identify an object in a scene, gaze must shift so that the image of that object projects onto the fovea. Because gaze can be directed to only one place at a time, some process must distinguish among possible locations to select the target for a saccade. Consequently, some items may be overlooked. The outcome of the selection process is purposeful in the context of visually guided behavior (Jovancevic-Misic and Hayhoe, 2009). Patterns of eye movements express regularities such as concentrating on conspicuous and informative features of an image under diverse conditions (Hayhoe and Ballard, 2005; Triesch et al., 2003).

Indeed, theories of primate evolution have long suggested that the development of visual acuity played an important role in the development of fine motor skills:

> Increased reliance upon the guidance of the sense of sight awakened in the creature [Tarsier] the curiosity to examine the objects around it with

> closer minuteness and supplied guidance to the hands in executing more precise and more skilled movements than the Tree Shrew attempts. Such habits not only promoted the development of the motor cortex itself, and cultivated the discriminative powers of the tactile and kinaesthetic senses, but they linked up their cortical areas in bonds of more intimate associations with the visual cortex.
>
> —G.E. Smith, *The Evolution of Man*, in Polyak (1957).

This chapter will review our current understanding of the neural basis of saccade target selection. The process of selecting the target for pursuit eye movements is similar (Carello and Krauzlis, 2004; Ferrera and Lisberger, 1995, 1997; Gardner and Lisberger, 2001; Krauzlis et al., 1999; Krauzlis and Dill, 2002). This topic has been reviewed recently (Bichot and Desimone, 2006; Fecteau and Munoz, 2006; Schall, 2003b, 2004b; Schall et al., 2003; Schiller and Tehovnik, 2005; Thompson and Bichot, 2005), so this chapter will frame the major issues and highlight more recent developments. A major theme will be that saccade target selection entails at least two processes, one that identifies locations in the image to which to shift attention and gaze and another that leads to the saccade.

1.2 Visual search, selection, attention and action

To investigate how the brain selects the target for an eye movement, multiple stimuli that can be distinguished in some way must be presented. This experimental design is referred to as visual search. The visual search paradigm has been used extensively to investigate visual selection and attention (e.g., Wolfe and Horowitz, 2004). In a visual search task, multiple stimuli are presented among which a target is discriminated and located. Search is efficient (with fewer errors and faster response

times) if stimuli differ along basic visual feature dimensions, such as color, form or direction of motion. Search becomes less efficient (more errors, longer response times) if the distractors resemble the target or no single feature clearly distinguishes the stimuli. Recently, another approach to investigating the visual and other factors guiding saccade target selection has required participants to locate a more or less vague target embedded in an image of random or structured noise or texture (e.g., Eckstein et al., 2001; Najemnik and Geisler, 2009). A general conclusion drawn from these studies is that humans can direct gaze under these circumstances in a statistically optimal manner. By introducing rapid variation over time in the structure of the image, it is possible to measure the interval of visual input that most effectively guides saccades (e.g., Caspi et al., 2004; Ludwig et al., 2005). These experiments have found that in the ~ 100 ms before a saccade is initiated, changes of visual input have little or no influence except on subsequent saccades.

Saccade target selection cannot be discussed without consideration of the allocation of visual attention. In fact, several lines of evidence indicate that visual target selection and the allocation of visual attention may be synonymous. For example, perceptual sensitivity is reduced and saccade latency is elevated if attention is directed away from the target for a saccade (Kowler et al., 1995; Deubel and Schneider, 1996), but this relationship varies with task demands (Deubel, 2008). Also, the visual conspicuousness of an oddball stimulus can drive covert (Theeuwes, 1991) and overt (Theeuwes et al., 1998) selection, and non-target elements that resemble a designated target can be inadvertently selected covertly (Kim and Cave, 1995) and overtly (Bichot and Schall, 1999a; Motter and Belky, 1998; Zelinsky and Sheinberg,

1997). Finally, target selection is influenced by implicit memory representations arising through short-term priming of location or stimulus features for covert (Maljkovic and Nakayama, 1994, 1996) and overt (Bichot and Schall, 1999a; McPeek et al., 1999) orienting. These observations are explained most commonly by postulating the existence of a map of salience derived from converging bottom-up and top-down influences (Itti and Koch, 2001; Rodriguez-Sanchez et al., 2007; Wolfe, 2007). One major input to the salience map is the maps of the features (color, shape, motion, depth) of elements of the image. Another major input is topdown modulation based on goals and expectations. Peaks of activation in the salience map that develop as a result of competitive interactions represent locations to which attention has become allocated for enhanced visual processing.

Some researchers have suggested that shifts of attention and eye movements are tightly linked (Chelazzi, 1995; Deubel and Schneider, 1996; Henderson, 1991; Hoffman and Subramaniam, 1995; Hunt and Kingstone, 2003; Kowler et al., 1995; Peterson et al., 2004; Sheliga et al., 1994, 1995; Shepherd et al., 1986). This view is known as the oculomotor readiness hypothesis (Klein, 1980; Klein and Pontefract, 1994) or the premotor theory of attention (Rizzolatti, 1983; Sheliga et al., 1994, 1995; Shepherd et al., 1986). However, the link between directing attention and shifting gaze is not obligatory (Crawford and Muller, 1992; Eriksen and Hoffman, 1972; Jonides, 1980; Klein et al., 1992; Posner, 1980; Remington, 1980; Reuter-Lorenz and Fendrich, 1992; Shepherd et al., 1986). Certainly, when observers scan an image, the timing of saccade production is not under immediate visual control (Hooge and Erkelens, 1996, 1998, 1999; Van Loon et al., 2002). These observations highlight the problem of explaining

the timing of saccade production. A recent study showed two distinct groups of fixations, one that increased in duration as the delay between saccade and visual scene reappearance increased, and one that displayed constant fixation duration as a function of delay (Henderson and Pierce, 2008). This suggests that some fixation durations are under top-down control, whereas others are not.

A key measurement in describing stages of processing during eye-movement decisions has been response time, the time taken from visual stimulus onset to saccade. Separating a task into stages of processing allows for experimental manipulation of one stage (e.g., target selection) while holding constant another (e.g., saccade preparation) (Donders, 1868/1969; Sternberg, 1969; Miller, 1988; Schall, 2004a). The decision to make a saccade to a target has been described using the principle of accumulation of evidence to a threshold (Carpenter and Williams, 1995; Reddi and Carpenter, 2000; Reddi et al., 2003; Smith and Ratcliff, 2004). As we shall see later in this chapter, the activity of distinct populations of neurons have been associated with different stages of processing during saccade decisions.

The neural processes described as saccade target selection occur throughout the visual pathway and ocular motor system. Pedagogically, it is easiest to review the experimental evidence for each part of the brain in turn, but the reader should not gain the mistaken impression that the various areas and structures operate in isolation or sequence. In fact, the neural processes responsible for selecting a target and shifting gaze transpire concurrently in an interconnected network woven through the brain from front to back, top to bottom.

1.3 Superior colliculus

The properties and function of the superior colliculus have been reviewed thoroughly elsewhere (Moschovakis et al., 1996; Sparks and Hartwich-Young, 1989; Wurtz and Albano, 1980, e.g.,). To learn how the superior colliculus contributes to selecting the target for a saccade, several studies have presented monkeys with multiple stimuli among which to locate the target for an eye movement. In some studies the target location was specified by the properties of the stimulus at the central fixation point (Horwitz and Newsome, 1999, 2001; Kustov and Robinson, 1996; Li and Basso, 2005) or by implicit cuing (Goldberg and Wurtz, 1972; Wurtz and Mohler, 1976). In other studies the target was identified by properties such as color distinct from non-target stimuli (Basso and Wurtz, 1998; Glimcher and Sparks, 1992; Ignashchenkova et al., 2004; Kim and Basso, 2008; McPeek and Keller, 2002; Olivier et al., 1999; Ottes et al., 1987; Port and Wurtz, 2009; Shen and Paré, 2007). The central observations have been made primarily on the visually responsive prelude and build-up neurons. While the design of each study was different, the results can be summarized briefly. Initially, when multiple stimuli are presented, activation increases at all locations in the superior colliculus map corresponding to the potential saccade targets. This happens because neurons in the macaque superior colliculus are not naturally selective for color, orientation, shape or direction of motion. Following the initial volley, activation becomes relatively lower at locations that would produce saccades to non-target elements and grows at locations corresponding to more conspicuous or important potential targets, ultimately yielding a burst that triggers the saccade produced by

activation centered on just one location in the motor map. When the target is easily distinguished from distractors (e.g., a red spot among green spots), then the difference in activity that signals target location arises 100-150 ms after the array appears. The elevated neural activity for the target revealed in these studies likely corresponds to the enhancement of visual responses originally described by Goldberg and Wurtz (1972). In general, the pattern of activity of neurons in the superior colliculus largely resembles what has been observed in cortical areas in the parietal and frontal lobes from which these signals may arise through direct cortical afferents.

Recent studies using microstimulation and inactivation have demonstrated a causal role of superior colliculus in target selection (Carello and Krauzlis, 2004; McPeek and Keller, 2004; McPeek, 2008). In one study, reversible inactivation of superior colliculus with lidocaine or muscimol caused deficits in target selection (McPeek and Keller, 2004). In this study, monkeys searched for a popout target among three distractors. Before superior colliculus inactivation, monkeys performed with 100% accuracy. After injections, monkeys made saccades to distractors on many trials when the target appeared in the location corresponding to the injection site. This deficit in target selection occurred without deficits in saccade production.

1.4 Primary visual cortex and the ventral stream

Selecting a particular element in an image requires that the element be distinguished from others in the image. Such a distinction can be derived from differences in color, shape, motion or depth. Therefore, selection of a target for a visually guided saccade must begin with neural signals that distinguish the features of elements in

the image. A cornerstone of visual neuroscience is the fact that neurons in the visual cortex respond selectively according to the color, shape, motion and depth of stimuli. A signal sufficient to distinguish the features of visual objects is available in the first few spikes produced by neurons in primary and extrastriate visual cortex (reviewed by Orban, 2008). Selectivity of neural responses for visual features forms the necessary substrate for visual target selection; however, it is not sufficient because targets are distinguished only through a comparison to the features of other stimuli in the image. When more than one stimulus is presented, interactions occur between neurons responding to stimuli in neighboring parts of the scene. Different forms of response modulation by surrounding stimuli has been observed in some neurons primary visual cortex (Knierim and van Essen, 1992; Rossi et al., 2001; Zipser et al., 1996), areas MT and MST (Saito et al., 1986) and area V4 (Desimone and Schein, 1987). Modulation of the response of neurons to a stimulus in the receptive field by stimuli present in the surrounding region provides the substrate for identifying the location of features that are conspicuously different from surrounding features.

Having larger receptive fields, the responses of neurons in area V4 appear to relate more directly to the guidance of saccades. Neurons in V4 exhibit modulated discharge rates before saccade initiation (Fischer and Boch, 1981) that seems to signal enhanced selectivity for the features of the stimulus at the location of the saccade (Moore, 1999; Moore and Chang, 2009). Also, the receptive fields of V4 neurons have been characterized as reducing in size to effectively focus around the target of the saccade (Tolias et al., 2001), resembling a shift of sensitivity within the receptive field in a spatial attention task (Connor et al., 1997). More direct information about how

extrastriate cortex select targets has been obtained in studies that present multiple stimuli. This line of research has been framed by the seminal observation that when two stimuli are presented in the receptive field of many neurons in area V4, the response to the preferred stimulus is modulated according to which of the two stimuli is selected for guiding a behavioral response (reviewed by Reynolds and Chelazzi, 2004). For example, several studies have shown that neurons in V4 respond initially indiscriminately to target and distractor stimuli in their receptive fields but then the activity is modulated to signal through maximal activation the location of the target stimulus, whether it is defined by similarity to a cue stimulus or distinctiveness relative to non-target distractors (Chelazzi et al., 2001; Mirabella et al., 2007; Motter, 1994; Ogawa and Komatsu, 2004, 2006). The selective activation took some time, on the order of 150 ms, to arise. The time needed to distinguish and locate a target depends on the similarity of the target to non-target objects in the image (Hayden and Gallant, 2005). Nevertheless, this selective activation occurs as well when targets are selected during natural scanning eye movements (Bichot et al., 2005; David et al., 2008; Gallant et al., 1998; Mazer and Gallant, 2003).

Measurements of event-related potentials over extrastriate visual cortex of human participants performing tasks that require target selection and attention allocation have identified a signature of the locus and time of attention allocation (Luck and Hillyard, 1994a,b; Woodman and Luck, 1999, 2003b). Referred to as N2pc, it is a slightly more negative polarization arising approximately 200 ms after stimulus presentation in electrodes contralateral as compared to ipsilateral to the attended hemifield. Source localization procedures indicate that the N2pc arises from an early

parietal source and a later occipito-temporal source (Hopf et al., 2000). A recent study demonstrated that a homologue of the N2pc can be recorded from electrodes in the surface of the skull in macaque monkeys (Woodman et al., 2007).

The modulation of neural activity that has been observed in, for example, area V4 has also been found in areas in inferior temporal cortex where neural representations of conjunctions of features and of objects arise. The stimulus selectivity of neurons in inferior temporal lobe seems the same during active scanning in a cluttered image as compared to passive presentation (DiCarlo and Maunsell, 2000). Studies have described modulation of neurons to attended versus non-attended stimuli (Richmond and Sato, 1987; Sato, 1988) and during natural scene viewing and search (Rolls et al., 2003; Sheinberg and Logothetis, 2001). The process of selection by modulation of neural activity for target and non-target stimuli that was described for V4 has also been observed in inferior temporal cortex (Chelazzi et al., 1998). A general conclusion of these studies is that multiple stimuli compete for an explicit neural representation, and the competition among stimuli can be biased by other neural signals that reflect experience or instruction (Desimone and Duncan, 1995). Ultimately, though, enhanced activity in visual cortex represents the features characterizing the target and not that it is a target per se. A more general representation of the location of a target regardless of its features is necessary to guide saccadic eye movements. Such a representation seems to be present in the parietal and frontal lobes.

1.5 Posterior parietal cortex

A great deal is known about parietal cortex contributions to attention and gaze (Andersen and Buneo, 2002; Behrmann et al., 2004; Constantinidis, 2006; Gottlieb, 2007), and we will only point to studies testing saccade target selection because a more comprehensive account can be found in Chapter 14 (NOPE; REVIEW HERE!). Posterior parietal cortex consists of multiple areas; we will focus on results from area 7a and the lateral intraparietal area (LIP).

The importance of LIP in performing visual search is demonstrated by the deficits observed consequent to inactivation of LIP (Wardak et al., 2002, 2004). Recent studies have investigated the responses of neurons in posterior parietal cortex in monkeys confronted with displays consisting of a target and one or more distractors (Balan et al., 2008; Buschman and Miller, 2007; Constantinidis and Steinmetz, 2001a,b; Gottlieb et al., 1998; Ipata et al., 2006; Ogawa and Komatsu, 2009; Platt and Glimcher, 1997; Thomas and Paré, 2007). Neurons in area 7a signal the location of a stimulus of one color among distractors of another color (Constantinidis and Steinmetz, 2001a). Other studies have examined how neural activity in area LIP participates in target selection (Balan et al., 2008; Buschman and Miller, 2007; Gottlieb et al., 1998; Ipata et al., 2006; Thomas and Paré, 2007). As observed in the superior colliculus and, as we shall see, the frontal eye field, the initial response to the array did not distinguish the location of the oddball, but when the target was easily distinguished from visual search distractors, then within 100-150 ms the activation increased if the oddball was in the receptive field and decayed if only distractors were in the receptive field.

This neural activity is sufficient to represent the location of a conspicuous target. A similar pattern of modulation has been observed in experiments in which monkeys shift gaze to the object in an array of eight distinct objects that matches a sample stimulus. If the object in the receptive field was designated the target, neurons exhibited a significant elevation of activity. When the sample was presented during fixation in the center of the array, the augmented activity for the target arose more than 200 ms after the target was specified. This time is longer than that observed in simple pop-out search because more time was needed to encode the properties of the sample and locate the matching element. The modulation of activity is probably related to the enhancement of responses if it is to be the target for a saccade (Bushnell et al., 1981; Mountcastle et al., 1981; Robinson et al., 1978) or the attenuation of responses to a stimulus appearing at a location where attention is already allocated (Powell and Goldberg, 2000; Robinson et al., 1995; Steinmetz et al., 1994; Steinmetz and Constantinidis, 1995).

Overall, current results indicate that the visual representation in posterior parietal cortex represents the location of conspicuous and relevant stimuli, i.e., likely targets for orienting either covertly or overtly. Thus, neurons in posterior parietal cortex embody the properties of units in a salience map (reviewed by Kusunoki et al., 2000; Gottlieb, 2007).

1.6 Frontal eye field

David Ferrier discovered over 130 years ago that electrically stimulating a localized region of the frontal cortex elicited eye movements:

> The results of the stimulation [were]...turning of the eyes and head to the opposite side.
>
> Ferrier (1874-1875)

FEF is an area in prefrontal cortex that contributes to transforming visual signals into saccade commands (Schall, 1997, 2003b, 2004b; Schall and Thompson, 1999). It is well known that microstimulation of FEF elicits saccades to the visual field contralateral to the stimulated hemisphere (Bruce et al., 1985)—indeed, it has been known for over 130 years (Ferrier, 1874-1875)—mediated by a population of neurons that controls whether and when saccades are initiated (Bruce and Goldberg, 1985; Hanes and Schall, 1996; Hanes et al., 1998). These neurons project to superior colliculus (Segraves and Goldberg, 1987; Sommer and Wurtz, 2000, 2001) and the brainstem (Segraves, 1992), which in turn generate saccades via outputs to the oculomotor nuclei (Moschovakis et al., 1996). Although traditionally regarded as a motor area, FEF is equally part of the visual system, being strongly interconnected with numerous visual areas, cortically (Barone et al., 2000; Jouve et al., 1998; Schall et al., 1995b) and subcortically (Huerta et al., 1986; Stanton et al., 1988). Most FEF neurons have transient or sustained responses to visual stimuli (Bruce and Goldberg, 1985; Mohler et al., 1973; Schall, 1991) with relatively fast latencies on the order of 50 ms after the appearance of the stimulus (Schmolesky et al., 1998).

Thus, the clear engagement of FEF in visual and motor processing make it a prime locus in which to investigate the signals involved in visual search and attentional target selection. This approach is validated by the observation that ablation or inactivation of FEF causes specific deficits in producing saccades when distractors are

present as in visual search (Schiller and Chou, 2000; Wardak et al., 2006). In addition, a number of studies in human participants have demonstrated that transcranial magnetic stimulation over FEF in a limited timeframe relative to array presentation influences visual search performance, especially when the target is more difficult to locate (Muggleton et al., 2003; O'Shea et al., 2004).

A series of investigations has described specific neural correlates of target selection for visually guided saccades by recording the activity of neurons in the FEF of monkeys trained to shift gaze directly to a target in visual search arrays (Bichot and Schall, 1999a,b; Bichot et al., 2001b,a; Cohen et al., 2009a; Murthy et al., 2001; Ogawa and Komatsu, 2006; Sato et al., 2001; Sato and Schall, 2003; Schall, 2004b; Schall and Hanes, 1993; Schall et al., 1995a, 2004; Thompson et al., 1996). The extensive evidence for the involvement of FEF in saccade target selection has led to the suggestion that it can be understood in terms of a saliency map (Thompson et al., 2001; Thompson and Bichot, 2005). However, we should not draw the unnecessary and mistaken conclusion that FEF performs this function uniquely and exclusively.

Following presentation of an array with a single target among uniform distractors, visually responsive neurons in FEF respond initially indiscriminately to the target or the distractors of the search array in their receptive field. However, before a saccade to the target was generated, a selection process proceeded by which visually responsive neurons in FEF ultimately signaled the location of the oddball target stimulus. If the target of the saccade was in the response field, FEF activity was greatest. If non-target distractors were in the response field, the activity was suppressed. This selection process requires more time when that target is less distinct from the distractors

(Bichot et al., 2001b; Cohen et al., 2009a; Murthy et al., 2001) and occurs if no overt response is made (Thompson et al., 1997) or if target location or property is signaled by through a manual response (Thompson et al., 2005b). The target selection process has also been described in local field potentials recorded from FEF (Monosov et al., 2008); in fact the spatially selective activity identifying the location of the target in the visual search array appeared in the spikes ~ 30 ms before it appeared in the local field potentials. If local field potentials reflect dendritic input and spikes measure neuronal output from a brain region, then this temporal relationship suggests that spatial selection necessary for attention and eye movements is computed locally in FEF from spatially nonselective inputs. When gaze shift errors occur during these visual search tasks, the selection process erroneously guides gaze to a distractor (Thompson et al., 2005a). However, when manual response errors occur, the selection process locates the singleton in the search array correctly (Trageser et al., 2008).

Clearly, the visual selection observed in FEF depends on the afferents from the various visual areas conveying feature selectivity. However, FEF also provides extensive feedback connections to extrastriate visual cortex (Barone et al., 2000; Schall et al., 1995b), so the state of neural activity in FEF can influence neural processing in visual cortex. In fact, this connection from FEF to visual cortex is a central feature of models of visual attention (Hamker and Zirnsak, 2006). Several recent studies have described the relationship between activity in FEF and extrastriate cortex. Microstimulation of FEF biases V4 activity in a manner similar to what is observed when attention is allocated (Armstrong et al., 2006; Armstrong and Moore, 2007; Moore and Armstrong, 2003).

In Chapter VI we compare the timing of target selection signals in FEF with the N2pc, the signal of target selection measured in an event-related potential over extrastriate cortex. In this study, three signals measuring target selection time were recorded simultaneously while monkeys searched for a target defined by form among distractors: FEF single neurons, FEF local field potentials and ERPs over extrastriate cortex. Single FEF neurons selected the target among distractors first, followed by FEF local field potentials, followed by ERPs. Recent anatomical work suggests that target-selecting neurons in the upper layers of FEF project to V4 (Pouget et al., 2009), providing the major anatomical substrate for the functional signals flowing from FEF to V4.

Evidence that FEF neurons can convey signals related to endogenous spatial attention has been presented recently (Zhou and Thompson, 2009). Neurons in FEF exhibit elevated activity when a cue informs monkeys that one of two choice stimuli would appear in their response field. This spatially selective anticipatory activity occurred without any visual stimulus appearing in the neuron's response field and was not related to motor preparation. These results provide evidence that FEF is a source of a purely top-down spatial attention signal in anticipation of visual stimuli that need to be discriminated.

The selection of targets for gaze shifts is influenced by experience. In one experiment monkeys were trained exclusively with search arrays that contained a single item of a constant color among distractor items of another constant color (e.g., red target among green distractors) (Bichot et al., 1996). These monkeys persistently directed gaze to stimuli possessing the learned target color even if the target and dis-

tractor colors switched. In monkeys trained exclusively on targets of one color, about half of FEF neurons show selective responses for stimuli of that color appearing in the earliest spikes. This result indicates that the visual system can be configured to provide preferential processing of selected stimuli.

In another experiment monkeys were trained to perform visual search for a conjunction of features (such as a red cross among red circles, green crosses and green circles); this requires an explicit memory representation to identify the target (Treisman and Sato, 1990). Monkeys' performance and the neural selection process in FEF exhibited two, separate contextual influences: visual similarity of distractors to the target and the history of target properties (Bichot and Schall, 1999a,b). The evidence for the influence of visual similarity was revealed by the pattern of occasional erroneous saccades during conjunction search. Erroneous saccades tended to direct gaze to distractors that resembled the current target. Similar observations have been made with human observers during covert (Kim and Cave, 1995) and overt orienting (Findlay, 1997; Motter and Belky, 1998). Now, when monkeys successfully shifted gaze to the target, following the initial indiscriminate response, FEF neurons not only discriminated the target from distractors but also discriminated among the non-selected distractors. More activation was present for distractors that were the same shape or color as the target than for a distractor that shared neither feature of the target. One consequence of this observation is that stimuli that are not selected overtly may still influence subsequent processing because of the differential neural representation. The history of stimulus presentation across sessions also affected the selection process during conjunction search. If an error was made, monkeys showed a significant

tendency (in addition to the visual similarity tendency just described) to shift gaze to the distractors that had been the target in the previous session. Recordings from FEF neurons during trials with correct saccades to the conjunction target revealed a corresponding discrimination among distractors with more activation for distractors that had been the target during the previous session. This effect was evident across sessions that were more than a day apart and persisted throughout experimental sessions.

Another expression of cognitive control of visual search is expressed on a shorter time scale. Humans and monkeys are affected by trial-to-trial changes in stimulus features and target location during pop-out visual search. For example, repetition of stimulus features improves performance. This feature-based facilitation of return was manifested in the target discrimination process in FEF; neurons discriminated the target from distractors earlier and better with repetition of stimulus features, corresponding to improvements in saccade latency and accuracy, respectively. In contrast to the repetition of features, repetition of target position increased saccade latency. This location-based inhibition of return was reflected in the neuronal discrimination process but not in the baseline activity in FEF. These results show adjustments of the target selection process in FEF contributing to changes in performance across trials due to sequential regularities in display properties.

A major question in this line of research concerns the relationship of the visual target selection process to saccade preparation and production. This question touches on multiple major questions. First, what is the origin of the variability of fixation duration between saccades made during scanning a scene or reading. Multiple studies

have found that the time spent fixating elements of an image cannot be explained just by the properties of the image (Hooge and Erkelens, 1996; Jacobs, 1987). In general, fixation duration seems to be adjusted according to the difficulty of finding the desired target, but moment-by-moment control of fixation duration based on the properties of the image does not seem to occur. This observation indicates that a form of executive control can be exerted on saccade production. Second, the relation of target selection and associated attention allocation with saccade production has been the focus of the oculomotor readiness or premotor theory of attention. Neurophysiological and anatomical data have been obtained that address specific claims of this theory. Finally, understanding how target selection leads to adaptive saccade production is an instance of the more general problem of understanding the mechanisms responsible for response times. A marriage of neurophysiological measurements and mental chronometry has provided new insights supporting the theory that response times are the outcome of successive, stochastic stages of processing.

The neural process of target selection occupies a certain amount of time that can be measured with reasonable accuracy. This provides an opportunity to determine how the time of visual target selection relates to the time of saccade initiation. This work is motivated by the general hypothesis that behavioral response times are occupied by more or less distinct stages of processing (Donders, 1868/1969; Miller, 1988; Schall, 2004a; Sternberg, 1969). Recent studies have investigated how the time taken to select a target relates to the time taken to initiate the saccade.

One approach to this is the well-known method of selective influence. Different stages of processing should be influenced by different manipulations. The time of tar-

get selection by FEF neurons depends on the quality of the stimuli and, as described above, the cognitive context. When the discrimination of the target is easy because the target is visually distinct from the distractors, then the time taken by neurons in FEF to locate the target is relatively short ($\sim$ 140 ms for pop-out displays) and on average does not account for the variability and duration of saccade latency. Note that studies of LIP (Ipata et al., 2006; Thomas and Paré, 2007) have not found this relationship. These investigators found that the time of target selection by LIP neurons was more correlated with response time. One possible account for this difference is the behavioral requirements in the respective experiments. In all of the experiments in our laboratory monkeys are required to produce a single saccade to the target; this emphasizes accuracy. In the experiments on LIP monkeys were permitted to produce multiple saccades to locate the target; this allows a strategy of speed over accuracy of the saccade. Experimental verification of this possibility has not been obtained to date. When the discrimination of the target is more difficult because the target more closely resembles the distractors, then the time taken by neurons in FEF to locate the target increases and accounts for a larger fraction but not all of the variability and duration of saccade latency (Bichot et al., 2001b; Cohen et al., 2009a; Sato et al., 2001). For example, in monkeys performing a search for a **T** (or **L**) among randomly oriented **L**s (or **T**s) with arrays of 2, 4 or 8 elements, the time taken for FEF neurons to locate the target increases with the number of objects in the array. However, even in the most difficult search in the 8-object array, saccades were initiated well after the target was selected (see Chapter VII).

If the time of visual target selection during search does not account for the full duration and variability of saccade initiation times, then some other process must occur to prepare and produce the saccade. As described above, a population of neurons in FEF and superior colliculus linked through the basal ganglia and thalamus provides the input to the brainstem network that produces the saccade. The activation of these neurons in FEF corresponds to the process of saccade preparation with the activation of these presaccadic movement neurons (also referred to as *build-up*, *prelude* or *long-lead burst neurons*). Saccades are initiated when the level of activation in this network reaches a certain level that may vary across task conditions but appears to be constant within a condition (Dorris et al., 1997; Fecteau and Munoz, 2007; Hanes and Schall, 1996). Most of the variability of the latencies of saccades to a visual target can be accounted for by randomness in the rate of growth of activity to the threshold (Hanes and Schall, 1996)(Hanes and Schall 1996), although other studies find variability of the baseline activity as well (Dorris et al., 1997; Fecteau and Munoz, 2007).

Thus, the picture that emerges is that the process of visual selection occupies a certain amount of time that can be shorter and less variable if the target is conspicuous, or it can be longer and more variable if the target is less conspicuous. If subjects wish to prevent a saccade to a non-target stimulus, then the preparation of the saccade can be delayed until the visual selection process has proceeded to a high degree of resolution (Woodman et al., 2008). Neural activity mediating saccade preparation begins to grow as the selection process is completed and (for reasons that are not clear) the rate of growth of activity leading to the movement varies apparently

randomly such that sometimes gaze shifts sooner and sometimes gaze shifts later. Systematic adjustments of saccade latency, though, appear to arise through changes in the time that the accumulation of activity begins. In fact, further evidence for the distinction between target selection and saccade preparation is the observation that the movement neurons in FEF do not discharge at all above baseline when monkeys maintain fixation when monkeys report target location through a manual response (Thompson et al., 2005b).

On the other hand, occasionally it is possible for the saccade preparation process to become activated before identification of the currently fixated element and selection of the next target are completed. For example, during visual search neurons in FEF with no visual response and only presaccadic movement activity can exhibit partial activation for non-target stimuli that resemble the target (Bichot and Schall, 1999a). Such activation of movement neurons can, if excessive, result in premature, erroneous saccades. Independence of visual selection and response preparation is also necessary to explain the production of saccades that are not directed to the location of the selected target.

The dynamics of visual selection and saccade preparation by the frontal eye field has been investigated in macaque monkeys performing a search-step task that combines the classic double-step saccade task with visual search (Camalier et al., 2007). In most trials the target appeared in an array of distractors and reward was earned for producing a saccade to the target. On random trials before the saccade was initiated, the target and one distractor swapped locations, and monkeys were rewarded for shifting gaze to the new target location. Performance of this task is unpredictable,

but on average, the longer the delay of the target step, the less likely will monkeys (or humans) correctly shift gaze to the new target location. If target selection and saccade preparation are too far advanced before the target step, then they will shift gaze to the old target location. These errors are commonly followed by corrective saccades to the new target location. Now, some investigators use double-step target presentation as an explicit means of dissociating retinal error from motor error, but performance of this task under the instruction to follow the target steps is different from performance under the instruction to redirect gaze to the final target location (Ray et al., 2004).

Performance of this task can be accounted for as the outcome of a race between processes producing the two saccades and a process that inhibits production of the first saccades (Camalier et al., 2007). The race model provides a powerful framework in which to interpret and understand the activity of the different types of neurons. Central to this model is the duration of the process that interrupts preparation of the first saccade on trials when the target steps. This interval is referred to as target step reaction time. The physiological properties of neurons in FEF of monkeys performing this task have been described in several papers (Murthy et al., 2001, 2007, 2009). When the target stepped out of a movement field, noncompensated saccades to the original target location were produced when movement-related activity grew rapidly to a threshold. Compensated saccades to the final target location were produced when the growth of the original movement-related activity was interrupted within target step reaction time and was replaced by activation of other neurons producing the compensated saccade. When the target stepped into a receptive field, visual

neurons selected the new target location regardless of the monkeys' response. In other words, even when gaze shifted away from the pop-out oddball of a search array, visual neurons in FEF represented the current location of the target. A modulation of this form has also been described in the superior colliculus (McPeek and Keller, 2002). When the target stepped out of a receptive field most visual neurons maintained the representation of the original target location, but a minority of visual neurons showed reduced activity. These findings indicate that visual activity in the frontal eye field signals the location of targets for orienting while movement-related activity instantiates saccade preparation.

During natural scanning eye movements one observes occasional instances of saccades initiated after fixation intervals that are too short to permit visual analysis of the image sufficient to guide gaze. In the double-step or search-step task corrective saccades are observed following similarly short fixation of the original target location (Becker and Jürgens, 1979; Camalier et al., 2007; Sharika et al., 2008). In fact, the race model provides an explanation for the incidence and timing of these corrective saccades that includes an account of why midflight corrections are rare. The latency of these corrective saccades is predicted by the timing of movement-related activity in the FEF. Preceding rapid corrective saccades, the movement-related activity of many neurons began before visual feedback of the error was registered and that of a few neurons began before the error saccade was completed. Corrective saccade can be produced, though, only if other neurons in the brain have located the new target location and maintain that representation through the production of the error. As noted above, this is just what the visual neurons in FEF do. However, this selection

process is itself a variable process that may be more or less complete at the time of saccade initiation. Thus, incomplete suppression of distractor-related activity results in curvature of saccades toward the distractor (McPeek et al., 2003; McPeek, 2006).

The double-step or search-step condition dissociates visual target location from saccade endpoint incidentally. The dissociation can also be accomplished explicitly through instruction. For example, it is possible to shift gaze in the direction opposite a visual target, referred to as antisaccade. In monkeys producing antisaccades visually responsive neurons in the superior colliculus and FEF respond if the target falls in the receptive field, and movement neurons are active for saccades into the movement field whether it is a prosaccade or an antisaccade (Everling et al., 1999; Everling and Munoz, 2000). To investigate the relationship of visual target selection to saccade preparation explicitly, monkeys were trained to make a prosaccade to a color singleton or an antisaccade to the distractor located opposite the singleton; the shape of the singleton cued the direction of the saccade (Sato and Schall, 2003; Schall, 2004b). As observed in previous studies, the response time for antisaccades was greater than that for prosaccades. A goal of this experiment was to account for this difference in terms of the neural processes that locate the singleton, encode its shape, map the stimulus onto the response, select the endpoint of the saccade and finally initiate the saccade. Two types of visually-responsive neurons could be distinguished in FEF. The first, called Type I, exhibited the typical pattern of initially indiscriminant activity followed by selection of the singleton in the response field through elevated discharge rate regardless of whether the singletons features cue a prosaccade or an anti saccade. Some of these Type I neurons maintained the representation of singleton location in

antisaccade trials until the saccade was produced. However, the majority of the Type I neurons exhibited a remarkable and dramatic modulation of discharge rate before the antisaccade was initiated. After showing higher discharge rates for the singleton as compared to a distractor in the receptive field, the firing rates changed such that higher discharge rates were observed for the endpoint of the antisaccade relative to the singleton location. This modulation could be described as the focus of attention shifting from one location to the other before the saccade. The second type of neuron, called Type II, resembled qualitatively the form of modulation of Type I neurons in prosaccade trials, but in antisaccade trials, these neurons did not select the location of the singleton and only selected the endpoint of the saccade. This endpoint selection was distinct from movement neuron activation, but the selection times of Type II, but not Type I, neurons accounted from some of the variability of saccade response time on prosaccade or antisaccade trials.

This experiment revealed a sequence of processes that can be distinguished in the modulation of different populations of neurons in FEF. The timecourse of these processes can be measured and compared across stimulus-response mapping rules. More details about the relationship of singleton selection time, endpoint selection time and response time are described in Sato and Schall (2003). To summarize, Type I neurons selected the singleton earlier than did Type II neurons. In the population of Type I neurons the time of selection of the singleton in prosaccade and antisaccade trials did not vary with stimulus response mapping or account for the difference in RT. However, the singleton selection time of Type II neurons in prosaccade trials was less synchronized with array presentation and more related to the time of saccade

initiation. In antisaccade trials the time of endpoint selection by Type I neurons was significantly later than that of Type II neurons. This result is as if the endpoint of a saccade must be identified before attention can shift to the location. The endpoint selection time of Type I neurons in antisaccade trials was too late to explain the increase in RT relative to prosaccade trials. In contrast, the endpoint selection time of Type II neurons in antisaccade trials, like the singleton selection time in prosaccade trials, accounted for some but not all of the delay and variability of RT.

This visual search task with prosaccades and antisaccades provided a powerful test of the pemotor theory of attention (Juan et al., 2004). The premotor theory of attention states that shifting visual spatial attention corresponds to preparing a saccade. The focus of attention was dissociated momentarily from the endpoint of a saccade by training monkeys to perform visual search for an attention-capturing color singleton and then shift gaze either toward (prosaccade) or opposite (antisaccade) this color singleton according to its orientation. Saccade preparation was probed by measuring the direction of saccades evoked by intracortical microstimulation of the frontal eye field at different times following the search array. Eye movements evoked on prosaccade trials deviated progressively toward the singleton that was the endpoint of the saccade. Eye movements evoked on antisaccade trials deviated not toward the singleton but only toward the saccade endpoint opposite the singleton. These results are interpreted in relation to previous work showing that on antisaccade trials most visually responsive neurons in frontal eye field initially select the singleton while attention is allocated to distinguish its shape. In contrast, preliminary data indicates that movement neurons are activated but do not produce a directional signal after the

saccade endpoint is selected. Evidence consistent with these observations has been obtained in a study of human participants using transcranial magnetic stimulation (Juan et al., 2008), and in a study probing explicitly the locus of attention (Smith and Schenk, 2007). Thus, the brain can covertly orient attention without preparing a saccade to the locus of attention. The premotor theory should be revised to accommodate these results.

To produce arbitrary responses to specific stimuli requires a mechanism to encode the rules and context of the task. This brings us to areas in prefrontal cortex rostral to the FEF.

1.7 Prefrontal cortex

Rostral to FEF are areas of ventrolateral and dorsolateral prefrontal cortex that have been the focus of extensive investigation and theory (e.g., Fuster, 2008). Before proceeding, we should note that the FEF is certainly an area in prefrontal cortex defined by the presence of a granular layer and afferents from the mediodorsal nucleus of the thalamus. Nevertheless, to simplify and summarize the function of the more rostral areas, we can state that they contribute to enacting flexible stimulus-response rules through time.

Recent lesion and microstimulation studies have established a general role of macaque dorsolateral prefrontal cortex in attention and saccade target selection (Opris et al., 2005; Rossi et al., 2007). However, we must note that the conditions of the experiments investigating prefrontal cortex were not typical of the visual search experiments reviewed above. For example, in one study, monkeys discriminated the

orientation of a colored target grating among distractor gratings. When the cue indicating which stimulus was the target was held constant across trials, monkeys with prefrontal cortex lesions were unimpaired. When the cue switched frequently across trials, however, monkeys with prefrontal cortex lesions were severely impaired in attending to the target.

The activity of neurons in prefrontal cortex areas rostral to FEF has been described during tasks that required different forms of visual target selection (Boussaoud and Wise, 1993; Buschman and Miller, 2007; Constantinidis et al., 2001b; Everling et al., 2006; Ferrera et al., 1999; Hasegawa et al., 2000; Kim and Shadlen, 1999; Rainer et al., 1998). In some of these studies the selection of the target appeared as effectively an all-or-none activation, largely because the responses began after the selection process was completed in visual areas of the cortex.

A common feature of neurons recorded in dorsolateral prefrontal cortex is the presence of activity during enforced delay periods in which monkeys must remember specific aspects of the stimuli to guide the eventual response. The characteristics of this delay period activation have been described in numerous studies. For example, one study presented monkeys with two stimuli, a bright target and a distractor with brightness that was varied across trials from that of the dim background to that of the bright target (Constantinidis et al., 2001b). In this way the discriminability of the target from the distractor was varied. After an instructed delay in which the stimuli had been removed, monkeys shifted gaze to the location occupied by the brighter stimulus. The activation during the delay period varied according to the brightness of the stimulus in the receptive field and the performance of the monkeys. Neurons

remained active during the delay period even if the stimulus in the receptive field had been the distractor. This affords an opportunity for the properties of the non-selected stimuli to influence subsequent performance. Also, the magnitude of the activation varied such that if the distractor was more similar to the target, the activation evoked by the distractor was more similar to the activation evoked by the target.

To summarize, the studies of dorsolateral prefrontal cortex have indicated that neurons may not participate directly in the target selection process but can encode the properties of selected and non-selected stimuli. Further work is needed to discover how the function of dorsolateral prefrontal cortex influences target selection in the more caudal parts of the brain.

1.8 Summary

Vision occurs naturally in a continuous cycle of fixations interrupted by gaze shifts. The guidance of these eye movements requires information about what is where in the image. The identity of objects is derived mainly from their visible features. Single neurons in the visual pathway represent the presence of specific features by the level of activation. Each point in the visual field is represented by populations of neurons activated by all types of features. Topographic representations are found throughout the visual and oculomotor systems; neighboring neurons tend to represent similar visual field locations or saccades.

When confronted by an image with many possible targets, the visual system compares the features of elements across the visual field. The retinotopic maps of the visual field facilitate local interactions to implement such comparisons; in particular, a

network of lateral inhibition can extract the locations of the most conspicuous stimuli in the visual field. The process of these comparisons can be influenced by knowledge so that inconspicuous but important elements in the image can be the focus of gaze. This selection process results in a state of activation in which neurons with potential targets in their receptive field are more active, and neurons with non-targets in their receptive field are less active.

The outcome of this selection process can be represented at a level of abstraction distinct from the representation of the features themselves. This is why the hypothetical construct of a salience map is useful. The state of neural selection of a salient target relative to surrounding non-target elements amounts to the covert allocation of attention that usually precedes overt shifts of gaze. The time taken for the brain to achieve an explicit representation of the location of a target varies predictably according to how distinct the target appears in relation to non-target elements.

Coordinated with this visual processing is activation in a network including FEF and superior colliculus that is responsible for producing the eye movement. A saccade is produced when the activation at one location within the motor map reaches a critical threshold. One job of visual processing influenced by memory and goals, is to insure that only one site–the best site–within the map of movements becomes activated. This is done when the neurons signaling the location of the desired target develop enhanced activation while the neurons responding to other locations are attenuated. When confronted with ambiguous images having multiple potential targets, partial activation can occur in parts of the motor map representing saccades to non-target elements that resemble the target. Saccade target selection converts

an initially ambiguous pattern of neural activation into a pattern that reliably signals one target location in a winner-take-all fashion. However, the representation of likely targets for orienting does not automatically and unalterably produce a saccade. Sometimes potential targets are perceived without an overt gaze shift or gaze can shift to locations not occupied by salient stimuli. The explanation of this flexible coupling between target selection and saccade production requires separate stages or modules that select a target for orienting and that produce gaze shifts. The flexible relationship between target selection and saccade production also affords the ability to emphasize speed or accuracy. Accuracy in fixating correctly can be emphasized at the expense of speed by allowing the visual selection process to resolve alternatives before producing a saccade. On the other hand, accuracy can be sacrificed for speed, allowing the visuomotor system to produce a saccade that may be inaccurate because it is premature relative to the target selection process.

1.9 Motivation: what we don't know

The preceding discussion emphasized the correlation of firing rates of single neurons across cortical and subcortical areas with attentional selection and eye movement production. The role of interactions between neurons within and across these brain areas and the timing of these interactions are poorly understood. To understand the relationship between neuronal interactions in FEF and visual target selection, we recorded from multiple FEF neurons simultaneously in monkeys performing visual search. To understand the timing of target selection within and across brain areas, we recorded FEF activity and visual event-related potentials over posterior cortex in

monkeys performing visual search tasks of varying difficulty.

1.10 Road map

Each of the following chapters, save the last one, is a published paper or one in preparation. Thus, each stands alone. I nevertheless encourage the reader to read them in sequence, as I have ordered them so that they follow the title of this thesis; I first present studies of neural coding of visual target selection, then studies of neural timing of visual target selection.

CHAPTER II

COOPERATION AND COMPETITION AMONG FRONTAL EYE FIELD NEURONS DURING VISUAL TARGET SELECTION

2.1 Abstract

The role of spike rate versus timing codes in visual target selection is unclear. We simultaneously recorded activity from multiple frontal eye field neurons and asked whether they interacted to select targets from distractors during visual search. When both neurons in a pair selected the target and had overlapping receptive fields (RFs), they cooperated more than when one or neither neuron in the pair selected the target, measured by positive spike timing correlations using joint peristimulus time histogram analysis. The amount of cooperation depended on the location of the search target: it was higher when the target was inside both neurons' RFs than when it was inside one RF but not the other, or outside both RFs. Elevated spike timing coincidences occurred at the time of attentional selection of the target as measured by average modulation of discharge rates. We observed competition among neurons with spatially non-overlapping RFs, measured by negative spike timing correlations. Thus, we provide evidence for dynamic and task-dependent cooperation and competition among frontal eye field neurons during visual target selection.[1]

[1]This chapter has been submitted as Cohen JY, Crowder EA, Heitz RP, Subraveti CR, Thompson KG, Woodman GF, Schall JD. Cooperation and competition among frontal eye field neurons during visual target selection.

2.2 Introduction

Complex behavior is the result of interactions among neurons in different brain areas. Saccadic visual search is one behavior ideal for understanding the role of neuronal interactions in perceptual decision making. Several studies have shown functional correlations between pairs of neurons involved in perception and decisions (Ahissar et al., 1992; Cohen et al., 2007; Das and Gilbert, 1999; Engel et al., 1991a,b; Narayanan and Laubach, 2006; Poulet and Petersen, 2008; Samonds et al., 2006; Snider et al., 1998; Stark et al., 2008; Ts'o et al., 1986; Vaadia et al., 1995; Zohary et al., 1994), but it is unclear to what degree these correlations are dynamic and how they depend on task demands.

During visual search for a target among distractors, the brain must allocate attention to the target while filtering out distractor objects (Wolfe, 1998). Do cortical neurons that discriminate between a search target and distractors interact to select the target, or do they each select the target independently? To answer this, we investigated the role of spike synchrony in visual target selection in the macaque frontal eye field (FEF). Visually-responsive FEF neurons signal the location of a target of visual search by increasing activity with the target inside their receptive field (RF) relative to when a distractor is in the RF (Cohen et al., 2009a; Sato and Schall, 2003; Sato et al., 2001; Schall and Hanes, 1993; Schall et al., 1995a; Thompson et al., 1996). We recorded activity from multiple FEF neurons simultaneously and measured spike rate and timing correlations between pairs of neurons.

We show that when both neurons in a pair selected the target of search and had

overlapping RFs, they cooperated through spike timing synchrony when the target was inside the intersection of both neurons' RFs around the time when each neuron selected the target as measured by its firing rate. Furthermore, when both neurons in a pair selected the target of search and had non-overlapping RFs, they competed through spike timing asynchrony when the target was inside one but not the other neuron's RF. These results reject the hypothesis that each FEF neuron selects the target independently and sends target selection signals to be pooled downstream. Rather, FEF neurons cooperate and compete to select targets during visual search, suggesting that spike timing, as well as spike rate, conveys information about target location.

2.3 Materials and Methods

2.3.1 Behavioral task and recordings

We recorded activity from pairs or groups of FEF neurons in both hemispheres of three male macaques (*Macaca radiata*) during color and form visual search tasks of varying difficulty (Table 2.1). Because we analyzed spike timing relationships in pairs of neurons, many neurons contributed data to more than one pair (107 out of 208). However, because the proportion of neurons contributing to the pairs of interest (the rightmost three columns in Table 2.1) was smaller (36 out of 164), we removed the neurons contributing data to multiple pairs and found similar results, albeit with weaker effects. Thus, we present data with those neurons included.

In the color search task (Fig. 2.1*A*, left), monkey F searched for a target (green

Monkey	Recording sessions	Total		Both neurons select target		One neuron selects target		Neither neuron selects target	
		Pairs	Neurons	Pairs	Neurons	Pairs	Neurons	Pairs	Neurons
F	28	154	97 (75)	17	25 (8)	27	39 (10)	12	18 (6)
Q	27	34	57 (6)	7	14 (0)	8	15 (1)	4	8 (0)
S	21	51	54 (26)	8	16 (0)	14	18 (8)	7	11 (3)
Total	76	239	208 (107)	32	55 (8)	49	72 (19)	23	37 (9)

Table 2.1: Numbers of neurons and pairs of neurons in each analysis of visual search data. Numbers in parentheses indicate neurons contributing to more than one pair.

disk) among seven distractors (Sato et al., 2001). Each trial began with the monkey fixating a central spot for approximately 600 ms. A target was then presented at one of eight iso-eccentric locations equally spaced around the fixation spot. The other seven locations contained distractor stimuli. Distractors could be red disks (efficient search) or yellow-green disks (inefficient search). The monkey was given a liquid reward for making a single saccade to the target location and fixating it for approximately 400 ms.

In the form search task (Fig. 2.1*A*, right), monkeys Q and S searched for a target (**T** or **L**) among distractors (**L** or **T**) (Cohen et al., 2009a; Woodman et al., 2007). Distractors could be homogeneous (e.g., upright **L**s) or heterogeneous (e.g., **L**s oriented differently). Each trial began with the monkey fixating a central spot for approximately 600 ms. A target was then presented at one of eight iso-eccentric locations equally spaced around the fixation spot. The other seven locations contained 1, 3 or 7 distractor stimuli (set sizes 2, 4 and 8, respectively). The monkey was given a liquid reward for making a single saccade within 2000 ms to the target location and

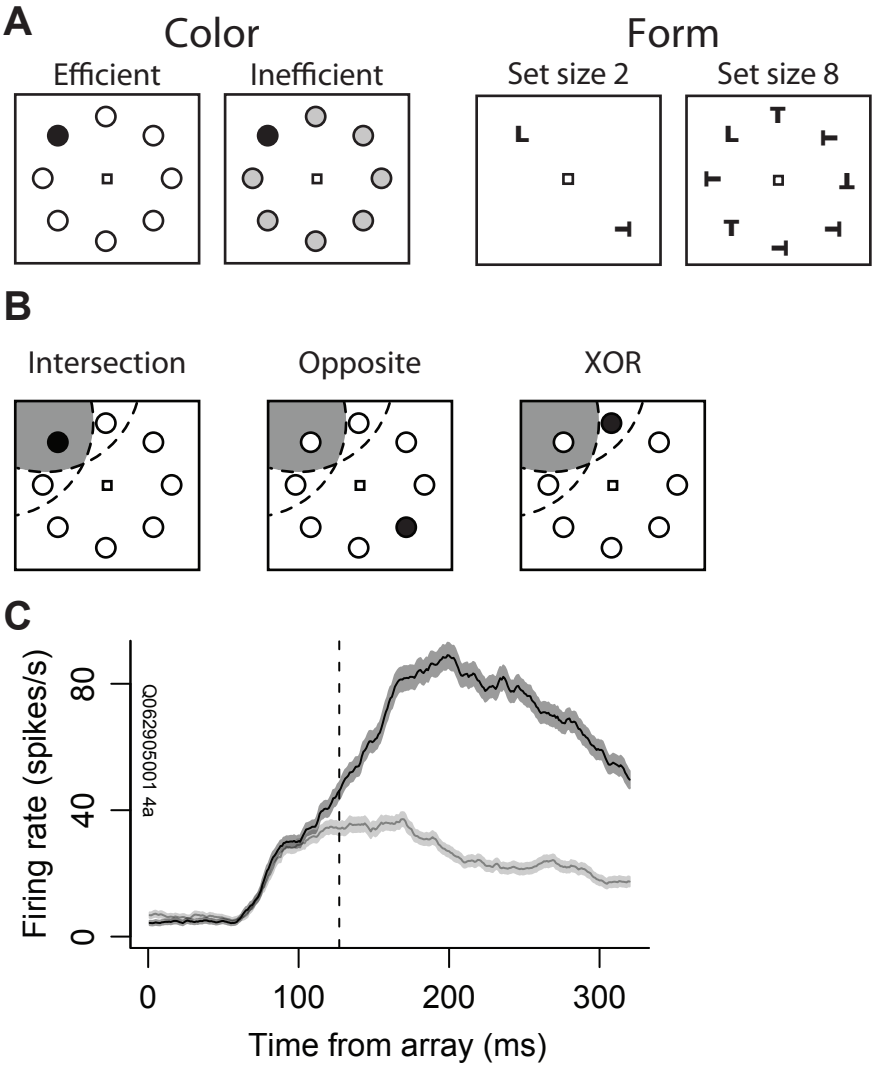

Figure 2.1: ***A***: Color and form visual search tasks. In each task, monkeys were required to make a single saccade to the target for reward. ***B***: Diagram of RF conditions. The dashed arcs represent the RFs of a pair of neurons. The shaded gray region represents the intersection of the RFs. The "Intersection" condition occurred when the target was inside the intersection of the pair of neurons' RFs (i.e., in the shaded gray region). The "Opposite" condition occurred when the target was in a location opposite the RF intersection. The "XOR" condition occurred when the target was in one neuron's RF but outside the other's RF. ***C***: Example neuron that selected the target during the form search task. The black curve with dark bands represents the mean ± SE firing rate when the target was inside the neuron's RF. The gray curve with light bands represents the mean ± SE firing rate when the target was opposite the RF. Initially, the neuron's firing rate did not discriminate between target and distractors, but after 130 ms its firing rate selected the target (dashed vertical line).

fixating it for 1000 ms. Across sessions the monkeys alternated between searching for **T**s with **L**s as distractors and **L**s with **T**s as distractors. Trials with incorrect behavioral responses were excluded from neural analyses. Behavioral analyses of these data have been published previously (Cohen et al., 2009a; Sato et al., 2001).

Activity from each neuron was recorded during a memory-guided saccade task to distinguish visual- from movement-related activity (Bruce and Goldberg, 1985; Hikosaka and Wurtz, 1983). The target (filled gray circle) was presented in isolation for 80-150 ms. Monkeys were required to maintain fixation for 400-1000 ms after the target onset. When the fixation spot disappeared, the monkey was rewarded for a saccade to the remembered location of the target. We used the data from the memory-guided saccade task to classify neurons according to the following criteria (Cohen et al., 2009b). Visual neurons had significantly greater activity in the 100 ms after the target flash than in the 100 ms before the target flash. Movement neurons had greater responses in the 100 ms leading up to the saccade than in the 100 ms before the target flash. Visuomovement neurons had greater responses in the 100 ms after the target flash and in the 100 ms leading up to the saccade than in the 100 ms before the target flash. All three classes of neurons were included in our preliminary analyses, as well as neurons that were not classified as visual, movement or visuomovement.

Monkeys were surgically implanted with a head post, a subconjunctival scleral eye coil and recording chambers. Surgery was conducted under aseptic conditions with animals under isofluorane anesthesia. Antibiotics and analgesics were administered postoperatively. All surgical and experimental procedures were in accordance with the National Institutes of Health Guide for the Care and Use of Laboratory Animals and

approved by the Vanderbilt Institutional Animal Care and Use Committee. Details have been described previously (Cohen et al., 2009a; Sato et al., 2001; Schall et al., 1995a).

Recordings were acquired from the rostral bank of the arcuate sulcus using tungsten microelectrodes (FHC, Bowdoin, ME). To confirm that electrodes were in FEF, we evoked saccades with low-threshold microstimulation ($< 50\,\mu$A) at each site (e.g., Bruce et al., 1985). Spikes were sorted online and offline using principal components analysis and template matching (Plexon, Dallas, TX). To ensure that spikes came from different neurons, we only analyzed pairs of neurons recorded from different electrodes. To measure the firing rate of each neuron, we used a spike density function, convolving each spike with a kernel resembling a postsynaptic potential (Thompson et al., 1996). Spike density functions were used to measure target selection time, but not in spike synchrony analyses.

2.3.2 Data analysis

2.3.2.1 Target selection time

To measure the time of target selection we used ms-by-ms Wilcoxon rank sum tests. Selection time was defined as the time at which the distribution of activity when the search target was inside a neuron's RF was significantly greater than the distribution of activity when the target was opposite the RF for ten consecutive ms with $p < 0.01$. For one neuron, we used a more conservative criterion of 50 consecutive ms based on visual inspection of the spike-density functions. This "neuron-antineuron"

approach presumes that a population of neurons in the brain representing the location of the target competes with a population of neurons representing the location of distractors opposite the target. Measuring selection time with a receiver operating characteristic analysis (Thompson et al., 1996) yielded indistinguishable results. Neurons from which we measured a target selection time were all classified as visual and visuomovement and had significant above-baseline activity during the memory delay period in the memory-guided saccade task. Fourteen neurons had phasic visual activity with no activity above baseline during the delay of the memory-guided saccade task; these neurons did not discriminate between target and distractors during the search task because their responses were too brief. There was no difference in target selection time between visual and visuomovement neurons. While movement neurons showed increased activity before a saccade was made to the target inside of their movement field relative to a distractor outside of their movement field, this activity was not considered "target selective" because these neurons select the endpoint of the saccade, not the location of the target (Murthy et al., 2001; Sato and Schall, 2003; Schall, 2004b; Thompson et al., 1997). Indeed, we observed that these neurons fired at their baseline rate when a saccade was made outside their movement fields. Thus, while we measured a "target selection time" for these movement neurons, we did not classify them as target selective; rather, they were saccade endpoint selective.

Figure 2.1*C* shows target selection in an example neuron. One of the factors of interest in this study was whether both, one or neither neuron in a pair selected the target. Of the neurons that did not select the target, some were movement neurons that were involved in preparing saccades, some were visual or visuomovement neurons

that did not select the target (typically transiently firing visual neurons) and some were not task-related. Of the 208 total neurons in the data set, 115 were visual or visuomovement neurons that selected the target.

2.3.2.2 Visuomovement index

To quantify the strength of visual- and movement-related activity, we computed a visuomovement index for each target-selecting visual and visuomovement neuron,

$$\frac{V - M}{V + M},$$

where V is the average firing rate from 50 ms to 150 ms after target onset in the memory-guided saccade task and M is the average firing rate in the 100 ms before saccades in the memory-guided saccade task. The visuomovement index is -1 for neurons with only movement-related activity and 1 for neurons with only visual-related activity.

2.3.2.3 Spike rate noise correlations

We measured spike rate noise correlations as the trial-by-trial spike rate correlation after the mean spike rate was subtracted from each neuron in the pair (Averbeck and Lee, 2004). The noise correlation is defined as

$$\left\langle \frac{\langle \lambda_1^i \lambda_2^i \rangle - \Lambda_1 \Lambda_2}{\sqrt{\langle (\lambda_1^i - \Lambda_1)^2 \rangle \langle (\lambda_2^i - \Lambda_2)^2 \rangle}} \right\rangle,$$

where λ_j is the spike rate from the j^{th} neuron and Λ_j is the mean spike rate from the j^{th} neuron, where i references a given trial and $\langle \cdot \rangle$ denotes expected value.

2.3.2.4 Spike synchrony

We measured spike-timing relationships using joint peristimulus time histograms (JPSTHs; Aertsen et al., 1989; Brody, 1999a,b). The shuffle-corrected, normalized JPSTH is defined as

$$J_N(t_1, t_2) = \frac{\langle S_1^i(t_1) S_2^i(t_2) \rangle - \langle S_1^i(t_1) \rangle \langle S_2^i(t_2) \rangle}{\sigma_1(t_1)\sigma_2(t_2)},$$

where t_1 and t_2 are time points within a trial, $S^i(t)$ is the spike train on the i^{th} trial at time t and $\sigma(t)$ is the standard deviation of the PSTHs $S(t)$. JPSTH measures correlations in spike timing over the time course of experimental trials at varying lags between spike trains. To compute JPSTHs, we used the time from 50 ms before search array onset to the 90^{th} percentile of the saccade response time distribution for a given pair of neurons. We used a 1 ms bin width for spike counts to search for precise spike timing relationships. To visualize trends in the JPSTH matrix we applied a two-dimensional mean filter with a 10×10 square kernel (Fig. 3); all statistical tests were performed on unfiltered data. Figure 2.3 shows the normalized JPSTH (J_N in the above equation).

From the JPSTH, we extracted two measures: a crosscorrelogram, which measures the overall correlation of spike times at varying lags, and a coincidence histogram, which measures the average spike timing correlation over time. Crosscorrelograms

(gray histograms in the upper right of each JPSTH in Fig. 2.3) and their 95% confidence intervals were computed using ±50 ms around a lag of 0 ms (Brody, 1999a,b). Crosscorrelograms were counted as significant if two consecutive values exceeded the confidence intervals. Coincidence histograms (black histograms to the right of JPSTHs in Fig. 2.3) were computed as the average JPSTH at ±10 ms around the main diagonal. To determine the effects of experimental manipulations on spike timing relationships, we measured the area under the crosscorrelograms in a 20 ms window around a lag of 0 ms and the area under the coincidence histograms. Each of these area measures (i.e., the integral) was the sum of the crosscorrelogram or coincidence histogram values in the appropriate time window, so that positive values were added to the area and negative values were subtracted from the area.

To avoid spurious crosscorrelation due to stimulus-induced firing rate increases, we used both an excitability correction (Brody, 1999a,b) and we simulated spike trains with the same average firing rates of the neurons in our data set. To generate a simulated spike train from a given neuron, we used that neuron's peristimulus time histogram (PSTH) as the probability of spiking at each time point over the course of a trial. For each simulated trial and time bin, we drew from a binomial probability distribution. If the value drawn was less than or equal to the PSTH at that time bin, the simulated trial would have a spike in that time bin. This ensured that while the average time-varying firing rate of the simulated neurons remained the same as the real neurons, the specific spike timing information was random, so any spurious JPSTH correlation caused purely by mean firing rate should also be present in the simulations. This confound is different from that controlled for by

Brody's excitability correction (Brody, 1999a,b), which is why we used this additional negative control. None of the comparisons described in Results (section 2.4) using the excitability correction or the simulated neurons were significant. Crosscorrelograms and coincidence histograms were fit with smoothing splines for visualization, but bar plots and statistics show results from unsmoothed data. All statistical tests were done with Bonferroni corrections for multiple comparisons. Analyses were done with R (`http://www.r-project.org/`) and Matlab (The MathWorks).

2.4 Results

We recorded from 239 pairs of neurons from different electrodes from three macaques (154 pairs from monkey F in the color search task, 34 from monkey Q in the form search task and 51 from monkey S in the form search task). We measured spike rate and timing correlations manipulating two experimental factors. The first factor, the number of neurons in the pair that selected the search target, had three levels: both neurons in the pair selected, one neuron selected or neither neuron selected. The second factor, the position of the target relative to the RFs, had three levels (Fig. 2.1*B*): target inside the intersection of the RFs ("Intersection"), target inside the RF of one neuron but not the other ("XOR") or target opposite the intersection of the RFs ("Opposite"). We analyzed the 104 pairs of neurons with overlapping RFs (comprised of the 32, 49, and 23 pairs in which both neurons, one neuron, or neither neuron selected the target; see Table 2.1). Nine pairs of neurons had completely overlapping RFs, so there was no XOR condition for these pairs.

We defined two types of neurons: (1) visual and visuomovement neurons that

selected the target from distractors (see Methods and Materials) and (2) neurons that did not select the target (some of these included movement neurons, which selected the target on correct trials but selected the distractor that was the endpoint of the saccade on incorrect trials). We recorded from 47 neurons that selected the target in the color search task and 68 that selected the target in the form search task. Table 2.1 shows the number of pairs of each type associated with each analysis.

2.4.1 Noise correlation

We first measured the spike rate noise correlation to determine whether the variability of spike rates of pairs of simultaneously recorded neurons tended to covary. Noise correlation was higher on trials when the target appeared at the intersection of the RFs than when it was opposite the intersection or in one RF but not the other (Fig. 2.2*A*; $F_{(2,181)} = 5.1$, $p < 0.01$).

We next analyzed 18 pairs of neurons in which both neurons in each pair selected the target and the RFs of each pair were non-overlapping in the visual field. These pairs can be considered to comprise neurons from different pools, whereas the pairs of neurons with overlapping RFs can be considered as derived from the same pool, analogous to neurons with similar or different direction tuning in MT (Cohen and Newsome, 2008). We found negative noise correlations for these 18 pairs of neurons when the search target was in one RF but not the other (Fig. 2.2*B*; mean $\pm$ SE, -0.077 ± 0.026, $t_{(17)} = -2.95$, $p < 0.01$). This indicates that signals arriving from neurons in different spatial pools in FEF exhibit a "push-pull" interaction in spike rate.

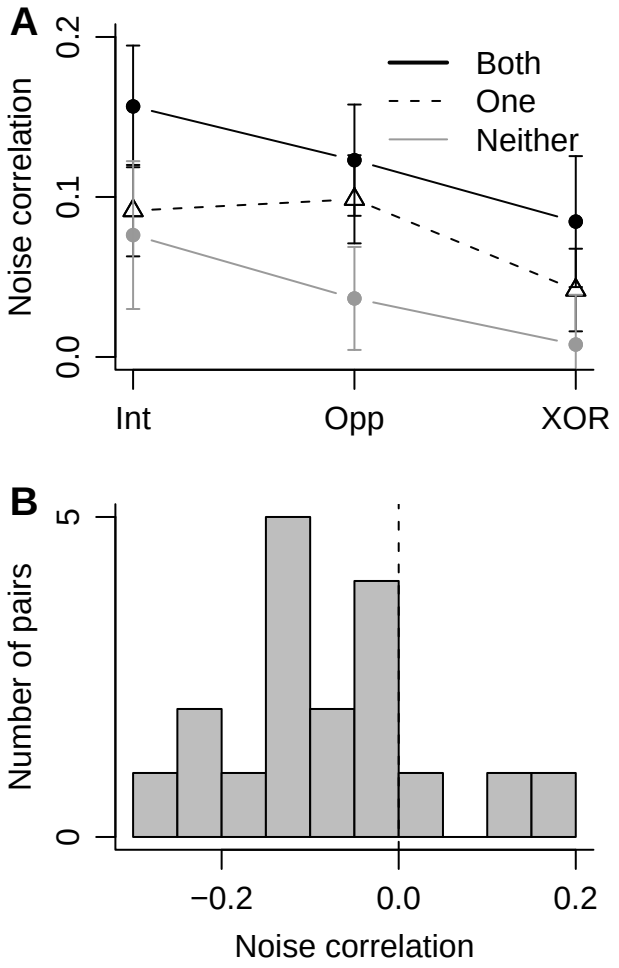

Figure 2.2: ***A***: Mean ± SE noise correlation between pairs of neurons in which both selected the target (black points and black lines), one selected the target (triangles and dashed lines) and neither selected the target (gray points and gray lines) when the target was inside the intersection of RFs (Int), opposite the intersection (Opp) and in one RF but not the other (XOR). ***B***: Histogram of noise correlation values for pairs of neurons with disjoint RFs that both selected the target.

2.4.2 Joint peristimulus time histogram analysis

Next, we measured JPSTHs for each pair of neurons. Figure 2.3 shows two example JPSTHs with crosscorrelograms and coincidence histograms. In Figure 2.3*A*, the left plot shows analysis of a pair of visual neurons that selected the target in the color search task. The right plot shows analysis of simulated neurons with the same time-varying average firing rates as the two visual neurons (note the similar PSTHs between data and simulated neurons). The data clearly show synchronous firing beginning around the time of target selection (dashed lines) in the two neurons that does not appear in the analysis of simulated neurons. This is apparent in the JPSTH, coincidence histogram and the crosscorrelogram. Figure 2.3*B* shows a pair of movement neurons recorded in the color search task with strong synchronous firing around the time of saccade onset, which does not appear in the analysis of simulated neurons with the same time-varying average firing rates.

2.4.3 Crosscorrelogram analysis

To measure the spike timing relationships between pairs of FEF neurons, we calculated crosscorrelograms. The crosscorrelogram measures the correlation between spiking in the pair of neurons, taking into account spurious correlations based on firing rate (see Methods and Materials, section 2.3), but ignoring the time course of correlations. Of the 239 pairs of neurons, 21 (8.8%) showed significant peaks in the crosscorrelogram, while none of the simulated pairs of neurons showed significant peaks, measured using 95% confidence intervals (see Methods and Materials, section

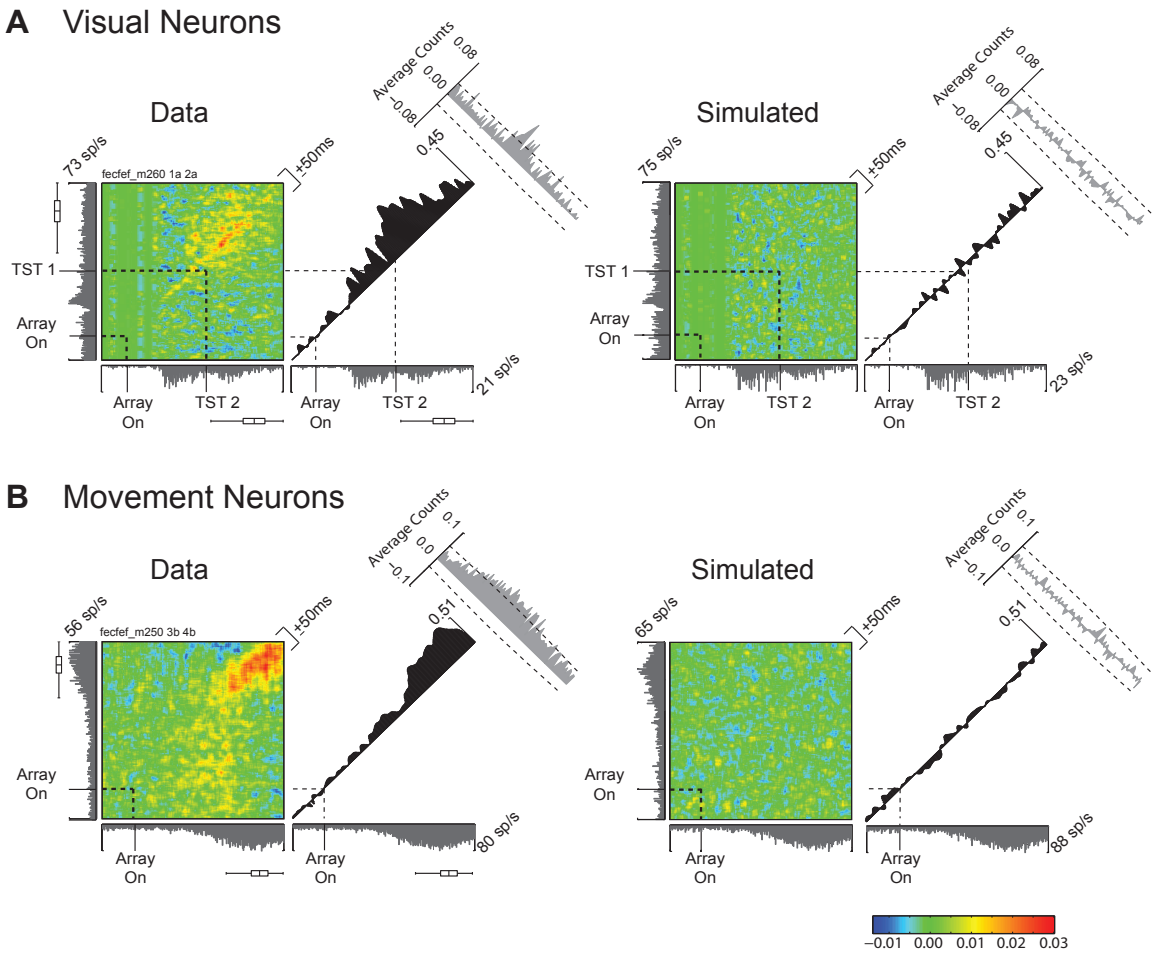

Figure 2.3: ***A***: JPSTH of a pair of target-selecting visual neurons (left panel) and a pair of simulated neurons with the same mean firing rates (right panel; see Materials and Methods). The color plots are JPSTH matrices. The gray histograms to the left and below the color plot are PSTHs from the two neurons. The time axis goes from −50 ms before array onset to 244 ms after array onset (90^{th} percentile of saccade response time distribution). The black histogram to the right of the color plot is the coincidence histogram, calculated from a ±10 ms window around the main diagonal of the JPSTH. The gray histogram in the upper right corner is the crosscorrelogram, calculated from a ±50 ms window collapsed across the main diagonal (see Materials and Methods). Dashed black lines indicate search array onset and target selection time (TST) for each neuron. Box-and-whisker plots next to each PSTH show the median, interquartile range and the range saccade response times. Note the increase in synchrony around the time of target selection in the real neurons but not the simulated neurons, evident in the JPSTH, the coincidence histogram and the crosscorrelogram. ***B***: JPSTH of a pair of movement neurons. Conventions are as in (***A***). The time axis goes from −50 ms before array onset to 315 ms after array onset (90^{th} percentile of saccade response time distribution). Note the synchrony around the time of saccades in the real neurons but not the simulated neurons.

2.3).

Figure 2.4 shows crosscorrelograms from each experimental condition collapsed across task difficulty. The left column shows the crosscorrelograms and the right column shows the area under the crosscorrelograms in a window ± 10 ms wide around zero lag. There was a significant effect of neuron pair type (i.e., both, one, or neither neuron in a pair selected the target; mixed-effects ANOVA, $F_{(2,98)} = 3.4$, $p < 0.05$) and target location (i.e., Intersection, XOR or Opposite; $F_{(2,180)} = 18.1$, $p < 0.001$) on crosscorrelogram area. When both neurons in a pair selected the target (32 pairs), and the target was inside the intersection of their RFs, they showed significantly higher positive correlations than when the target was opposite the intersection (Fig. 2.4; paired $t_{(31)} = 3.9$, $p < 0.001$). The same effect held for pairs in which one neuron, but not the other, selected the target and the target was inside the intersection of the RFs versus in one RF but not the other (49 pairs; paired $t_{(48)} = 3.4$, $p < 0.01$) or opposite the intersection ($t_{(39)} = 2.9$, $p < 0.01$). Comparing across pair type, when the target was inside the intersection of RFs, pairs of neurons in which both selected the target showed significantly higher positive correlations than pairs in which neither neuron selected the target (Fig. 2.4, Welch's $t_{(53)} = 2.2$, $p < 0.05$).

To ensure that these effects were not due to changes in firing rate, we simulated neurons with the same time-varying average firing rates (see Methods and Materials, section 2.3). There were no significant correlations or pairwise differences in any correlations (Fig. 2.4, gray bars). Thus, pairs of neurons showed the strongest positive correlations when the target of search was inside both of their RFs and both neurons selected the target from distractors.

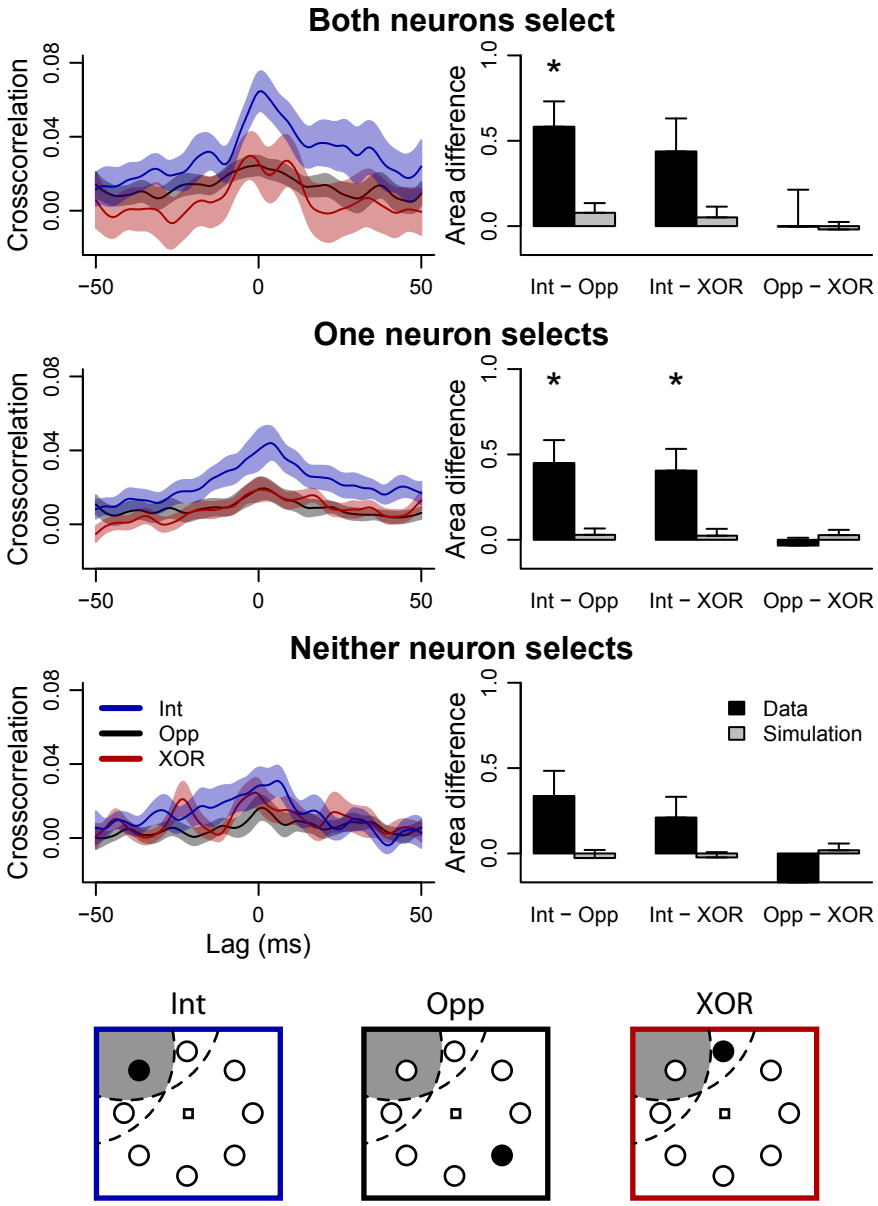

Figure 2.4: Crosscorrelograms and crosscorrelogram areas for each experimental condition, combined across task difficulty. The left column shows mean ± SE crosscorrelograms when the target was inside the intersection of the RFs ("Intersection" condition; blue), in one RF but not the other ("XOR" condition; red) and opposite the intersection of the RFs ("Opposite" condition; black). The right column shows mean ± SE of the differences in the area (i.e., integral) of the crosscorrelograms in a ±10 ms window around a lag of 0 ms for each paired comparison. Asterisks denote significance. The top row shows results from pairs in which both neurons selected the target. The middle row shows results from pairs in which one neuron, but not the other, selected the target. The bottom row shows results from pairs in which neither neuron selected the target.

2.4.4 Coincidence histogram analysis

To measure the time course of spike correlations, we extracted coincidence histograms from the JPSTHs. The coincidence histogram is a measure of the time course of correlations in a window ± 10 ms wide around zero lag, ignoring the spike timing relationships in terms of lag. Figure 2.5 shows coincidence histograms from each experimental condition collapsed across task difficulty, aligned to the time of search array onset (left column) and saccade onset (right column). Note that the increase in coincidence histograms occurred after the initial increase in firing rate in response to the onset of the search array (dashed line in Fig. 2.5, top left), suggesting that the increased spike timing correlations were not due solely to increased firing rates.

There was a significant effect of neuron pair type (i.e., both, one, or neither neuron in a pair selected the target; mixed-effects ANOVA, $F_{(2,98)} = 3.1$, $p < 0.05$) and target location (i.e., Intersection, XOR or Opposite; $F_{(2,195)} = 26.0$, $p < 0.001$) on coincidence histogram area. Coincidence histogram area was significantly larger when both neurons in a pair selected the target than when one or neither neuron selected the target (Welch's $t(170) = 2.6$ and $t_{(151)} = 3.9$, $p < 0.01$).

2.4.5 Relationship to target selection time

We noticed that around the time of target selection for individual neurons (vertical gray line in Fig. 2.5 shows the mean target selection time), correlations rapidly increased from baseline when both neurons in a pair selected the target. Therefore, we used target selection time to divide the time course of synchrony into two inter-

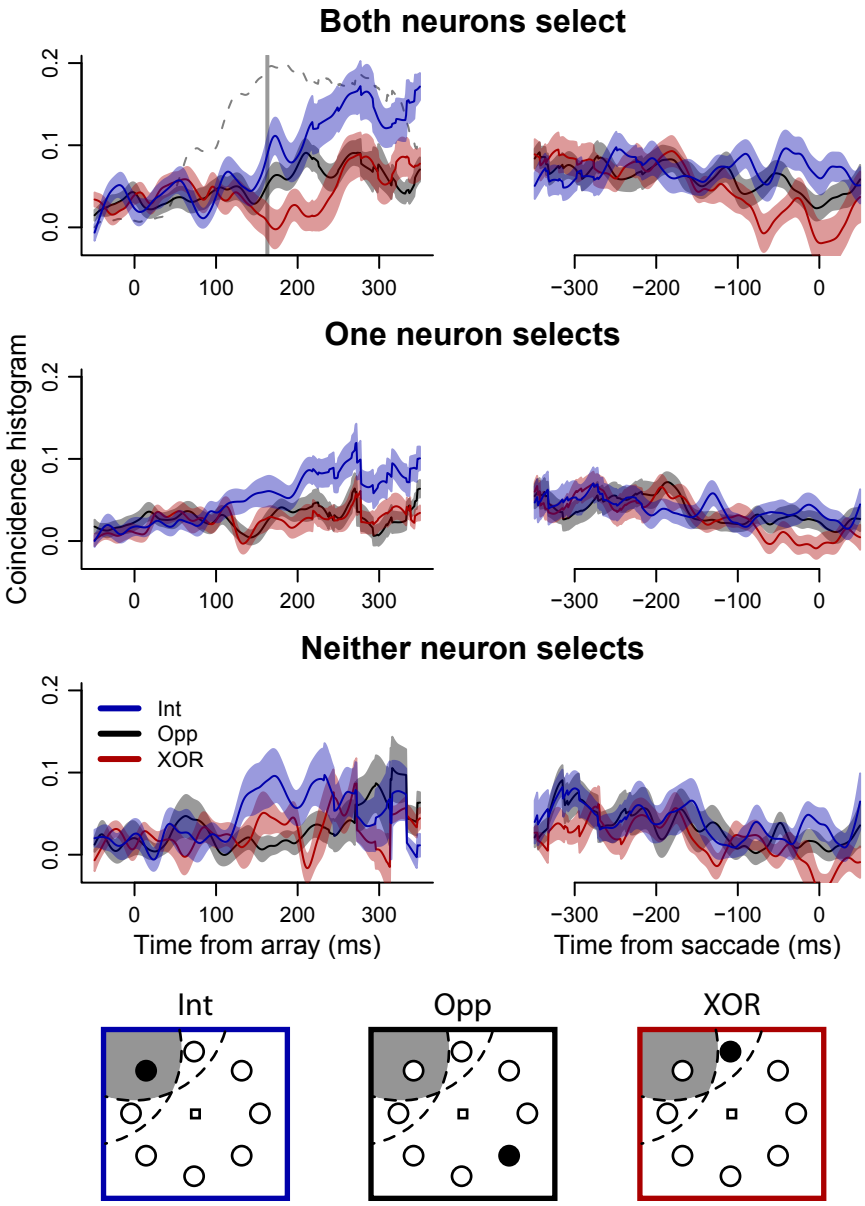

Figure 2.5: Coincidence histograms for each experimental condition, combined across task difficulty. The top row shows mean ± SE coincidence histograms when both neurons selected the target, aligned to array onset (left) and saccade onset (right) when the target was inside the intersection of the RFs ("Intersection" condition; blue), in one RF but not the other ("XOR" condition; red) and opposite the intersection of the RFs ("Opposite" condition; black). The middle row shows the same when only one neuron in the pair selected the target. The bottom row shows the same when neither neuron in the pair selected the target. Vertical line indicates mean target selection time in individual neurons when both neurons selected the target. Dashed line in upper left plot shows the average firing rate when the target was inside RFs, normalized between 0 and 0.2, indicating that the increase in coincidence was not a result of the initial increase in firing rate of individual neurons.

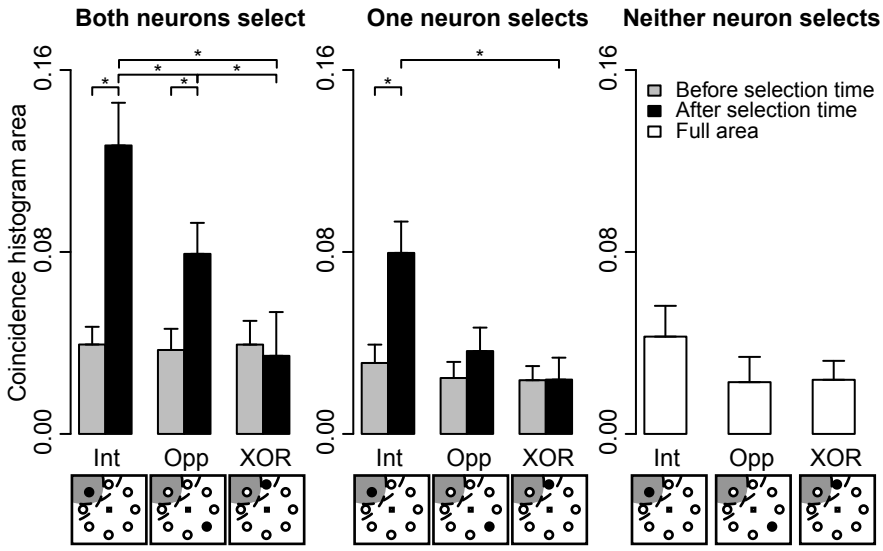

Figure 2.6: Mean ± SE area under coincidence histograms under three target location conditions (Intersection, Opposite and XOR; depicted below the abscissa labels; see Fig. 1 for details) when both neurons in the pair selected the target (left panel), when one neuron selected the target (middle panel) and when neither neuron selected the target (right panel). Asterisks indicate significant differences (see text) between RF conditions within each group of pair type ("both," "one" or "neither"). All coincidence histogram areas from simulated neurons were not significantly different from zero, and are not shown here. Areas are normalized by the length of the interval.

vals. The first was from array onset to target selection time, the second from target selection time to the 90^{th} percentile of saccade response times. For pairs of neurons in which both selected the target, the first interval ended at the earlier of the two target selection times and the second interval began at the later of the two target selection times (the median difference between target selection times for these pairs was 23 ms; the median difference between target selection times from pairs of neurons recorded at different times was 30 ms, which was significantly larger measured by Wilcoxon rank sum test, $p < 0.05$). We measured the time course of spike synchrony in the two intervals using the area of the coincidence histogram in each (Fig. 2.6).

There was a significant effect of interval (before vs. after target selection time) on

coincidence histogram area (mixed-effects ANOVA, $F_{(1,77)} = 29.9$, $p < 0.001$). When both neurons in a pair selected the target, there was significantly larger area in the coincidence histogram after target selection time than before selection time both when the target was inside the intersection of the RFs and when the target was opposite the RFs (paired $t_{(31)} = 5.2$ and 3.1, $p < 0.01$). Similarly, there was significantly larger coincidence histogram area after as opposed to before selection time when one neuron in the pair selected the target and the target was inside the intersection of the RFs (paired $t_{(48)} = 4.2$, $p < 0.001$).

Next, we tested whether there was a difference in coincidence histogram area across neuron pair types as a function of target location (Intersection, Opposite or XOR) and interval (before or after target selection time; Fig. 2.6). When both neurons in a pair selected the target, we found significantly larger coincidence histogram area after target selection time than when one or neither neuron in a pair selected the target. This effect was present when the target was inside the intersection of the RFs (Welch's $t_{(62)} = 2.1$ and $t_{(52)} = 3.6$, $p < 0.05$) and when the target was opposite the intersection (Welch's $t_{(63)} = 2.5$ and $t_{(53)} = 3.2$, $p < 0.05$). There were no differences between any coincidence histogram areas before target selection time, suggesting that the increase in synchrony when the target was inside the intersection of the RFs was associated with the target selection process.

There was a significant effect of target location on coincidence histogram area ($F_{(2,156)} = 22.5$, $p < 0.001$). When the target was inside the intersection of RFs coincidence histogram area was larger than when the target was opposite the intersection (Welch's $t_{(57)} = 2.2$, $p < 0.05$) or in one RF but not the other ($t_{(62)} = 3.4$, $p < 0.01$)

for pairs of neurons in which both selected the target. When one neuron in the pair selected the target, coincidence histogram area was larger when the target was in the intersection of RFs than when it was in one RF but not the other ($t_{(86)} = 3.3$, $p < 0.01$).

2.4.6 Effects of distance between neurons

To determine whether the strength of spike timing correlations varied as a function of distance between neurons, we performed two analyses. First, we split crosscorrelograms and coincidence histograms from pairs of neurons with overlapping RFs into two groups: pairs of neurons recorded in the same hemisphere and pairs recorded in different hemispheres. Crosscorrelogram area was significantly larger for intra- versus interhemispheric pairs of neurons when the target was in the intersection of RFs (Fig. 2.7*A*; Welch's $t_{(79)} = 2.3$, $p < 0.05$).

Coincidence histogram area after target selection time, but not before, was larger within the same hemisphere than across different hemispheres. When the target was inside the intersection of the RFs, coincidence histogram area was significantly larger when the neurons were recorded from the same hemisphere than from different hemispheres (Fig. 2.7*B* and *C*; Welch's $t_{(90)} = 3.5$, $p < 0.01$). To rule out the possibility that these differences were due to differences in the magnitude of target selection between pairs of neurons in the same versus different hemispheres, we measured the firing rate difference between when the target was inside each neuron's RF and when the target was opposite the RF, yielding an index of the magnitude of target selectivity. We found no difference in the magnitude of target selection between pairs

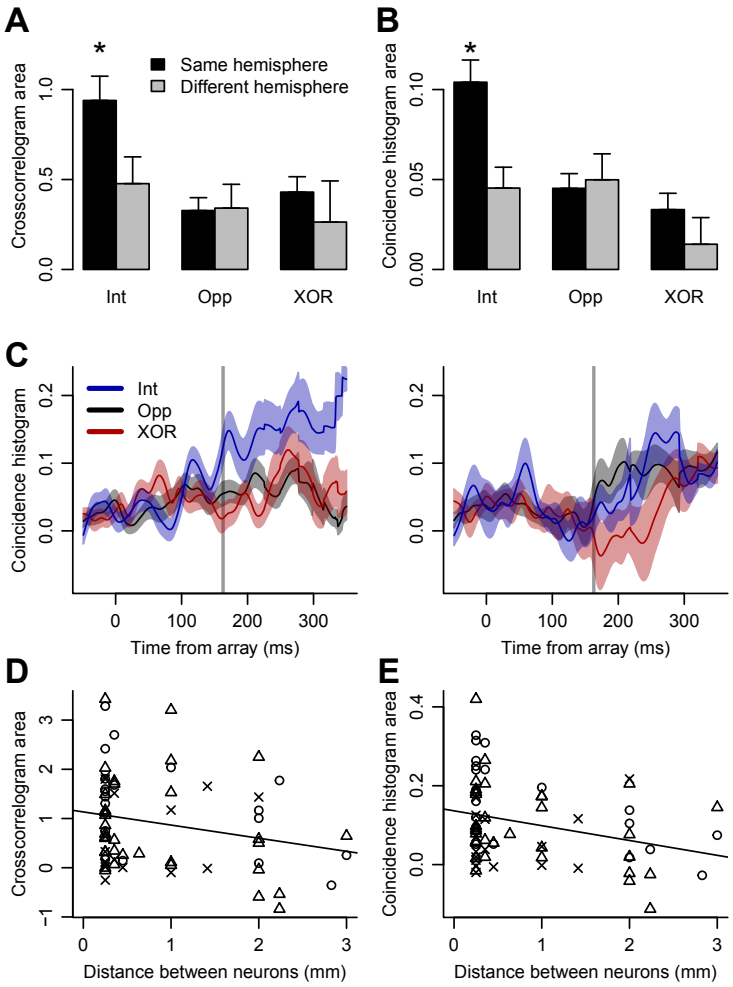

Figure 2.7: Effects of distance between neurons. ***A***: Mean ± SE crosscorrelogram area in a ±10 ms window around a lag of 0 ms when the target was inside the intersection of a pair of neurons' RFs (Int), opposite the intersection (Opp) and in one RF but not the other (XOR), when the pair of neurons came from the same (black bars) and different (gray bars) hemispheres. Asterisk indicates that when pairs of neurons came from the same hemisphere and the target was inside the intersection of RFs, crosscorrelogram area was the largest. ***B***: Mean ± SE coincidence histogram area after target selection time (gray vertical lines in ***C***). Other conventions are as in (***A***). ***C***: Coincidence histograms when both neurons selected the target when the neurons were recorded in the same (left panel) and different (right panel) hemispheres. Shown are mean ± SE coincidence histograms when the target was inside the intersection of RFs (blue), opposite the intersection (black) and in one RF but not the other (red). Vertical lines indicate mean target selection time in individual neurons when both neurons selected the target. ***D***: Crosscorrelogram area as a function of distance between neurons when the target was in the intersection of RFs and both neurons selected the target (circles), one neuron selected the target (triangles), or neither neuron selected the target (Xs), for pairs of neurons recorded in the same hemisphere. Regression line is shown superimposed. ***E***: Coincidence histogram area after target selection time as a function of distance between neurons recorded in the same hemisphere. Conventions are as in (***D***).

of neurons recorded in the same versus different hemispheres (Welch's $t_{(90)} = 0.44$, $p > 0.6$). We also tested for differences in the amount of overlap between RFs of pairs of neurons in the same versus different hemispheres. ANOVAs with number of overlapping RF locations and same/different hemisphere revealed no significant effect of the number of overlapping RF locations on crosscorrelogram area ($F_{(1,101)} = 0.013$, $p > 0.9$) or coincidence histogram area ($F_{(1,101)} = 0.059$, $p > 0.8$).

Second, we correlated the area under the crosscorrelograms and coincidence histograms with the distance between pairs of neurons recorded in the same hemisphere. We found that area under the crosscorrelograms decreased as a function of distance between neurons (Fig. 2.7*D*; linear regression slope $= -0.27 \pm 0.14$, intercept $= 1.13 \pm 0.16$, $p < 0.05$). Similarly, area under the coincidence histogram after target selection time decreased as a function of distance between neurons (Fig. 2.7*E*; linear regression slope $= -0.04 \pm 0.01$, intercept $= 0.14 \pm 0.02$, $p < 0.05$).

2.4.7 Relationship to saccade response time

To determine whether increases in synchrony varied with saccade response time, we divided the data from each pair of neurons into two groups: trials faster than the median and slower than the median response time for each session. Previous studies have shown that these neurons select the target later with longer response times (Bichot et al., 2001b; Cohen et al., 2009a; Sato et al., 2001). The increase in the coincidence histogram when the target was inside the intersection of RFs relative to when the target was inside one RF but not the other first became significant (ms-by-ms Wilcoxon signed rank test, $p < 0.05$) at 163 ms after array onset for fast trials

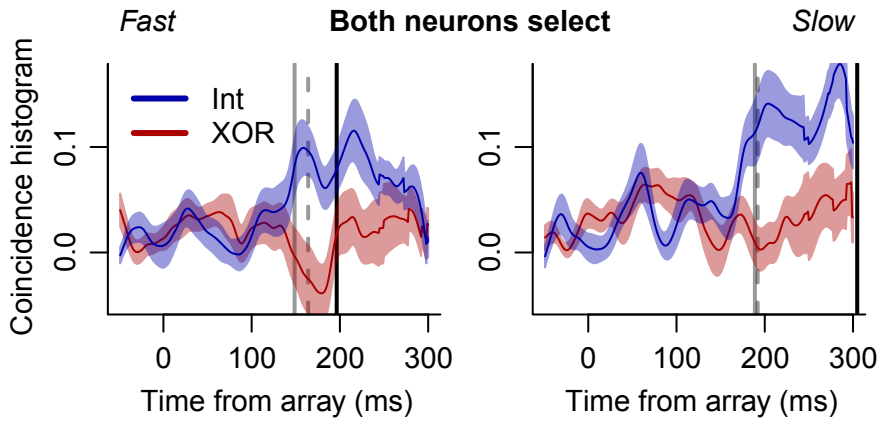

Figure 2.8: Mean ± SE coincidence histograms for pairs of neurons in which both selected the target, when the target was inside the intersection of RFs (blue) versus in one RF but not the other (red) for trials faster (left) and slower (right) than the median saccade response time in each session. Solid gray vertical lines indicate mean target selection times for individual neurons. Dashed gray vertical lines indicate the time at which the blue curves exceeded the red ones statistically (see text). Solid black vertical lines indicate mean saccade response times.

(Fig. 2.8, dashed gray lines; ms-by-ms Wilcoxon signed rank test, $p < 0.05$). For slow trials, the coincidence histogram when the target was inside the intersection of RFs exceeded that when the target was in one RF but not the other 191 ms after array onset. This earlier onset of coincidence histogram difference for fast trials than slow ones correlated with the difference in target selection time between fast and slow trials (Fig. 2.8, solid gray lines; mean ± SE fast trials, 148 ± 3.0 ms; slow trials, 188 ± 3.8 ms; Welch's $t_{(101)} = 8.2$, $p < 0.001$). The difference in saccade response time was also significant (Fig. 2.8, solid black lines; mean ± SE fast trials, 195 ± 3.4 ms; slow trials, 304 ± 8.8 ms; Welch's $t_{(97)} = 11.4$, $p < 0.001$). A similar pattern of effects, albeit weaker, was observed when we divided data into easy (efficient search in the color task and set size 2 in the form task) and hard (inefficient search in the color task and set size 8 in the form task) trials.

2.4.8 Visuomovement index

To determine whether the strength of spike synchrony varied with the relative amount of visual- versus movement-related activity in pairs of neurons, we computed a visuomovement index for the 55 target-selecting neurons that comprised the pairs in which both selected the target. The distribution of visuomovement indices happened to be significantly larger than zero (mean $\pm$ SE, 0.22 ± 0.06; $t_{(54)} = 3.4$, $p < 0.01$), indicating that target-selecting neurons tended to have stronger visual- than movement-related activity during the memory-guided saccade task. There was no significant correlation between the area under the crosscorrelogram or coincidence histogram and the mean visuomovement index or difference between visuomovement indices between pairs of neurons (all $p > 0.2$).

2.4.9 Spike correlations during the memory-guided saccade task

To determine whether the observed spike timing correlations were present during saccade target selection without distractors, we calculated JPSTHs during the memory-guided saccade task for the same pairs of neurons analyzed above. Of the 32 pairs of neurons in which both selected the target, 25 of them had sufficient numbers of trials (> 50) to calculate JPSTHs. For this sample of 25 pairs of neurons, we calculated crosscorrelograms and coincidence histograms (Fig. 2.9). There was significantly larger crosscorrelogram area when the target was in the intersection of RFs than when the target was in one RF but not the other (paired $t_{(24)} = 2.99$, $p < 0.01$). The area under the coincidence histogram from 50 ms to 200 ms after the target flash

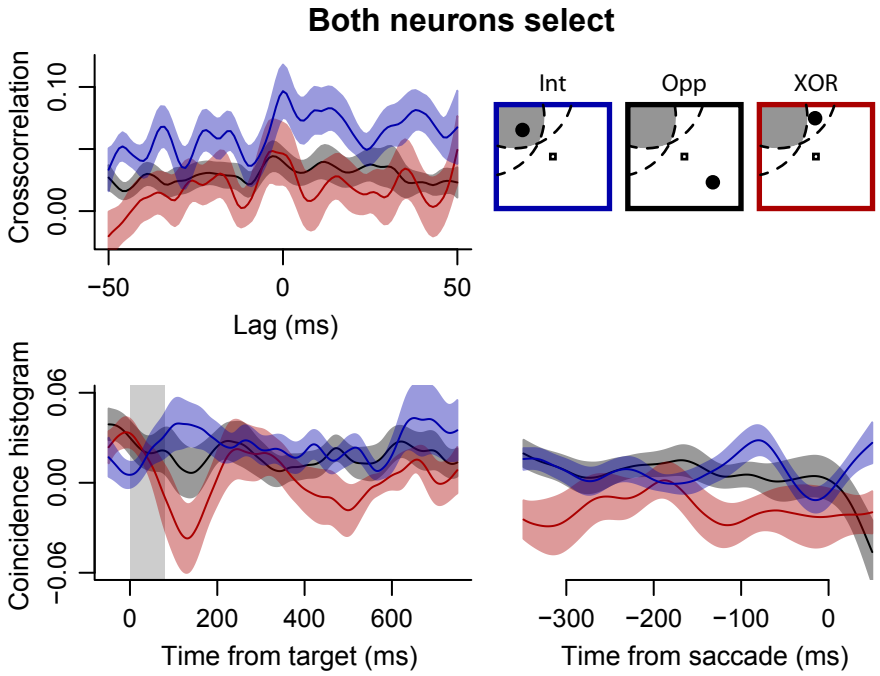

Figure 2.9: Mean ± SE crosscorrelograms (upper left) and coincidence histograms (bottom row; left, aligned to target flash, indicated by gray bar; right, aligned to saccade onset) during the memory-guided saccade task. Data from 25 of 32 pairs of neurons with sufficient trials to compute JPSTH are shown when the target was inside the intersection of the RFs ("Intersection" condition; blue), in one RF but not the other ("XOR" condition; red) and opposite the intersection of the RFs ("Opposite" condition; black).

was significantly larger when the target was in the intersection of RFs than when it was in one RF but not the other (paired $t_{(24)} = 3.20$, $p < 0.01$).

We compared the coincidence histograms between the memory-guided and visual search tasks for these 25 pairs of neurons. Coincidence histogram area was significantly larger during the search task than the memory-guided task (paired $t_{(24)} = 4.62$, $p < 0.01$), suggesting that target-distractor competition enhanced cooperation among neurons with overlapping RFs.

2.4.10 Spike correlations among neurons with non-overlapping receptive fields

Thus far, we have measured spike timing correlations among pairs of neurons with overlapping RFs (i.e., from the same pool). Next, we measured JPSTH for the 18 pairs of neurons analyzed in Figure 2.2*F*: those pairs in which both neurons selected the target and the RFs were spatially non-overlapping. We found that around the time of target selection for these neurons, the coincidence histograms shifted to negative correlation values when the target was in one RF but not the other ("XOR") relative to when the target was in neither RF (Fig. 2.10). This decrease was significant in the interval from target selection time to saccade (paired $t_{(17)} = 2.47$, $p < 0.05$) but not from array onset to target selection time (paired $t_{(17)} = 1.03$, $p > 0.3$), as measured by the area under the coincidence histogram in each interval. These results suggest that neurons with spatially non-overlapping RFs compete during target selection.

2.4.11 Effects of firing rate

In the analyses reported above, we used three control analyses (shuffle correction, excitability correction and simulation) to ensure that the spike timing relationships we observed were not due to covariations in firing rate between pairs of neurons. However, these controls do not rule out the possibility that the magnitude of spike timing correlations was related to the magnitude of the firing rates (but see Fig. 2.5). To test this possibility, we plotted the absolute value of the area under the crosscorrelogram as a function of the mean of the mean firing rates from search array onset to saccade onset for all pairs of neurons. Across the population of 239 pairs of neurons, we

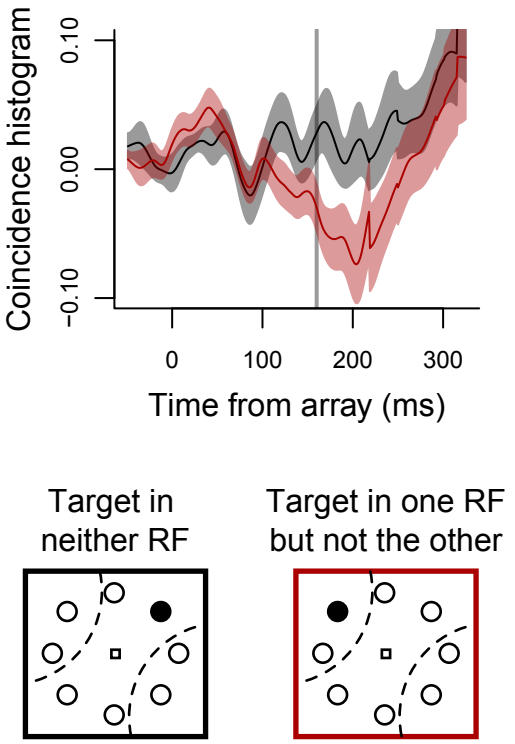

Figure 2.10: Mean ± SE coincidence histograms for the 18 pairs of neurons with disjoint RFs that both selected the target, when the target was inside one RF but not the other ("XOR" condition; red) and in neither of the RFs (black).

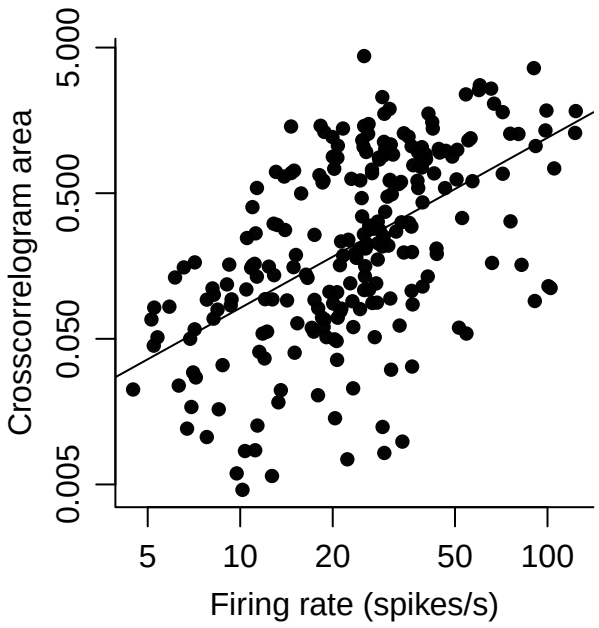

Figure 2.11: Log-log plot with linear regression of the absolute value of the area under crosscorrelograms versus the mean of the mean firing rates from search array onset to saccade for all 239 pairs of neurons with the target in all locations.

found a significant power law between crosscorrelogram area and firing rate: $\mathrm{CCA} = 0.0055 \cdot \mathrm{FR}^{1.17}$, where CCA is the crosscorrelogram area and FR is the mean of the mean firing rates (Fig. 2.11; $p < 0.001$ for slope and intercept). Thus, we cannot rule out that common driving input is a source of cooperation and competition in FEF, although we cannot distinguish between this interpretation, one in which cooperation and competition occur exclusively in FEF, and a combination of the two.

2.5 Discussion

We show that interactions between neurons are time varying and depend on whether and how neurons are involved in a task. Pairs of FEF neurons cooperated to select a visual search target from distractors by increasing their probability

of firing synchronously when the firing rates of both neurons discriminated target from distractors and when the target was inside both of their RFs. The timing of cooperative synchrony was aligned to the presentation of the visual search array, not saccade onset (Fig. 2.5), suggesting that the observed synchrony was involved in target selection and not saccade preparation. This is not surprising given that this effect was present in pairs of visual and visuomovement neurons that selected the target individually. The onset of cooperative synchrony also scaled with saccade response time (Fig. 2.8).

We found greater cooperative synchrony in pairs of neurons located in FEF in the same versus different hemisphere and competitive synchrony in pairs of neurons with non-overlapping RFs. This supports models of selective attention that propose that populations of neurons compete for representation of stimuli (Desimone and Duncan, 1995). However, it is unclear how such models would account for our observation of weak but significant synchrony during the memory-guided saccade task, in which a single target was flashed without distractors (Fig. 2.9). We showed previously, using a multivariate analysis, that movement neurons were engaged in greater interactions with visual and visuomovement neurons than vice versa (Cohen et al., 2007). Although we could not assess the direction of the interactions in this study given our limited sample of movement neurons, we did find surprisingly precise timing of the onset of synchrony in target-selecting visual and visuomovement neurons that varied with RT and task difficulty (e.g., Fig. 2.8). This is a significant advance over Cohen et al. (2007) because the previous study did not examine the time-dependence of neuronal interactions.

We observed some crosscorrelograms with broad peaks (Fig. 2.3*B*), which have been interpreted as evidence for common synaptic input or co-modulation (Averbeck and Lee, 2004; König and Engel, 1995; Nowak et al., 1995; Ts'o et al., 1986). Most crosscorrelograms, however, had sharper peaks on the order of 20 ms (Fig. 2.3*A* and Fig. 2.4), consistent with those observed in other cortical areas across species, including primary visual cortex (Das and Gilbert, 1999; DeAngelis et al., 1999; Samonds et al., 2006; Toyama et al., 1981; Ts'o et al., 1986), visual area MT (Bair et al., 2001), inferior temporal cortex (Gochin et al., 1991), somatosensory cortex (Celikel et al., 2004; Poulet and Petersen, 2008), auditory cortex (Ahissar et al., 1992; deCharms and Merzenich, 1996; Tomita and Eggermont, 2005), gustatory cortex (Yokota and Satoh, 2001), motor cortex (Allum et al., 1982; Jackson et al., 2003; Narayanan and Laubach, 2006) and prefrontal cortex (Constantinidis et al., 2001a,b; Constantinidis and Goldman-Rakic, 2002; Funahashi and Inoue, 2000; Narayanan and Laubach, 2006; Tsujimoto et al., 2008; Vaadia et al., 1995). These peaks probably do not reflect direct synaptic connections between pairs of recorded neurons, although the percent of significant crosscorrelations is consistent with anatomical studies estimating the probability of corticocortical connections using probability models (Abeles, 1991) and fluorescent labeling and patch clamping (Brown and Hestrin, 2009). Recent work has shown synchrony between unconnected neurons in vitro (de la Rocha et al., 2007) and zero-lag peaks that reflect long-range synaptic connections (Vicente et al., 2008). Previous work in cat visual cortex has shown interhemispheric synchrony (Nowak et al., 1995). Thus, we do not claim that the neurons we recorded were synaptically connected, but we emphasize that at a population level these inter-

actions are modulated by the task and could therefore contribute to the decision to select a target.

Given our observation that FEF neurons cooperate to locate a search target, how many neurons are required to make a decision about the target location? A recent study showed that weak correlations in spike timing between cortical neurons can imply strongly correlated networks of neurons (Schneidman et al., 2006). Thus, our observation of small correlation values could have profound effects in FEF population codes. Several studies report optimal or sufficient decision making with a population of 10-100 neurons (Newsome et al., 1989; Panzeri et al., 2003; Schoppik et al., 2008; Shadlen et al., 1996; Shadlen and Newsome, 1998; Zohary et al., 1994), including in FEF (Bichot et al., 2001b). Thus, models of networks of neurons that do not account for weak but informative temporal correlations between neurons may overestimate the amount of information a population can encode (Averbeck et al., 2006; Averbeck and Lee, 2004; Panzeri et al., 1999; Pouget et al., 2000). Indeed, a previous study of FEF neurons found that 7-14 neurons were sufficient to select a search target from distractors; they noted that this may have been an underestimate because they did not account for neuronal correlations (Bichot et al., 2001b).

We measured noise correlation to determine whether variability in spiking was correlated trial-by-trial. Previous studies have shown that noise correlation depends on the amount of time used to calculate it (Averbeck and Lee, 2003, 2004; Constantinidis and Goldman-Rakic, 2002; Reich et al., 2001), so we used the spike rates from search array onset to saccade, scaled by that duration. A previous study of MT neurons showed noise correlation values of about 0.12 for pairs of neighboring neurons

(Zohary et al., 1994). We find similar values of noise correlation in FEF, but the precise values vary as a function of neurons' involvement in a task (Fig. 2.2*A*) for pairs of neurons recorded as far away as opposite hemispheres.

Our noise correlation results suggest that population coding models need to be modified to account for positive and negative noise correlations among neurons in the same versus different pool, respectively. Recent work has shown that MT neurons representing different pools (disparate motion direction preferences) have lower noise correlation values than pairs of neurons representing the same pool (neurons with similar motion direction preferences) (Cohen and Newsome, 2008, 2009). Analogously, we may define pairs of neurons with overlapping RFs as part of the same pool and neurons with non-overlapping RFs as belonging to different pools. FEF neurons tend to have contralateral RFs (Bruce and Goldberg, 1985; Mohler et al., 1973; Schall, 1991), so it may be natural to think of each FEF as representing a different population of neurons involved in target selection and attention. Our data are consistent with a model in which neurons with spatially overlapping RFs excite each other as well as a population of interneurons that inhibit neurons with nonoverlapping RFs (Fig. 2.12).

Of course, FEF is not the only brain area containing target-selecting neurons. Neurons in posterior parietal cortex (e.g., Constantinidis and Steinmetz, 2001a; Thomas and Paré, 2007) and superior colliculus (e.g., McPeek and Keller, 2002) show similar behavior during visual search tasks. The question arises, then, whether neurons in these areas also cooperate to select targets, and how the three areas interact. One hypothesis is that neurons in all three areas cooperate independently within each area and are then pooled downstream (in the superior colliculus, for example). An

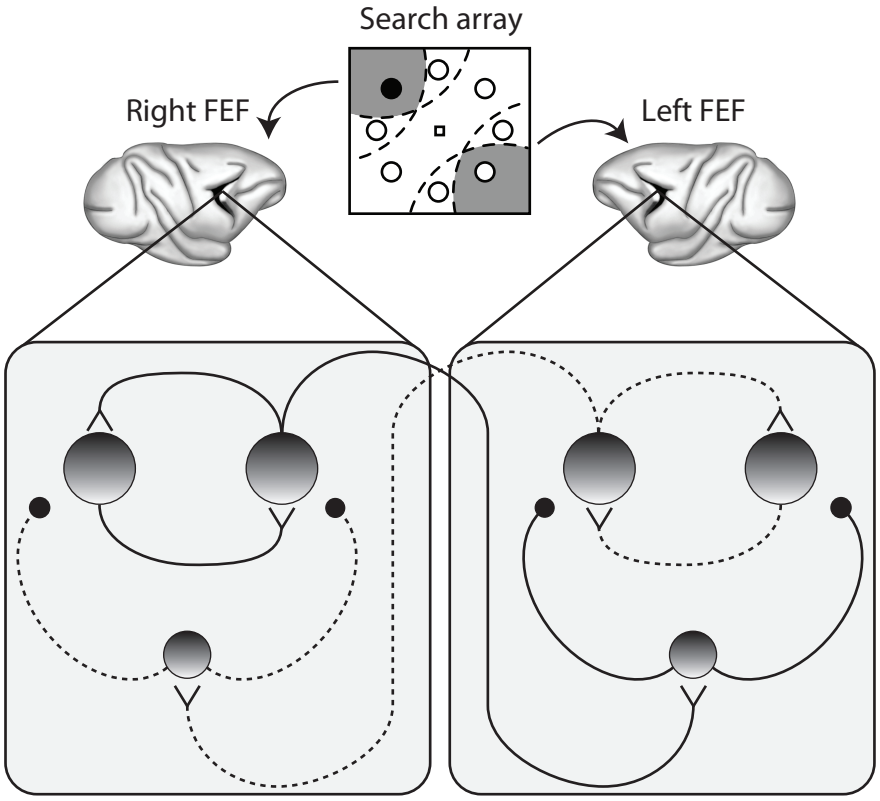

Figure 2.12: Circuit illustrating interactions among FEF neurons representing the target (in the left visual field, represented by right FEF) and distractors during visual search. Large shaded circles represent excitatory neurons. Small shaded circles represent inhibitory interneurons. V-shaped symbols represent excitatory synapses. Small black circles represent inhibitory synapses. Solid lines represent strong connections. Dotted lines represent weak connections. Dashed lines in the search array represent the RFs of the pair of excitatory neurons in each FEF.

alternative hypothesis is that neurons in all three areas interact as one large population of target-selecting neurons. Multiple-neuron recordings are required to address this question and, given their anatomical connections, it seems likely that a combination of the two hypotheses is at work. Given the power law between crosscorrelation magnitude and firing rate (Fig. 2.11), future experiments should distinguish between common input versus local interactions as the source of cooperation and competition in FEF.

In conclusion, we wish to draw a speculative analogy that we believe relates our findings to decision-making studies across different scientific fields. Increased synchrony around the time of target selection may signal formation of a quorum, a feature of many biological systems (Couzin, 2009), including groups of ants (Pratt et al., 2002), bees (Passino et al., 2008; Seeley and Visscher, 2004), bacteria (Waters and Bassler, 2005) and yeast (De Monte et al., 2007). Individuals in a group (e.g., neurons) do not need to know the outcome of the group decision; each individual signals its choice based on local interactions with other individuals, and the decision forms, often very quickly (Taylor et al., 2009). We suggest that it may be useful to view the self-organization evident in neuronal interactions within a framework used by behavioral ecologists to understand large-scale biological patterns.

CHAPTER III

DIFFICULTY OF VISUAL SEARCH MODULATES NEURONAL INTERACTIONS AND RESPONSE VARIABILITY IN THE FRONTAL EYE FIELD

3.1 Abstract

The frontal eye field (FEF) is involved in selecting visual targets for eye movements. To understand how populations of FEF neurons interact during target selection, we recorded activity from multiple neurons simultaneously while macaques performed two versions of a visual search task. We used a multivariate analysis in a point process statistical framework to estimate the instantaneous firing rate and compare interactions among neurons between tasks. We found that FEF neurons were engaged in more interactions during easier visual search tasks compared with harder search tasks. In particular, eye movementrelated neurons were involved in more interactions than visual-related neurons. In addition, our analysis revealed a decrease in the variability of spiking activity in the FEF beginning ~ 100 ms before saccade onset. The minimum in response variability occurred ~ 20 ms earlier for the easier search task compared with the harder one. This difference is positively correlated with the difference in saccade reaction times for the two tasks. These findings show that a multivariate analysis can provide a measure of neuronal interactions and characterize the spiking activity of FEF neurons in the context of a population of

neurons.[1]

3.2 Introduction

Neuronal activity in the primate frontal eye field (FEF) reflects visual target selection and eye movement commands (Bichot and Schall, 1999a; Murthy et al., 2001; Schall and Thompson, 1999; Thompson et al., 1996, 1997). Information from the visual system converges on the FEF (Schall et al., 1995b) and is integrated into eye movement commands through inputs to oculomotor structures (Hanes and Schall, 1996; Helminski and Segraves, 2003; Sommer and Wurtz, 1998, 2001). Three functional classes of neurons have been described in the FEF: visual-related, visual-and-movementrelated, and movement-related (Bruce and Goldberg, 1985; Schall, 1991; Schall and Hanes, 1993; Schall and Thompson, 1999; Schall et al., 1995a; Segraves and Goldberg, 1987). How these classes of neurons in the FEF interact to contribute to target selection remains unknown. To address how such visual-to-motor integration occurs, we analyzed the activity of FEF neurons recorded during a visual search task, emphasizing interactions that occurred among simultaneously recorded neurons. We compared neuronal interactions associated with hard and easy visual search tasks. A hard task was defined as one with a high degree of similarity between the target of the search and the distractor stimuli to be ignored. An easy task was defined as one with a low degree of target-distractor similarity (Duncan and Humphreys, 1989).

Recent developments in multivariate point process modeling of neural responses

[1]This chapter was published as Cohen JY, Pouget P, Woodman GF, Subraveti CR, Schall JD, Rossi AF. Difficulty of visual search modulates neuronal interactions and response variability in the frontal eye field. *J Neurophysiol* 98: 2580-2587, 2007.

have provided an analytical framework to characterize neural activity in the context of interactions between simultaneously recorded neurons (Brown et al., 2002; Okatan et al., 2005; Truccolo et al., 2005). This analysis models the instantaneous firing rate of a neuron using its own spiking history and that of other simultaneously recorded neurons as covariates in the model. The significance of each covariate provides an estimate of its contribution to the response of the modeled neuron. If the multivariate model's estimate of instantaneous firing rate is significantly improved by including covariates representing the activity of other neurons, it is evidence of interactions among neurons in the recorded ensemble. Such interactions may be direct synaptic connections between neurons or may be mediated polysynaptically or by shared input. Compared with conventional univariate estimates of neuronal activity, such as the peristimulus time histogram (PSTH), the multivariate approach can distinguish between a neuron's response and its response in the context of interactions in a population of neurons. Furthermore, point process modeling of neural activity preserves spike timing information which is distorted by measures that average over time-interval windows (e.g., PSTH). Traditional approaches for analysis of interactions between neurons, such as the covariogram and joint PSTH (Aertsen et al., 1989; Brody, 1999a,b; Constantinidis et al., 2001a), are limited to pairwise comparisons and do not provide adequate measures of ensemble interactions. The multivariate point process model estimates the instantaneous firing rate of a neuron in real-time without limits on ensemble size. Nonetheless, it can extract the same interactions as pairwise measures.

We show that the multivariate approach can accurately model spiking activity

in the FEF and characterize interactions among simultaneously recorded neurons while monkeys perform a visual search task. To better understand how neuronal interactions in the FEF contribute to target selection, we addressed the following questions. 1) Do interactions among FEF neurons differ for hard and easy search? 2) Are there differences in interactions between the three classes of FEF associated with saccade onset times?

3.3 Methods

3.3.1 Behavioral task and recording

Activity of FEF neurons was recorded in macaques performing a visual search task in which they were required to saccade to a singleton target defined by color (Sato et al., 2001). Each trial began with the monkey fixating a central spot for ~ 600 ms. A target was presented at one of eight isoeccentric locations equally spaced around the fixation spot (Fig. 3.1*A*, inset). The other seven locations contained distractor stimuli. Monkeys were given a juice reward for making a saccade to the target location and holding their gaze on the target for ~ 400 ms. There were two levels of task difficulty, hard and easy, determined by the degree of target-distractor similarity. The hard task contained a green target among yellow-green distractors. The easy task contained a green target among red distractors. Recordings were made simultaneously from two to four tungsten electrodes placed in the rostral bank of the arcuate sulcus. A neural ensemble was defined as a set of simultaneously recorded neurons with overlapping receptive fields. Our data set consisted of 91 neurons in 29 ensembles from one

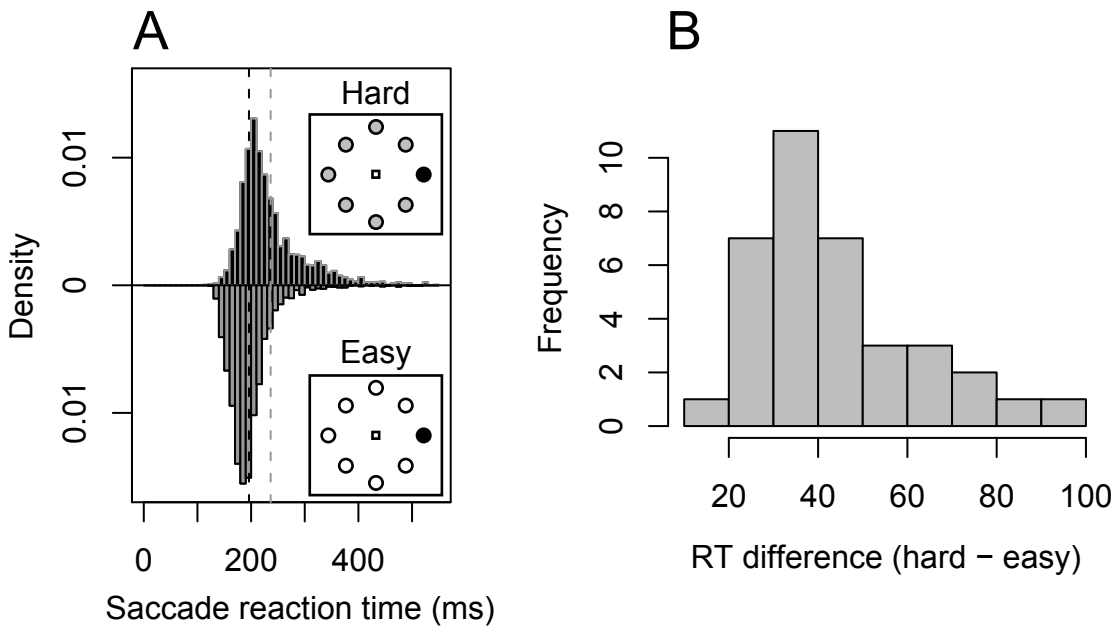

Figure 3.1: *Behavioral task and performance.* ***A***: top: density of saccade reaction times (RTs) for hard task (gray dashed line denotes mean). Bottom: density of RTs for easy task (black dashed line denotes mean). Hard search task consisted of a green target among yellow-green distractors. Easy task consisted of a green target among red distractors. Data are pooled across all sessions for both monkeys. ***B***: histogram of session-by-session RT differences (hard minus easy).

monkey (*Macaca mulatta*) and 21 neurons in 7 ensembles from a second monkey (*Macaca radiata*). Of the 36 ensembles, 15 contained two neurons, 10 contained three neurons, 6 contained four neurons, 4 contained five neurons, and 1 contained eight neurons. Spikes were sorted off-line using principal components analysis (Plexon). Because data from each monkey were collected during the same behavioral tasks and were similar, we pooled data from both monkeys.

Monkeys were trained on a memory-guided saccade task to distinguish visual- from movement-related activity (Bruce and Goldberg, 1985; Hikosaka and Wurtz, 1983). The target was flashed alone for 80 ms. The monkey was required to maintain

fixation for 400-1000 ms after the target offset. When the fixation spot disappeared, the monkey was rewarded for a saccade to the remembered location of the target. The movement-related neurons analyzed here had significantly greater responses in the 100 ms leading up to the saccade than in the 100 ms after the target flash. Visual- and visual-and-movementrelated neurons had greater responses in the 100 ms after the target flash than in the 100 ms before the target flash.

Each monkey was surgically implanted with a head post, a scleral eye coil, and a recording chamber. Surgery was conducted under aseptic conditions with isofluorane anesthesia (Schall et al., 1995a). Antibiotics and analgesics were administered postoperatively. All experimental procedures were performed in accordance with the National Institutes of Health Guide for the Care and Use of Laboratory Animals and approved by the Vanderbilt Institutional Animal Care and Use Committee.

3.3.2 Data analysis

To assess simultaneously the interactions of several neurons, we used a point process multivariate analysis (Okatan et al., 2005; Truccolo et al., 2005). The point process framework can provide for comparisons of arbitrarily large ensembles of simultaneously recorded neurons that pairwise measures cannot. We constructed a statistical model of the firing rate of a neuron by incorporating its firing history and the firing history of other neurons in its ensemble from stimulus onset to saccade onset (5315 correct hard search trials, 7414 correct easy search trials). We used a modified version of the generalized linear model (GLM) approach recently applied by (Truccolo et al., 2005). The modification was necessary because the fitted GLMs for

the hard and easy tasks may be different. Therefore unless they are nested, comparing such models statistically is intractable. We modified the GLM in the following way so that the data for both the hard and the easy tasks (for a particular neuron) were combined in a single GLM.

Using the theory of point processes, we represented recorded spike trains as sets of discrete event times. We modeled the instantaneous firing rate (conditional intensity function) of a neuron as a combination of terms of covariates (Truccolo et al., 2005). The conditional intensity function (λ_t) is more informative of the instantaneous firing rate than univariate measures (e.g., PSTH) because its estimate is derived in the context of interacting neurons. We predicted the firing of a neuron using its firing history (autoregressive process) and the firing history of other neurons recorded simultaneously (crossregressive process). We concatenated data from all correct trials for each neuron and used a GLM to predict the firing rate of a neuron as

$$\log(\lambda_t) = (\mu x_1 + \phi x_2) + \sum_{i=1}^{Q} (\alpha_i x_1 + \beta_i x_2)\delta N_{t-i} + \sum_{c} \sum_{j=1}^{R} (\eta_j^{(c)} x_1 + \nu_j^{(c)} x_2)\delta N_{t-j}^{(c)},$$

where λ_t is the firing rate at time t, μ is a baseline term associated with the hard search condition, ϕ is a baseline term associated with the easy search condition, $\{\alpha_i\}$ is the set of hard search autoregressive (AR) parameters, $\{\beta_i\}$ is the set of easy search AR parameters, $\{\eta_j\}$ is the set of hard search crossregressive (CR) parameters (1 for

each neuron in the ensemble at each lag), $\{\nu_j\}$ is the set of easy search CR parameters, and $\delta N_{t-k}^{(c)}$ is the spike count in the k^{th} ms before the current time t, for neuron c in the ensemble. Q and R are the AR and CR lags of the model, respectively. The indicator variables x_1 and x_2 combine the parameters associated with each task into a single model. x_1 is 0 for easy search trials and 1 for hard search trials. x_2 is 1 for easy search trials and 0 for hard search trials. Because of constraints on the length of the recordings (relative to the firing rate) we set $Q = R = 30$. This constraint was not of consequence to our analysis because the parameter fits stabilized well before lags of 30 ms. In the GLM above, the AR parameters describe the timing of the modeled neurons dependence on its firing history and the CR ones describe the timing of interactions between neurons. To compare models of hard and easy visual search trials, x_1 and x_2 terms were merged to create a separate GLM for each task.

We fit the GLM using an iteratively reweighed least squares algorithm (McCullagh and Nelder, 1989). This algorithm provides a robust maximum likelihood estimate of model parameters. If the assumptions of the GLM are met, the fitted model's residuals should have a normal distribution around mean 0 and constant variance with no autocorrelations (McCullagh and Nelder, 1989; Truccolo et al., 2005). Thus we examined the residuals of each of our model fits.

To compare the fit of nested models, we used likelihood ratio tests. For each neuron, we compared the model deviance ($D = -2 \log L$) for AR-only models and for AR-CR models for hard and easy search trials separately. This deviance comes from a χ^2 distribution. Thus we can test the hypothesis that adding CR terms to an AR model does not improve the GLM fits (McCullagh and Nelder, 1989). If

the likelihood ratio is large, the modeled neuron's response depends heavily on the ensemble neuron's responses. We measured variability in λ_t across neurons using a standardized measure of variability, the coefficient of variation (CV) (SD/mean). All analyses were performed in R (`http://r-project.org/`).

3.3.3 Model fits

To show that the GLM accurately accounted for the firing of FEF neurons, we compared the conditional intensity functions (λ_t, instantaneous firing rates) against the observed spike trains. Figure 3.2 shows the modeled intensity (black curve) and the observed spike train (gray vertical lines) for one example neuron over the course of 300 ms. The model covariates are the neuron's spiking history and the history of a second neuron in the ensemble. The modeled rate closely follows the observed spike times. Note that the magnitude of the intensity increases with the frequency of spikes. The brief (1 ms) decrease in the intensity after a spike likely corresponds to the neuron's absolute refractory period (Truccolo et al., 2005). This decrease is evident in Fig. 3.2*B*, which depicts the spike-triggered average intensity for the neuron in Fig. 3.2*A*. We also examined the Pearson residuals for each model. If the Pearson residuals were distributed normally with mean 0 and variance 1, the firing left unexplained by the model was insignificant McCullagh and Nelder (1989). For the model in Fig. 3.2, which was representative of the model fits of FEF neurons in our sample, the mean of the Pearson residuals was 6.08×10^{-4}, the variance was 0.892, and they were distributed normally. Models for all neurons had normally distributed Pearson residuals (Shapiro-Wilk test, $p < 0.05$).

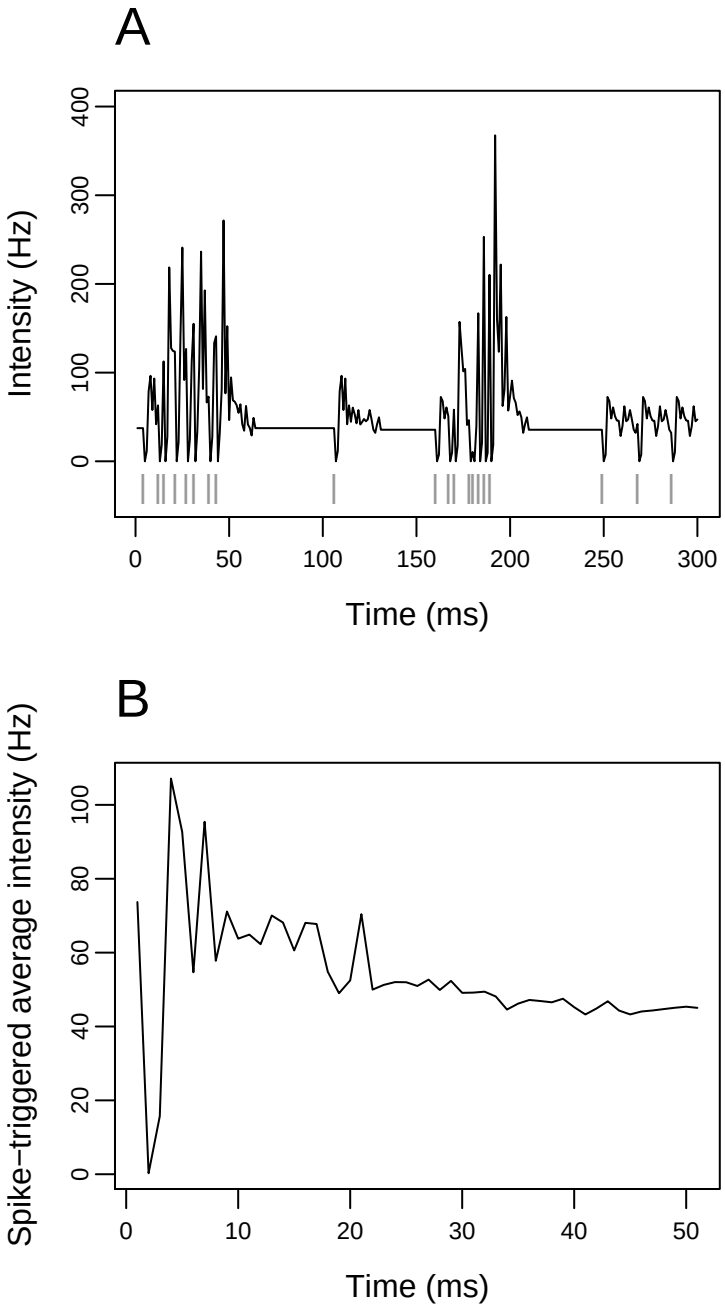

Figure 3.2: *Example model fit.* ***A***: spike train and modeled intensity for 1 frontal eye field (FEF) neuron over 300 ms. Gray vertical lines denote spike times. Black curve is modeled conditional intensity. ***B***: spike-triggered average intensity for neuron in ***A*** over course of entire recording.

3.3.4 Simulation and interpretation of parameters

A simulation was performed to test whether the GLM analysis extracted the same interactions that standard measures of pairwise interactions do. Figure 3.3, *A* and *B*, shows a comparison of the GLM fitting results for a simulated pair of spike trains with a standard measure of interactions between pairs of neurons, the covariogram Brody (1999a). The CR parameter values in Fig. 3.3*B* match the lags of high correlation between the pair of simulated spike trains in Fig. 3.3*A*. Significant parameters (by Wald Z test, $p < 0.05$) corresponded to interactions between the covariate and the target neuron at that lag, although not necessarily "monosynaptically." Positive parameter values corresponded to high probability that the covariate neuron excited the modeled neuron. Negative values corresponded to high probability of inhibition. Nonsignificant parameters (gray points) corresponded to low probability that the covariate interacted with the modeled neuron at those lags.

Figure 3.3, *C* and *D*, shows boxplots of parameter values at each time lag for all hard and easy models for all FEF recordings. Both AR and CR parameter values were stable past 15 ms, making it unnecessary to use a history of > 30 ms. The neurons' own history dependence (AR parameters) typically included ~ 10 ms and was inhibitory (negative parameter values). This likely corresponded to effects of absolute and relative refractory periods (Truccolo et al., 2005). Neurons' dependence on ensemble neurons' history (CR parameters) was, overall, relatively uniform except for at a lag of 1 ms. Baseline rates differed by < 1 spike/s between hard and easy tasks.

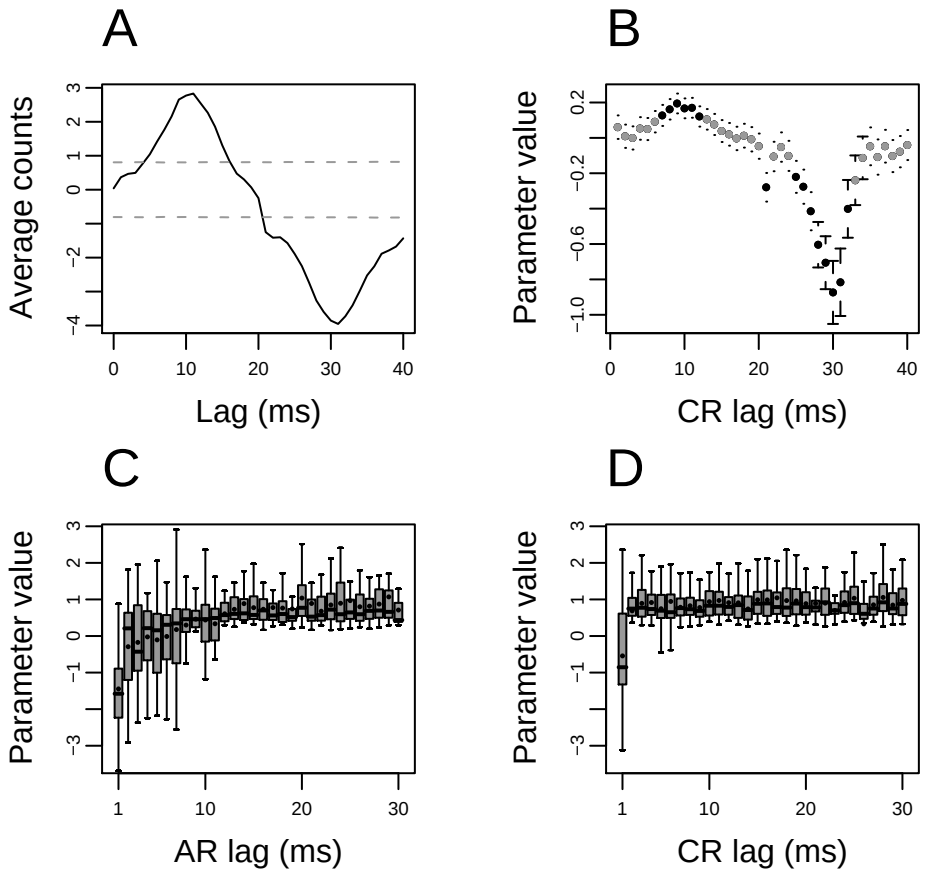

Figure 3.3: *Model interpretation.* ***A***: covariogram between a pair of simulated neurons. Dashed lines indicate significance. ***B***: crossregressive (CR) parameter values with SE (from Wald Z test) from the generalized linear model (GLM) fit for the same pair. Gray points are not significantly different from 0. ***C***: autoregressive (AR) parameter values significantly different from 0 for hard and easy search models. Filled point is mean, horizontal bar is median, box delimits interquartile range, and whiskers extend to point no more than 1.5 times interquartile range. Outliers are not shown in figure but are included in analyses. ***D***: same for CR parameters.

There were no significant differences between AR or CR parameters between hard and easy tasks. Figure 3.3, C and D, displays the overall pattern of history dependence on a neurons firing.

3.4 Results

Activity of 112 neurons was recorded in the FEF of two macaques performing two versions of a saccade-to-oddball visual search task (Fig. 3.1A, inset). These neurons were recorded in 36 ensembles. An ensemble was defined as a set of simultaneously recorded neurons with overlapping receptive fields. Ensemble sizes ranged from two to eight neurons.

Because both monkeys showed similar differences in performance for the easy and hard search tasks, these data were pooled. The easy and hard search tasks resulted in significant differences in percent correct (hard task = 71.6%; easy task = 96.6%; Wilcoxon rank sum test, $p < 10^{15}$) and mean saccade reaction time (hard task = 237 ms; easy task = 196 ms; $p < 10^{15}$). Figure 3.1A shows the densities of saccade reaction times (RTs) for the hard and easy search tasks. In addition to the significant difference in the mean RT (44.3 ms) for the two tasks, the variability of saccade RT was greater for the hard search task (SD = 65.3 ms) than the easy search task (SD = 41.2 ms). The mean difference in reaction time (hard minus easy) within each session was 44.4 ± 3.6 (SE) ms, with a minimum of 15.4 ms (Fig. 3.1B).

3.4.1 Do interactions among FEF neurons differ for hard and easy search?

We asked whether the amount of interactions among neurons in the FEF was affected by the difficulty of the visual search task. To measure interactions between neurons, we used a point process multivariate analysis to model the instantaneous firing rate of each neuron for each task (hard and easy) taking into account the firing history of all neurons in the recorded ensemble (see 3.3). The model estimated the conditional intensity function (instantaneous firing rate) of the neuron with respect to the covariates (AR and CR) when a saccade was made to a target located within the receptive field. We computed the likelihood ratios of models for each neuron for each task by subtracting the deviance of the AR-CR model from the deviance of the AR model. Large likelihood ratios indicated that including ensemble neurons in the model of a neuron greatly improved the prediction of the firing of that neuron. Because the likelihood ratio is distributed as χ^2, it is an ideal measure of the degree to which addition of CR covariates improved the estimate of the firing rate McCullagh and Nelder (1989).

We found that for 63.7% of easy task models and 51.6% of hard task models, χ^2 p-values were < 0.05, indicating that the inclusion of CR covariates improved the prediction of firing rate in the majority of models. We compared the likelihood ratios of the two pairs of models (hard vs. easy) to determine under which task the addition of ensemble responses (CR covariates) improved the model the most. The model that benefited the most from addition of CR covariates was judged to convey more interactions. Figure 3.4*A* is a histogram of the difference between likelihood

ratios for each neuron (easy minus hard). The histogram is shifted significantly to the right of zero (paired Wilcoxon rank sum test, $p = 3.05 \times 10^{-3}$). Thus we could better predict the firing of neurons in the easy task than the hard task when including the firing history of other neurons recorded simultaneously, indicating that neurons interacted more with each other during easy visual search. Simulations revealed that, regardless of visual search task, adding randomly firing simulated neurons to models of FEF neurons did not improve those model fits. Therefore improvements to models of FEF neurons by adding CR covariates were caused by neuronal interactions, whether monosynaptic, polysynaptic, or through shared input. There was no significant correlation ($p = 0.490$) between RT difference (hard minus easy) and likelihood ratio difference (easy minus hard), possibly because of low variability in RTs.

We cannot completely rule out that differences in interactions were not caused by differences in trial lengths or spike counts between hard and easy trials. This seems unlikely, however, for two reasons. First, the average firing rate difference between hard and easy trials was < 1 spike/s. Second, an analysis in which we equated for trial length yielded similar results. In this analysis, we removed data from the end of the spike train for each trial to equate with the length of the spike train of the shortest trial in each session. Before equating for trial length, 63.7% of neurons in the easy task and 51.6% in the hard task showed improved fits on addition of CR covariates, a difference of 12.1%. After equating for trial length, the number of neurons that showed improved fits decreased because of loss of data, but the same trend remained: 31.9% of neurons in the easy task and 20.9% in the hard task showed improved fits on addition of CR covariates, a difference of 11.0%. Thus

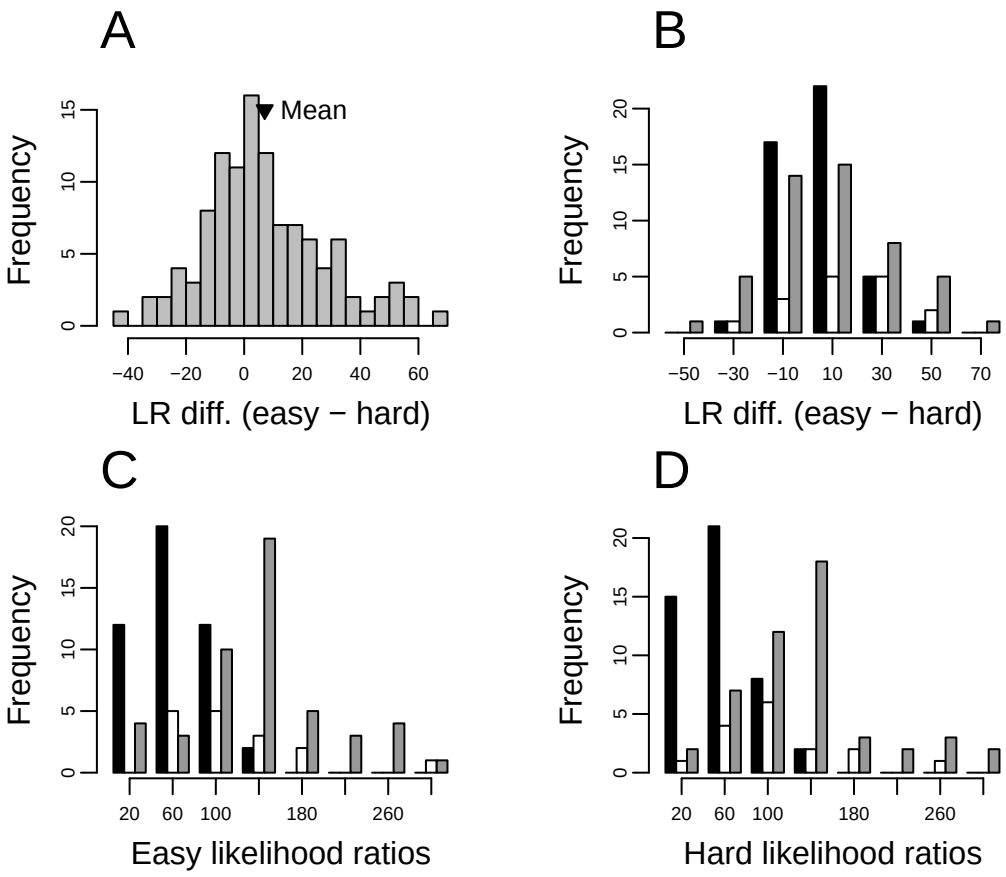

Figure 3.4: *Likelihood ratio analysis.* ***A***: histogram of likelihood ratio (LR) differences (easy minus hard) for each neuron. ***B***: histogram of LR differences split by neuron class (black: visual-related neurons; gray: visual-and-movement-related neurons; white: movement-related neurons). ***C***: histogram of LRs in easy task models split by neuron class. ***D***: histogram of LRs in hard task models split by neuron class.

despite discarding a considerable amount of data to equate for trial length, we found that neurons exhibited more interactions during easy trials than during hard trials.

3.4.2 Are there differences in interactions between the three classes of FEF neurons?

We classified each neuron as visual-related, movement-related, or visual-and-movementrelated. There were 46 visual-related neurons, 16 movement-related neurons, 49 visual-and-movementrelated neurons, and 1 that was unclassified. Figure 3.5 shows the responses of representative neurons of each class from our sample of recordings. The model for each showed improved fit on addition of CR covariates. Each PSTH in this figure shows the average firing rate of the neuron when the target was presented in the neuron's receptive field. Visual-related neurons had clear responses $\sim 50\,\text{ms}$ after target onset (Fig. 3.5A), visual-and-movementrelated neurons had similar visual latencies and increased firing leading up to saccades (Fig. 3.5B), and movement-related neurons fired at baseline until $\sim 60\,\text{ms}$ before saccades (Fig. 3.5C). The difference in visual-and-movement and movement-related responses during the hard and easy tasks correlated with the difference in mean RT between the hard (gray arrowhead) and easy (black arrowhead) tasks.

We tested whether there were systematic differences in interactions based on neuron class. Figure 3.4B shows likelihood ratio differences (easy minus hard) by neuron class. There were no significant differences in the distributions of likelihood ratio differences between visual- and movement-related neurons (Wilcoxon rank sum test, $p = 0.203$), visual- and visual-andmovement related neurons ($p = 1.00$), and visual-and-movement and movement-related neurons ($p = 0.329$). Figure 3.4, C

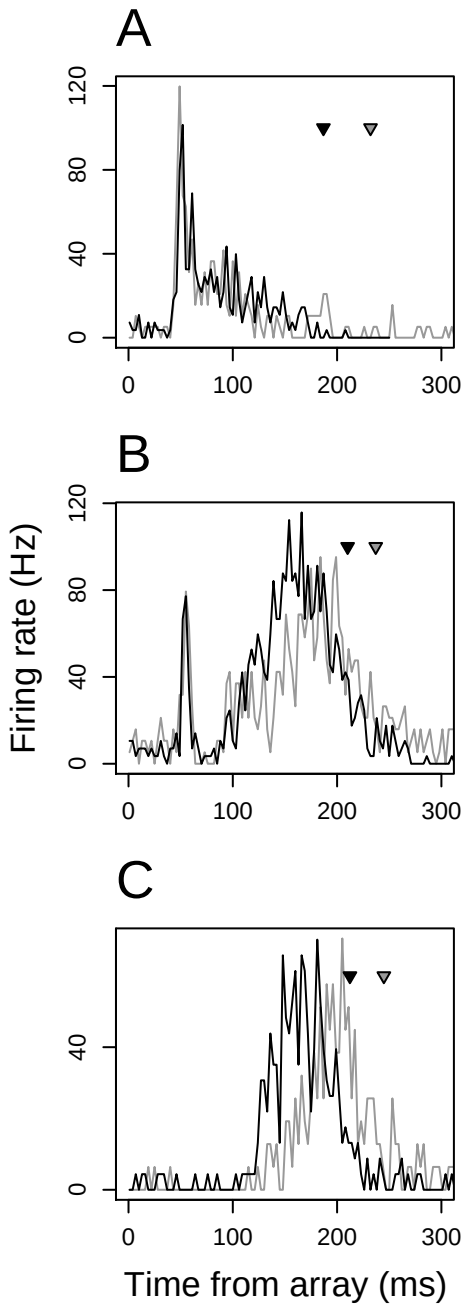

Figure 3.5: *Example neurons of each class.* ***A***: peristimulus time histogram (PSTH) for a visual-related neuron for the hard (gray) and easy (black) tasks aligned to array onset. ***B***: same for a visual-and-movement-related neuron. ***C***: same for a movement-related neuron. Bin size is 3 ms. Black arrowhead denotes mean saccade reaction time during recording session for easy task; gray arrowhead is for hard task.

and D, shows likelihood ratios for easy and hard tasks split by neuron class. We found that the likelihood ratios were significantly larger for movement-related neurons (white bars) than for visual-related neurons (black bars) for both hard (Fig. 3.4D; $p = 1.90 \times 10^{-3}$) and easy tasks (Fig. 3.4C; $p = 2.18 \times 10^{-5}$). Likewise, the ratios were larger for visual-and-movement related neurons (gray bars) than for visual-related neurons for both tasks (hard: $p = 6.34 \times 10^{-12}$; easy: $p = 7.36 \times 10^{-11}$). This indicates that movement- and visual-and-movementrelated neurons were engaged in greater interactions than the visual-related neurons. Likelihood ratios were significantly larger for the easy task than the hard task for visual-related neurons (paired Wilcoxon rank sum test, $p = 0.0425$) and movement-related neurons ($p = 0.0443$) and approached significance for visual-and-movementrelated neurons ($p = 0.0990$). This indicates that the model better predicted the firing of neurons in the easy task on addition of CR covariates than the hard task and that addition of CR covariates significantly improved firing predictions. The percent of neurons of each class with improved fits on addition of CR covariates was larger for neurons with movement-related activity than for neurons with only visual-related activity. For the easy task, 48.0% of visual-related neurons, 87.5% of movement-related neurons, and 63.3% of visual-and-movementrelated neurons showed improved fits. For the hard task, 32.0% of visualrelated neurons, 56.3% of movement-related neurons, and 59.2% of visual-and-movementrelated neurons showed improved fits. There were no differences in mean firing rate between neurons that showed improved fits and those that did not for each neuron class (Wilcoxon rank sum test, $p > 0.287$).

3.4.3 Are interactions among FEF neurons time-locked to saccade onset?

Because movement-related neurons in the FEF characteristically increase their firing leading up to saccades (Hanes and Schall, 1996) (see Fig. 3.5*C*), we analyzed the conditional intensity functions (λ_t, instantaneous firing rates) for movement-related neurons to determine whether the timing of interactions reflected the decision of the monkeys to move their eyes. To observe the neuronal responses around saccades, we modeled the intensity of these neurons from target onset to 50 ms after the saccade. Figure 3.6 shows the mean intensity (λ_t) for the 16 movement-related neurons during the hard task (Fig. 3.6*A*) and during the easy task (Fig. 3.6*B*). The gray curves show the mean intensities of AR models during the 100 ms leading up to saccades for the hard task; the black curves are the mean intensities of AR-CR models.

Figure 3.6, *C* and *D*, shows the difference between AR-CR and AR models of mean intensities for hard trials (*C*) and easy trials (*D*). For both hard and easy tasks, addition of CR covariates increased λ_t leading up to saccades, relative to λ_t for AR models. Thus interactions between neurons statistically accounted for a significant portion of the presaccadic activity in movement-related neurons. Figure 3.6, *E* and *F*, shows the normalized mean PSTH (gray curve) and intensity function (black curve) for hard trials (*E*) and easy trials (*F*). A comparison of the intensity functions and PSTHs shows that the AR-CR models accurately describe both the magnitude and the dynamics of the PSTHs for the two search tasks. The intensity functions are shifted ~ 30 ms to the right of the PSTHs, reflecting the integration of 30 ms of firing history into the estimate of the intensities.

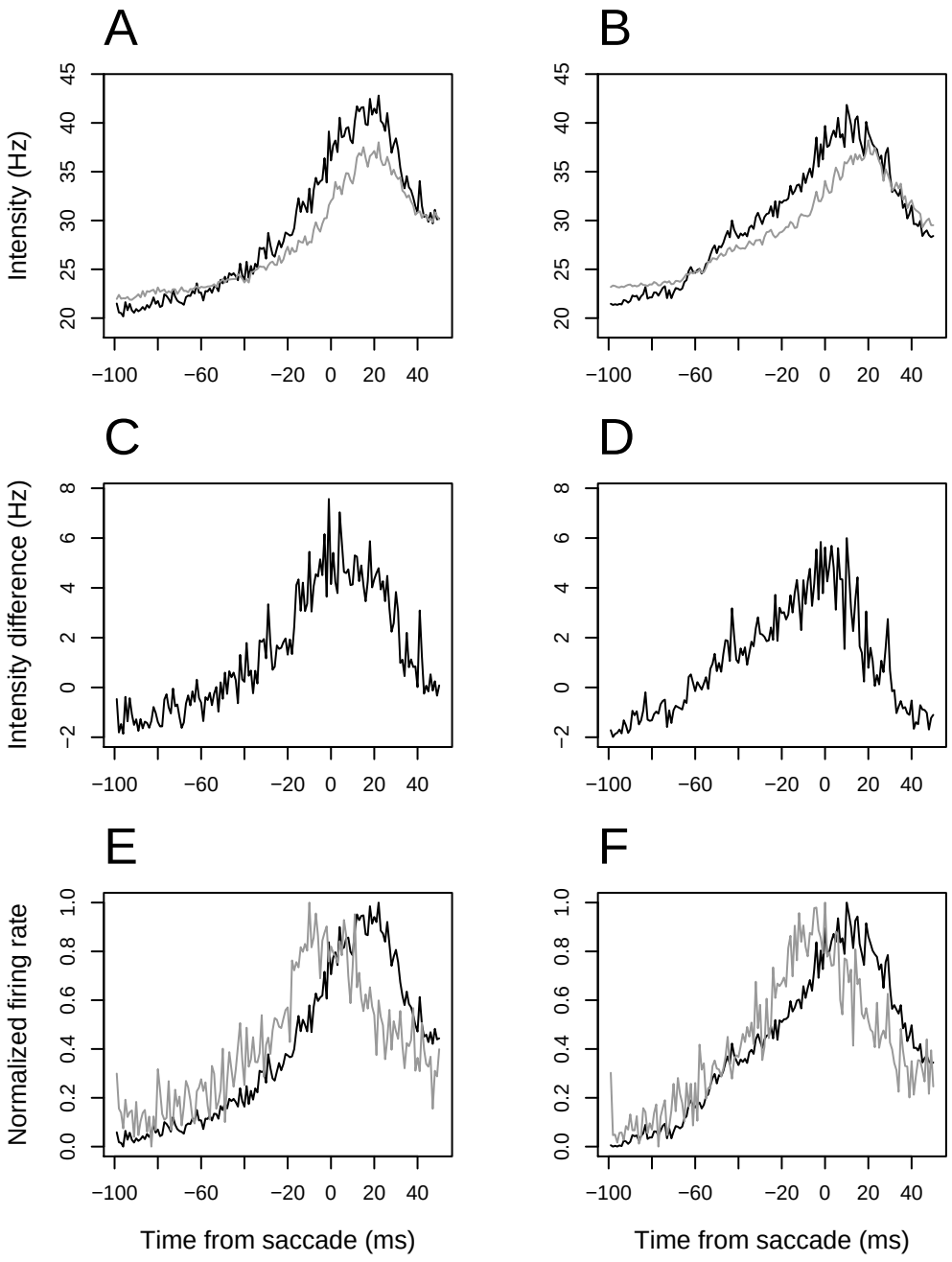

Figure 3.6: *Mean instantaneous firing rate of movement-related neurons before saccade.* ***A***: black curve is mean intensity function for 16 movement-related neurons during hard search task, averaged over all trials for AR-CR models. Gray curve is the same for AR models. Curves are aligned to each trial's saccade. ***B***: same for AR-CR models (black) and AR models (gray) for easy task. ***C***: difference between AR-CR and AR intensities for hard task, i.e., difference between black and gray curves in ***A***. ***D***: difference between AR-CR and AR intensities for easy task. ***E***: comparison of intensities and PSTHs. Normalized mean intensity function (black curve) and PSTH (gray curve, 1-ms bins) for hard task. ***F***: same for easy task.

To further explore the effect of ensemble interactions on the activity of movement-related neurons, we compared the variability of the conditional intensity functions for each search task. The CV (SD/mean) is a measure of standardized variability frequently used in neuroscience and may be interpreted as a "noise-to-signal" ratio (de Ruyter van Steveninck et al., 1997; Feng and Brown, 1999; Stein and Matthews, 1965; Stevens and Zador, 1998). We used the CV to measure changes in instantaneous firing rate of movement-related neurons that occurred just before saccades. Decreases in the CV over time reflected less variability (or noise) in the system.

Figure 3.7 shows the CV of the mean intensity function for the movement-related neurons for the hard (gray curves) and easy (black curves) tasks for AR-CR models (Fig. 3.7*A*) and AR models (Fig. 3.7*B*). For both hard and easy tasks, the CV decreased leading up to saccades in the AR-CR models until just before saccades, at which point the CV increased. Thus addition of CR covariates decreased standardized variability (CV) leading up to saccades.

Remarkably, there was a clear difference between the time at which the CV began to increase preceding saccades for hard and easy tasks. We fit smoothing splines to each curve to estimate the time at which each curve attained its minimum. In the AR-CR models, the CV started increasing 28 ms before saccades for the easy task and 7 ms for the hard task. This difference suggests that the movement-related neurons responded with the least variability ~ 20 ms earlier in the easy task, despite the fact that we aligned intensities on saccade times. The difference in minimum CV times between easy and hard search was closer for AR-CR models (Fig. 3.7*A*) than for AR models (Fig. 3.7*B*). Presumably, this was because of poorer fits of AR models. It is

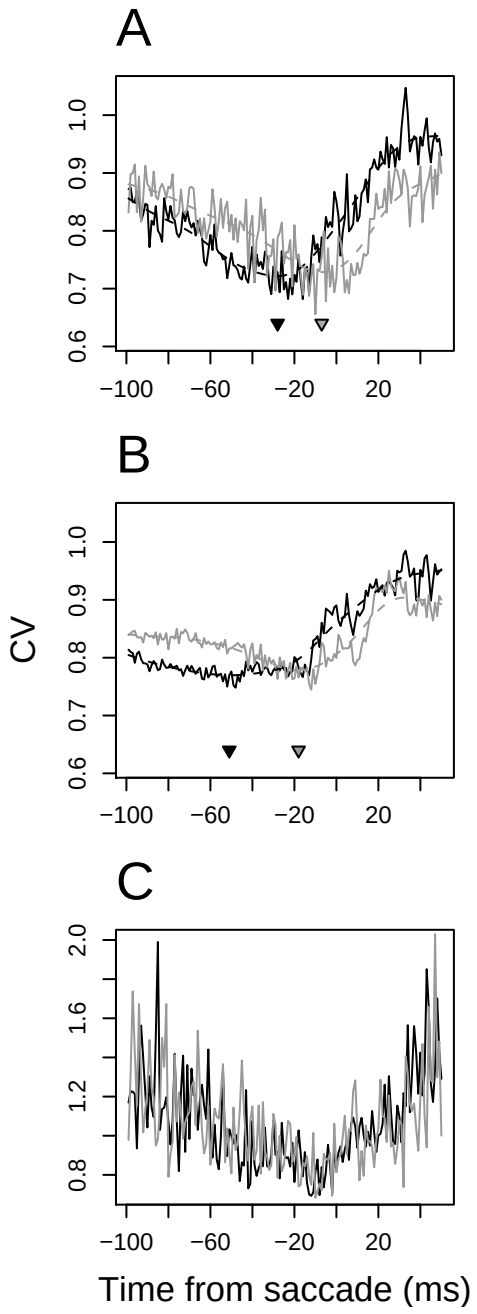

Figure 3.7: *Coefficient of variation (CV) of intensities and PSTHs.* ***A***: gray curve is CV of mean intensity functions for movement-related neurons during hard task; black curve is during easy task, averaged over all trials for AR-CR models. Dashed curves are smoothing splines used to estimate the minima of curves. Arrowheads denote these minima. ***B***: same for AR models. ***C***: gray curve is CV of mean PSTH during hard task; black curve is during easy task.

important to note that, although intensities were shifted to the right of PSTHs, the timing results in Fig. 3.7 compare identical measures to each other (i.e., intensity to intensity and PSTH to PSTH). Thus the differences in time course of the CV between the hard and easy tasks reflect the dynamics of the conditional intensity functions.

We compared the results using the intensity function to a standard model of the firing rate, the PSTH. Figure 3.7*C* shows the CV of the PSTHs of movement-related neurons. Similar to the results obtained from the intensity functions (Fig. 3.7, *A* and *B*), the PSTH CV decreased leading up to saccades and increased 510 ms before saccades. However, there was no difference between time of increase for hard and easy tasks. It is important to keep in mind that comparing changes in the PSTH between hard and easy tasks cannot reveal the same information as the intensity can, because the latter measures changes in the system in the context of interacting neurons. Thus the intensity function is a better measure of instantaneous firing rate than the PSTH to measure time of response variability in the FEF.

3.5 Discussion

An outstanding problem in neuroscience is determining how populations of neurons interact to produce behavior. We have recorded simultaneous activity from multiple FEF neurons while monkeys performed two versions of a visual search task, one hard and one easy, defined by similarity between the target and distractors.

These results indicate that easier visual search tasks are associated with greater interactions among populations of FEF neurons. This is seemingly counterintuitive. After all, why should neurons interact more during a task that seemingly requires

fewer resources to solve? The average firing rates are not significantly different between the two conditions, so there must be a difference in the structure of the spike trains. There are at least two potential explanations. 1) During hard tasks, FEF neurons fire less randomly, requiring fewer interactions to accomplish the same goals (target selection and saccade preparation). 2) FEF neurons fire more randomly during hard tasks, requiring more information from other neurons. We measured the CV of the interspike intervals during hard and easy tasks. We found no significant difference between the two ($p = 0.255$), although there was a trend toward larger CV during the easy task. Further studies are required to determine whether FEF neurons' firing patterns differ between tasks.

Hanes and Schall (1996) determined that single movement-related neurons in the FEF could reliably predict saccade reaction time. This finding leads to the question of how movement-related neurons integrate visual information. It is possible that interactions between the three neuron classes in the FEF fully predict the timing of saccades. Simultaneous recordings from the FEF and other prefrontal areas (e.g., area 46) or parietal areas (e.g., lateral intraparietal cortex) would address this issue. In concert with a point process analysis, such an experiment would describe the timing of interactions between areas and determine how neurons in other cortical areas interact with FEF neurons to decide to move the eyes.

We propose that the timing of changes in the intensity function of movement-related neurons reveals the time at which networks of neurons decide to initiate a saccade. For models that include ensemble activity, the CV decreases until just before saccades, which coincides with the period of time when information about the decision

to saccade accumulates. The CV is a second-order measure. As such, it reflects changes in noise in the system. Thus it provides an estimate of the time between the saccade decision time of FEF movement-related neurons and execution of the saccade. Because the CV reflects noise in the system, remarkably, this also suggests that the noise in the system actually decreases as the firing rate of these neurons increases leading up to saccades (until the increase in CV just before saccades). Therefore we show not only that movement-related neurons have activity sufficient to trigger a saccade (Hanes and Schall, 1996), but that their presaccadic activity reflects a decrease in firing variability.

The difference in time of increase of CV between hard and easy tasks has important implications for when the decision to make a saccade occurs. In our experiments, the neurons spent 20 ms longer reaching their minimum in response variability in the hard task than in the easy one. This may correspond to earlier decision times in the easy task than in the hard one. Therefore it seems that the decision to move the eyes is mediated by the movement-related neurons. The larger likelihood ratios for movement-related neurons versus visual-related neurons suggest that the movement-related neurons receive greater interactions from other FEF neurons. This agrees with models of visual search in the FEF, which assert that projections from visual-related neurons to movement-related neurons transform information about visual stimuli into a saccade execution plan (Thompson et al., 1996).

How does the estimate of 20-ms difference in time of minimum response variability correspond to differences in saccade RT? The mean RT difference between the hard and easy tasks was 44.3 ms. The CV during the 100 ms after target onset did not

decrease for visual-related neurons (data not shown). This may be because of the location of presynaptic neurons connecting with these visual-related neurons. If, as the anatomy suggests (Schall et al., 1995b), visual-related neurons receive synaptic connections from visually responsive neurons in the parietal, temporal, and occipital cortices, we would not have observed visual-related FEF neurons in the context of those interactions. Simultaneous recording from the FEF and cortical areas that project to the FEF would address this issue. Such an experiment would address whether sensorimotor integration occurs in a single bottom-up volley or is the result of continued flow of information between neurons with sensory responses and those with motor responses (Riehle et al., 1997; Woodman et al., 2008).

We showed that accounting for ensemble activity is a powerful method of modeling the firing rate of a neuron. There are several ways to measure activity of single neurons, however. A continuous function best represents the firing of a neuron if it accounts for the synaptic input to the neuron (a network property) and approximates the instantaneous firing rate of the neuron. The intensity function has two advantages over other measures of neuronal firing, such as the PSTH. First, it accounts for network activity (the CR covariates) and second, it approximates instantaneous firing rate better than the PSTH (Truccolo et al., 2005). We have shown that using the intensity function to describe the firing of FEF neurons reveals the time-course of activity leading to the decision to saccade more sensitively than the PSTH.

Although the point process model can account for a large number of influences on a neuron's firing, it is not a mechanistic model. It cannot, therefore, distinguish between neurons that are synaptically connected and neurons that share common

input. This limitation is shared by other common techniques such as the covariogram and joint PSTH. A challenge for future studies of neuronal interactions is to include knowledge about anatomical connections and biophysical properties of neurons in mechanistic models of networks of neurons.

We postulate that the distinction between easy and hard tasks, as detected by our results (e.g., difference in lag between minimum CV and saccade) is continuous, rather than dichotomous. Theoretically, there must exist a minimal set of neurons that are required to complete a given visual search task and a latest time before saccade that the decision is made. Our results show that easier visual search tasks are associated with greater interactions among populations of FEF neurons and may result in earlier saccade decision times.

CHAPTER IV

NEURAL VARIABILITY IN FRONTAL EYE FIELD DURING VISUAL SEARCH

4.1 Introduction

When presented with the same stimulus repeatedly, we respond with variable response times (RTs). What is the source of this variability in behavior? Can it be identified with particular stages of processing during perceptual decisions? The mean firing rates of neurons in several cortical areas correlate with RT and can explain variability in RT in a variety of tasks, including in extrastriate visual cortex (Britten et al., 1992), posterior parietal cortex (Thomas and Paré, 2007) and prefrontal cortex (Cohen et al., 2009a; Sato et al., 2001). Can firing variability account for variability in RT?

Recent work has shown that firing variability in dorsal premotor cortex accounts for variability in RT in a reaching task in monkeys (Churchland et al., 2006). This suggests that some of the variability in RT lies in variability in movement preparation.

We trained two macaques to perform a visual search task in which they made a single saccade to a target presented among distractor stimuli. We recorded spiking from frontal eye field (FEF) neurons and measured their firing variability. We asked whether firing variability in FEF accounts for variability in RT during visual search. In this task, at least two populations of neurons in FEF correlate with two processing stages: target selection and saccade preparation. The mean firing rates of visually-responsive FEF neurons select the target of visual search among distractors by firing

more when the target versus a distractor is in their receptive fields (RFs). The mean firing rates of other neurons, called movement neurons, increase to a threshold before purposive saccadic eye movements to their movement fields (MFs) but fire at their baseline rate before saccades outside their MFs (Bruce and Goldberg, 1985; Hanes and Schall, 1996).

We show that (1) variability decreased to a minimum after search array onset, (2) variability decreased more when the search task was easier versus harder and (3) variability decreased more when the search target was inside versus outside RFs. The first two findings suggest that the brain reaches a minimum variability in spiking to make a decision and that this minimum correlates with the difficulty of the task. The third finding suggests that neurons use the variability as well as the mean to discriminate between target and distractors during visual search decisions.

4.2 Methods

4.2.1 Behavioral task and recording

Activity of FEF neurons was recorded in both hemispheres of two male macaques (*Macaca radiata*) performing memory-guided saccade and visual search tasks. Recordings were acquired from the rostral bank of the arcuate sulcus using tungsten microelectrodes (FHC). In the search task, monkeys searched for a target (**T** or **L**) among distractors (**L** or **T**) (Woodman et al. 2007). Distractors could be homogeneous (e.g., upright **L**s) or heterogeneous (e.g., **L**s oriented differently). Each trial began with monkeys fixating a central spot for about 600 ms. A target was then presented at one

of eight isoeccentric locations equally spaced around the fixation spot (Fig. 7.1*A*). The other seven locations contained seven distractor stimuli, three distractors, or one distractor. During each recording session, the target was a **T** or an **L** rotated by 0, 90, 180, or 270 °. Monkeys were given a liquid reward for making a saccade to the target location and fixating it for 1000 ms.

Activity from each neuron was recorded during a memory-guided saccade task to distinguish visual- from movement-related activity (Bruce and Goldberg, 1985; Hikosaka and Wurtz, 1983). The target was flashed alone for 80 ms. Monkeys were required to maintain fixation for 500-1000 ms after the target onset. When the fixation spot disappeared, the monkey was rewarded for a saccade to the remembered location of the target.

Our data set consists of 68 neurons from monkey Q and 27 neurons from monkey S. Spikes were sorted on-line and off-line using principal components analysis and template matching (Plexon, Dallas, TX).

Monkeys were surgically implanted with a head post, a subconjunctival eye coil, and recording chambers. Surgery was conducted under aseptic conditions with animals under isoflurane anesthesia. Antibiotics and analgesics were administered postoperatively. All surgical and experimental procedures were in accordance with the National Institutes of Health Guide for the Care and Use of Laboratory Animals and approved by the Vanderbilt Institutional Animal Care and Use Committee.

4.2.2 Data analysis

To measure the firing rate of each neuron, we used a spike density function, convolving each spike with a kernel resembling a postsynaptic potential (Thompson et al., 1996).

We used a memory-guided saccade task to classify neurons. Visual neurons had significantly greater activity in the 100 ms after the target flash than in the 100 ms before the target flash. Movement neurons had greater responses in the 100 ms leading up to the saccade than in the 100 ms before the target flash. Visuomovement neurons had greater responses in the 100 ms after the target flash and in the 100 ms leading up to the saccade than in the 100 ms before the target flash. Of the 95 neurons in the data set, 83 were visual and visuomovement neurons and had significant above-baseline activity during the memory delay and 12 were movement neurons.

To measure the time of target selection we used millisecond-by-millisecond Wilcoxon rank-sum tests. Selection time is defined as the time at which the distribution of activity when the search target was inside a neuron's RF was significantly greater than the distribution of activity when the target was opposite the RF for ten consecutive milliseconds with $p < 0.01$. This "neuron-antineuron" approach presumes that a population of neurons in the brain representing the location of the target competes with a population of neurons representing the location of distractors opposite the target. Measuring selection time with a receiver operating characteristic analysis (Thompson et al., 1996) yielded similar results. There was no difference in target selection time between visual and visuomovement neurons.

To measure firing variability, we used a metric similar to the Fano factor (variance/mean), but scaled by the time-varying mean firing rate (Churchland et al., 2006).

To quantify the timing of mean and variability changes in firing rate, we used a receiver operating characteristic (ROC) analysis, in which we calculated the area under the curve of probability of mean or variability exceeding a particular criterion for target versus distractor. Area values close to 0.5 indicate the absence of selectivity. Area values close to 1 indicate strong discrimination between target and distractor activity.

All statistical tests were done with Bonferroni corrections for multiple comparisons. All analyses were done with R (`http://www.r-project.org/`).

4.3 Results

4.3.1 Normalized variability

Visual and visuomovement neurons

Figure 4.1 shows the mean firing rate of an example visuomovement neuron when the target was inside and opposite its RF. This neuron selected the target by increasing its firing rate when the target was in its RF.

Figure 4.2 shows the mean firing rate of 83 visual and visuomovement neurons by set size for each monkey when the target was inside or opposite RFs.

Figure 4.3 shows the time-varying firing variability of the 83 visual and visuomovement neurons from Figure 4.2. The firing variability decreased regardless of which

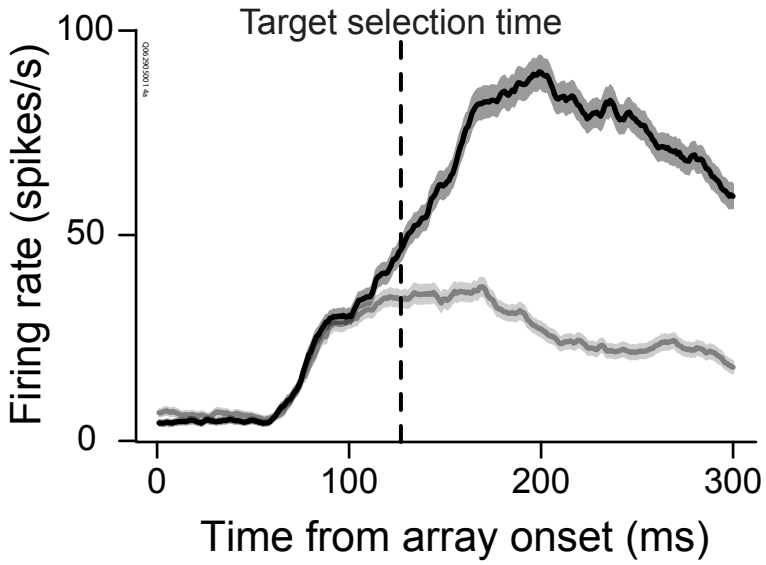

Figure 4.1: Example neuron that selected the target during the visual search task. The black curve with dark bands represents the mean ± SE firing rate when the target was inside the neuron's RF. The gray curve with light bands represents the mean ± SE firing rate when the target was opposite the RF. Initially, the neuron's firing rate did not discriminate between target and distractors, but after 130 ms its firing rate selected the target (dashed vertical line).

stimulus was inside RFs, but it decreased more when the target was inside RFs than when distractors were inside RFs. Thus, the firing variability discriminated between target and distractors just as the mean firing rates did.

Figure 4.4 shows the ROC area for each set for the variability and the mean firing rate for the population of visual and visuomovement neurons. Target selection was later for larger set sizes.

Movement neurons

Figure 4.5 shows the mean firing rate of 12 movement neurons by set size when the target was inside or opposite MFs. As with the visual and visuomovement neurons, the firing variability decreased with time when the target was inside MFs, but, in

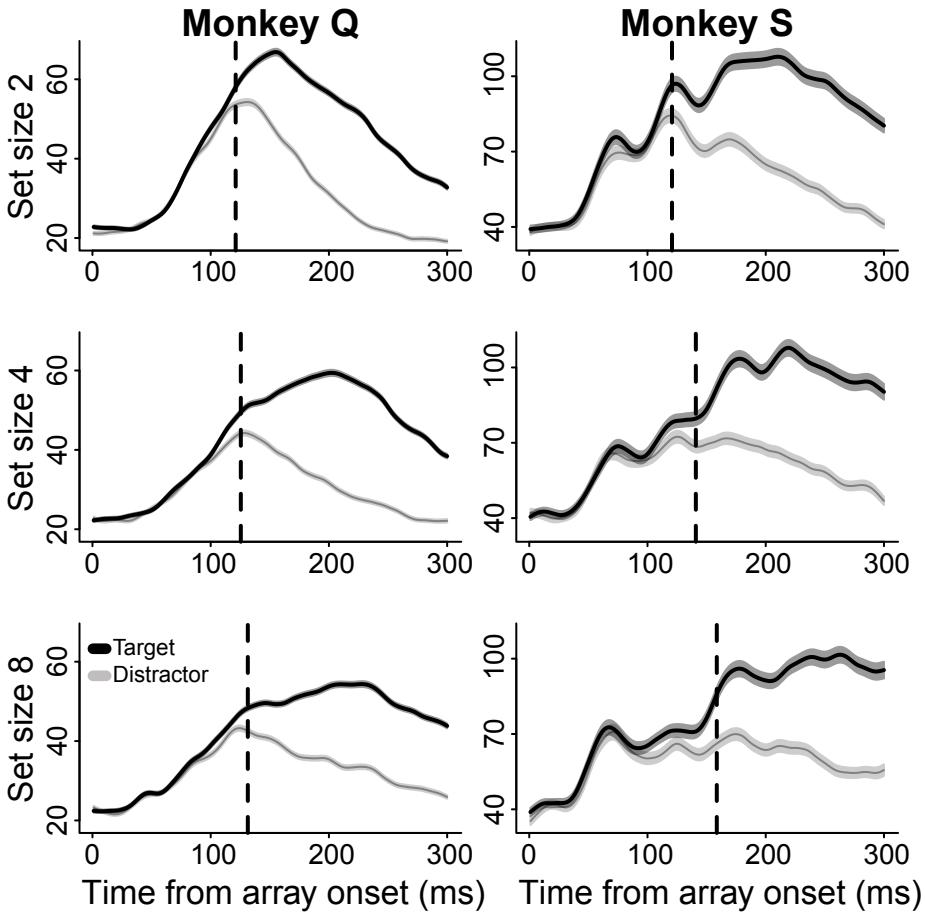

Figure 4.2: Mean ± SE population mean firing rates when the target was inside (dark) and opposite (light) neurons' RFs as a function of set size.

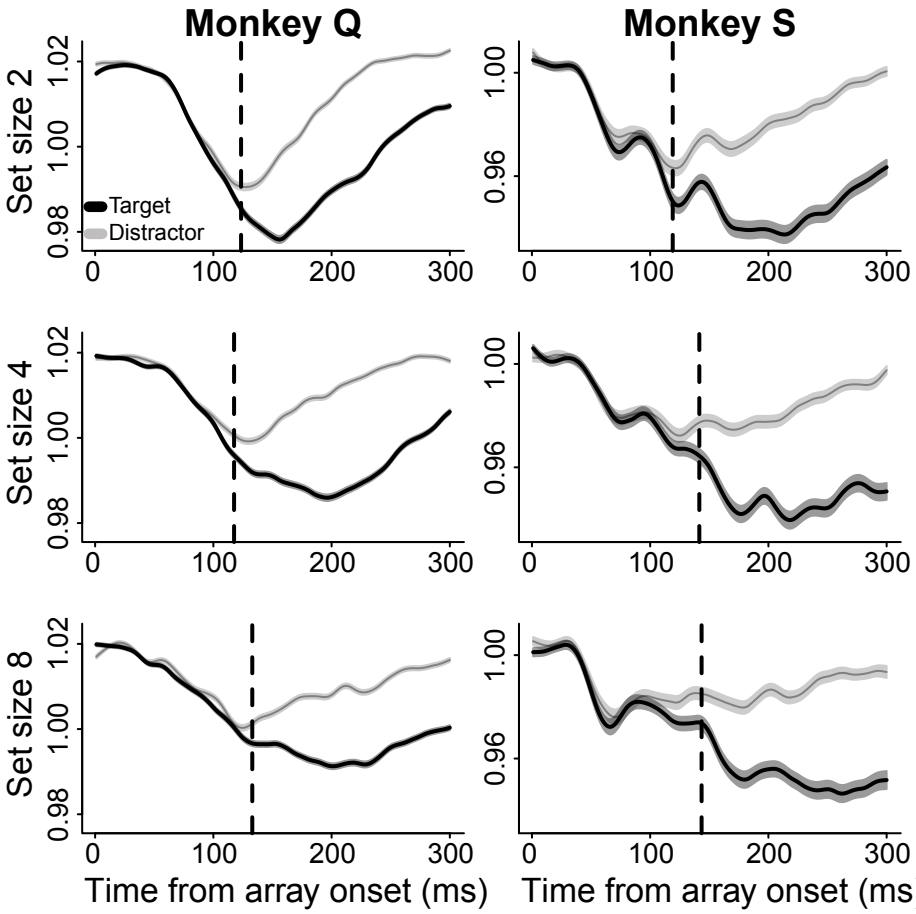

Figure 4.3: Mean ± SE population firing variability when the target was inside (dark) and opposite (light) neurons' RFs as a function of set size.

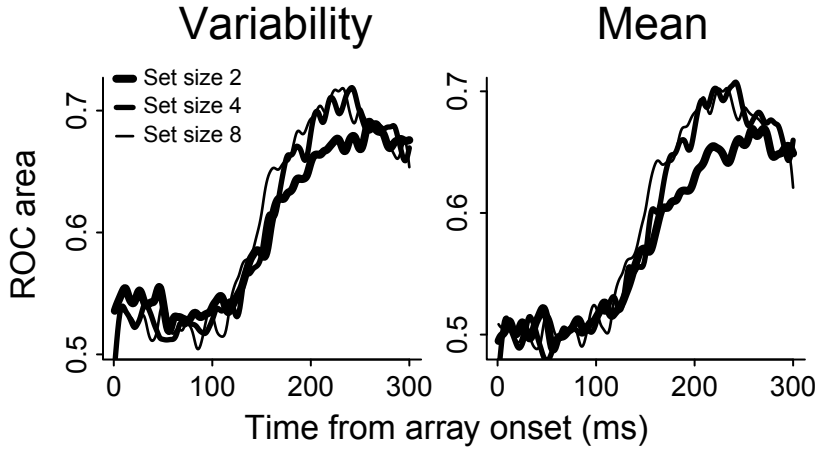

Figure 4.4: ROC area for each set size between target and distractor mean and variability of firing rate.

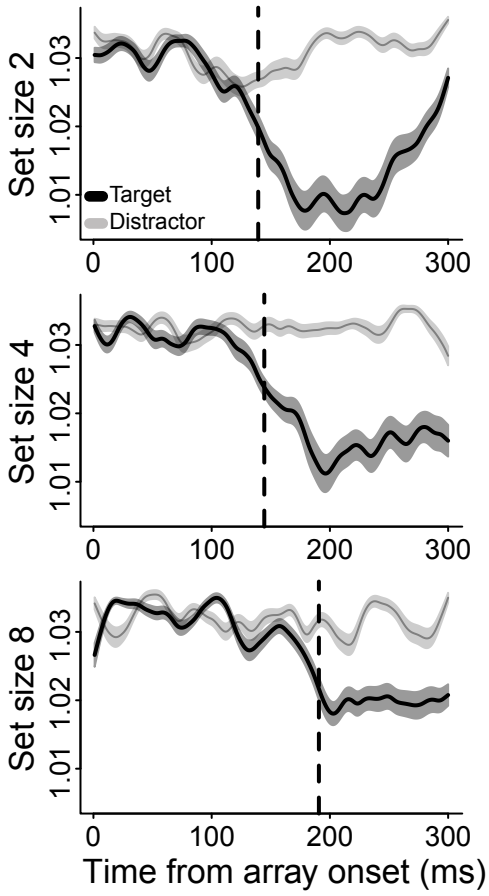

Figure 4.5: Mean ± SE population firing variability when the target was inside (dark) and opposite (light) neurons' RFs as a function of set size for movement neurons.

contrast to visual and visuomovement neurons, did not decrease when the target was outside MFs.

4.3.2 Relationship between firing rate and response time

We asked whether monkey's RTs were fastest when neurons had the highest firing rate or when they fired closest to their mean rate. Figure 4.6 shows scatterplots of RT versus deviation from each neuron's mean firing rate for all neurons and all trials in the data set. The top row shows the quadratic fits of curves for visual and

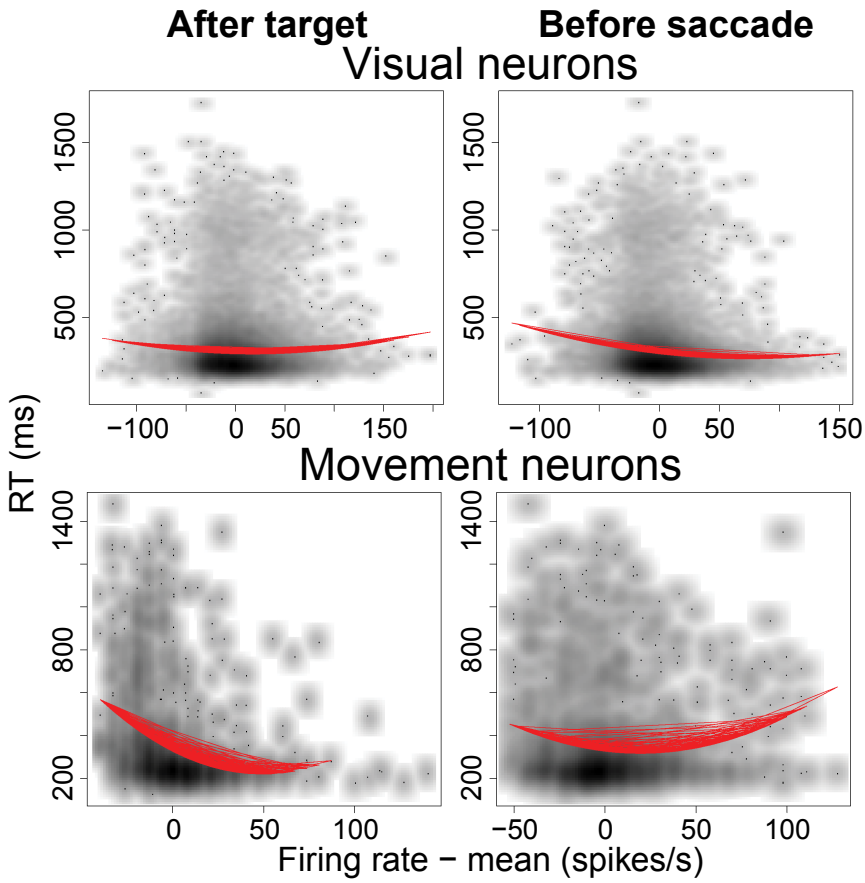

Figure 4.6: Scatterplots of RT versus deviation from mean firing rate with quadratic fits.

visuomovement neurons from 50 to 150 ms after search array onset (left panel) and from 100 ms before saccade onset to saccade onset (right panel). The bottom row shows the same scatterplots for movement neurons.

RT was fastest when visually-responsive neurons fired closest to their mean after target presentation and movement neurons fired closest to their mean before saccade onset. This suggests that the population of neurons selecting the search target and the population of neurons preparing the saccade each reached an optimal firing rate for the monkey to have its fastest RT. This suggests that neurons downstream of FEF movement neurons (e.g., in the superior colliculus) may not reach their threshold

fastest when receiving the most input from FEF quickly. Rather, an optimal network state may be required to activate burst neurons in the superior colliculus, consisting of balanced input from FEF movement neurons, and neurons in other areas, including within superior colliculus. On the other hand, the quadratic fits in Figure 4.6 were to over 30000 data points, so this conclusion must be taken with a degree of skepticism.

CHAPTER V

BIOPHYSICAL SUPPORT FOR FUNCTIONALLY DISTINCT CELL TYPES IN THE FRONTAL EYE FIELD

5.1 Abstract

Numerous studies have described different functional cell types in the frontal eye field (FEF), but the reliability of the distinction between these types has been uncertain. Studies in other brain areas have described specific differences in the width of action potentials recorded from different cell types. To substantiate the functionally defined cell types encountered in FEF, we measured the width of spikes of visual, movement, and visuomovement types of FEF neurons in macaque monkeys. We show that visuomovement neurons had the thinnest spikes, consistent with a role in local processing. Movement neurons had the widest spikes, consistent with their role in sending eye movement commands to subcortical structures such as the superior colliculus. Visual neurons had wider spikes than visuomovement neurons, consistent with their role in receiving projections from occipital and parietal cortex. These results show how structure and function of FEF can be linked to guide inferences about neuronal architecture.[1]

[1]This chapter was published as Cohen JY, Pouget P, Heitz RP, Woodman GF, Schall JD. Biophysical support for functionally distinct cell types in the frontal eye field. *J Neurophysiol* 101: 912-916, 2009.

5.2 Introduction

This paper concerns the general problem of how the primate brain transforms visual input into eye-movement output. Several cortical areas and subcortical regions contribute to this visual-motor mapping. One such area, the frontal eye field (FEF), contains at least three main functional types of neurons: visual, movement, and visuomovement neurons (Bruce and Goldberg, 1985; DiCarlo and Maunsell, 2005; Goldberg and Bushnell, 1981; Hanes et al., 1998; Kodaka et al., 1997; Schall, 1991; Segraves, 1992; Segraves and Goldberg, 1987; Umeno and Goldberg, 1997). In FEF, a population of visual and visuomovement neurons selects the target of search by increasing their firing rate in response to the presence of the target in their receptive fields (RFs) relative to when a distractor is situated in their RFs (e.g., Schall and Hanes, 1993; Thompson et al., 1996). A different population of neurons, called movement neurons, increases their firing rate leading up to saccades into their movement fields (MFs) (e.g., Hanes and Schall, 1996). Visuomovement neurons also increase their firing rate leading up to saccades. Despite these differences, distinctions between these cell types have relied largely on firing-rate patterns as opposed to inherent biophysical properties of the neurons being studied. Moreover, disagreements persist about the reliability of the distinction between cell types.

Understanding how visuomotor transformations occur requires knowledge of the underlying circuitry, which is composed of different types of neurons. Cortical neurons have been distinguished by morphology (Kawaguchi, 1995; Krimer et al., 2005), neurotransmitter (Connors and Gutnick, 1990), laminar distribution (Bullier and Henry,

1979; Condé et al., 1994; Dow, 1974), molecular composition (Cauli et al., 1997; Martina et al., 1998), functional property (González-Burgos et al., 2005), and developmental origin Letinic et al. (2002). Differences between neuron types have typically been distinguished in vitro or intracellularly. Several studies, however, have distinguished types of neurons by the shape of extracellularly recorded action potentials (Barthó et al., 2004; Chen et al., 2008; Constantinidis and Goldman-Rakic, 2002; Csicsvari et al., 1999; Henze et al., 2000; Mountcastle et al., 1969). For example, extracellular recordings of neurons in extrastriate visual cortex (V4) have shown that neurons with thin spikes (putative interneurons) showed stronger attentional modulation than neurons with wider spikes (Mitchell et al., 2007).

To determine whether functional cell types in FEF exhibit biophysical differences, we measured spike waveforms of functional cell types distinguished by their responses following visual stimuli or before saccades. The results are consistent with the hypothesis that different functional cell types correspond to different anatomical cell types.

5.3 Methods

5.3.1 Behavioral task and recording

All experimental procedures were performed in accordance with the National Institutes of Health Guide for the Care and Use of Laboratory Animals and approved by the Vanderbilt Institutional Animal Care and Use Committee. Activity of FEF neurons was recorded in four male macaques (*Macaca radiata*) performing three dif-

ferent tasks that have been described in detail previously. Monkey Q performed visual search for a singleton target defined by color (Cohen et al., 2007; Sato et al., 2001). Monkeys Q and S performed visual search for a target (**T** or **L**) among distractors (**L**s or **T**s, respectively) (Woodman et al., 2007). Monkeys M and U performed a saccade stop signal (countermanding) task (Hanes et al., 1998). All monkeys were trained on a memory-guided saccade task. Activity from each neuron was recorded during this task to distinguish visualfrom movement-related activity (Bruce and Goldberg, 1985; Hikosaka and Wurtz, 1983).

Our data set consists of 12 neurons from monkey Q during the color singleton visual search task, 48 neurons from monkey Q during the form visual search task, 20 neurons from monkey S during the form visual search task, 9 neurons from monkey M during the countermanding task, and 5 neurons from monkey U during the countermanding task, for a total of 94 neurons. Spikes were sorted on-line and off-line using principal components analysis (Plexon). A neuron was only considered for analysis if its spike waveforms were clearly discriminable and its activity was clearly visual related, movement related, or visual and movement related.

5.3.2 Data analysis

To measure the firing rate of each neuron, we used a spike density function, convolving each spike with a kernel resembling a postsynaptic potential (Thompson et al., 1996). We used the memory-guided saccade task to classify neurons. Visual neurons had significantly greater activity in the 100 ms after the target flash than in the 100 ms before the target flash. Movement neurons had greater responses in the 100 ms lead-

ing up to the saccade than in the 100 ms before the target flash. Visuomovement neurons had greater responses in the 100 ms after the target flash and in the 100 ms leading up to the saccade than in the 100 ms before the target flash.

Because spike amplitude, but not width, is dependent on the distance from electrode tip (Henze et al., 2000), we used spike width as a measure of action potential shape. We applied a smoothing spline to each mean spike waveform. Spike width was computed as the time from trough to peak (Mitchell et al., 2007) (see Fig. 5.2*A*). This measure resulted in smaller spike width values than those reported in other studies (e.g., Constantinidis and Goldman-Rakic, 2002), which measured spike width as the time from first to second trough. Spike waveforms were sampled at 40 kHz for 800 μs.

In addition to classifying neurons based on their activity during the memory-guided saccade task, we computed a visuomovement index for each neuron based on activity during the search or countermanding task in the RF location that elicited the largest response during the memory-guided task. The index was computed as

$$\frac{V - B}{M - B},$$

where V is the neuron's average visual-related firing rate from 50 to 150 ms after target onset, M is its average movement-related firing rate from 100 ms before saccades to the time of saccades and B is its average baseline firing rate 100 ms before target onset. We did not use spike density functions to compute visuomovement indices.

We measured spiking variability using the coefficient of variation (CV) (Softky and Koch, 1993) in bins of 100 interspike intervals. The CV is defined as the ratio of

the SD to the mean of the interspike intervals.

To measure differences between groups of neurons, we used Wilcoxon rank-sum tests with Bonferroni corrections for multiple comparisons. All analyses were performed in R (`http://www.r-project.org/`).

5.4 Results

We analyzed the activity of 94 FEF neurons from four monkeys during memory-guided visual search and countermanding tasks. We classified neurons as visual, movement or visuomovement and compared spike widths across functionally defined neuron types.

5.4.1 Types of FEF neurons

To classify neurons, we measured responses during the memory-guided saccade task. We classified 33 neurons as visual, 28 as movement, and 33 as visuomovement. The fraction of visuomovement neurons is lower than reported in previous studies (Bruce and Goldberg, 1985; Schall, 1991). Figure 5.1 shows average firing rates for a representative neuron of each type during the memory-guided task. Figure 5.1*A*, left, shows the firing rate of a visual neuron aligned to target onset. The neuron had its largest response following the target flash in its RF (cumulative distribution of saccade times shown as dashed gray curve). Figure 5.1*A*, right, shows the firing rate of the same neuron aligned to the time of saccade (dashed line). The neuron did not fire above baseline prior to saccades. Figure 5.1*B* shows the response of a movement neuron. This neuron increased its firing rate leading up to saccades (right). It did

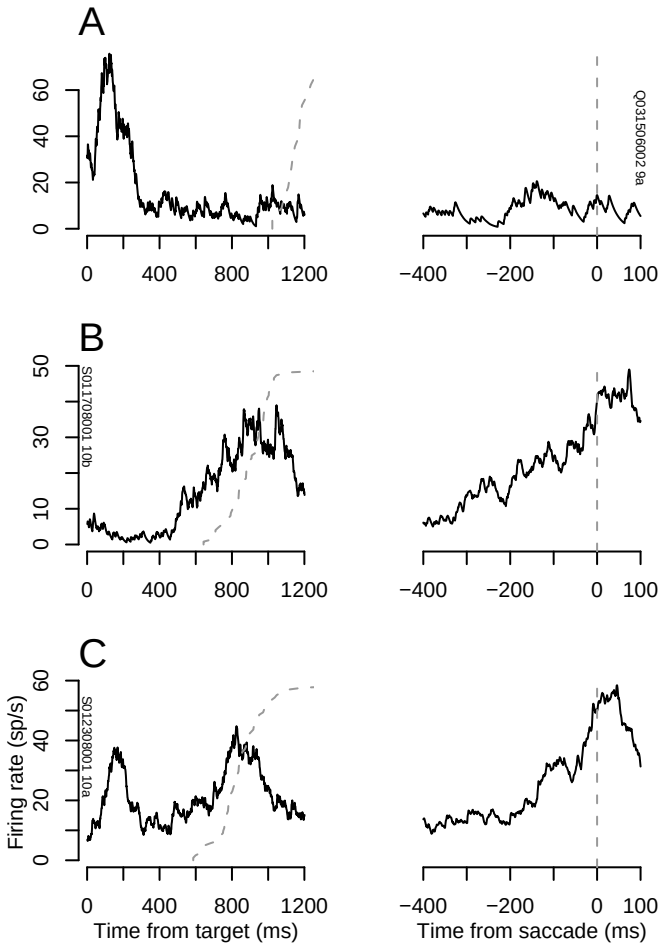

Figure 5.1: Representative visual (***A***), movement (***B***), and visuomovement (***C***) neurons. Left: average firing rate during the memory-guided saccade task aligned to the time of presentation of the target inside the neuron's receptive field. Dashed gray line plots the distribution of response times. Right: average firing rate aligned on the time of saccade initiation (dashed gray line).

not fire above baseline in response to the target flash (left). Figure 5.1*C* shows the response of a visuomovement neuron. This neuron responded to the visual stimulus and before saccades. We found no difference in spike amplitude or firing rate between types of neurons.

5.4.2 Spike widths

After categorizing neurons, we measured the width of the mean spike waveform for each neuron from trough to peak (Fig. 5.2). Figure 5.2*A* shows an example mean spike waveform from a visuomovement neuron and demonstrates our method for computing spike width. This neuron had a mean spike width of 250 μs. Figure 5.2*B* shows all the normalized mean spike waveforms for visual neurons (black), movement neurons (red) and visuomovement neurons (blue) fitted with smoothing splines. Each mean spike waveform was normalized by dividing its values by the difference of its maximum and minimum values. Figure 5.2*C* shows histograms of spike widths of all neurons of each type, and Fig. 5.2*D* shows the cumulative distributions of spike widths for each type of neuron. The mean spike widths ($\pm$ SE) were $329 \pm 20.5\,\mu$s for visual neurons (V), $352 \pm 19.5\,\mu$s for movement neurons (M), and $218 \pm 16.4\,\mu$s for visuomovement neurons (VM).

A Kruskal-Wallis rank sum test revealed a significant effect of neuron type ($\chi^2 = 28.1$, $p < 0.001$). Spike widths were significantly larger for movement neurons than for visuomovement neurons (Wilcoxon rank sum test with Bonferroni correction for multiple comparisons, $p < 0.001$) and larger for visual neurons than for visuomovement neurons ($p < 0.005$). There was no significant difference between visual and movement neuron spike widths ($p > 0.3$).

To verify that the demands of the task did not affect the shape of a neuron's spike, we compared the spike widths during the intertrial intervals and during the period from target onset to saccade onset. All neurons showed no difference in spike width

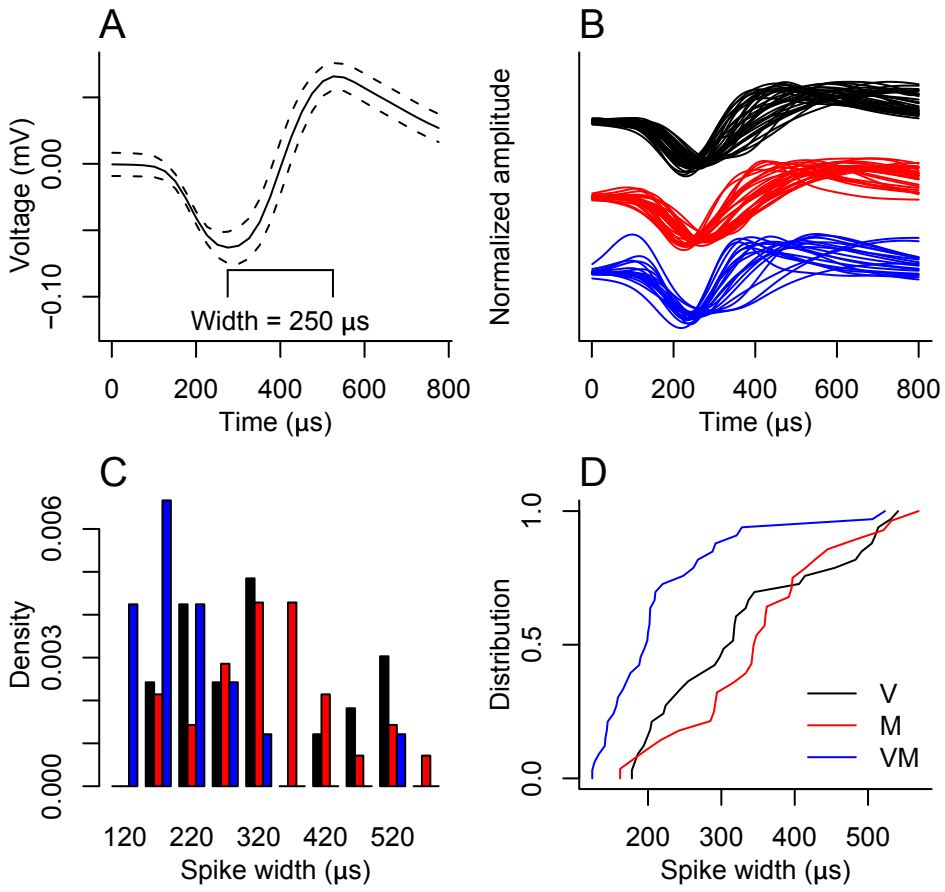

Figure 5.2: *Spike width by neuron type.* ***A***: mean (—) and mean ± SD (- - -) spike waveforms from a representative visuomovement neuron. ***B***: all mean, normalized spike waveforms for visual (V, black), movement (M, red) and visuomovement (VM, blue) neurons. ***C***: histogram of spike widths for each type of neuron. ***D***: cumulative distribution of spike widths for each type of neuron.

between task performance and baseline activity ($p > 0.9$).

We computed a visuomovement index for each neuron defined as the ratio of the difference between visual activity and baseline activity and movement activity and baseline activity during the search or countermanding task. Classifying neurons using the visuomovement index reproduced classification using the activity during the memory-guided task. Figure 5.3*A* shows boxplots of visuomovement indices grouped by neuron type as defined in the memory-guided task. Visuomovement indices were significantly different between visual and movement neurons (Wilcoxon rank sum test with Bonferroni correction for multiple comparisons, $p < 0.001$), between visual and visuomovement neurons ($p < 0.001$) and between movement and visuomovement neurons ($p < 0.001$). To obtain an independent classification of neurons, we divided the distribution of visuomovement indices into three groups. Figure 5.3*B* shows this division and the classification of neurons into visual (V), movement (M), and visuomovement (VM) categories. Two visuomovement neurons were classified differently using the visuomovement index, one as a visual neuron and one as a movement neuron. These are shown as gray points in Fig. 5.3*B*. Using this classification, spike widths were significantly larger for visual than visuomovement neurons ($p < 0.001$) and for movement than visuomovement neurons ($p < 0.001$). There was no significant difference in spike width between visual and movement neurons ($p > 0.7$).

Neuron classification using the visuomovement index was robust within a small range of boundaries between classes of neurons. Figure 5.3, *C* and *D*, show the number of misclassified neurons as a function of the boundary between movement and visuomovement neurons and visuomovement and visual neurons for each type of

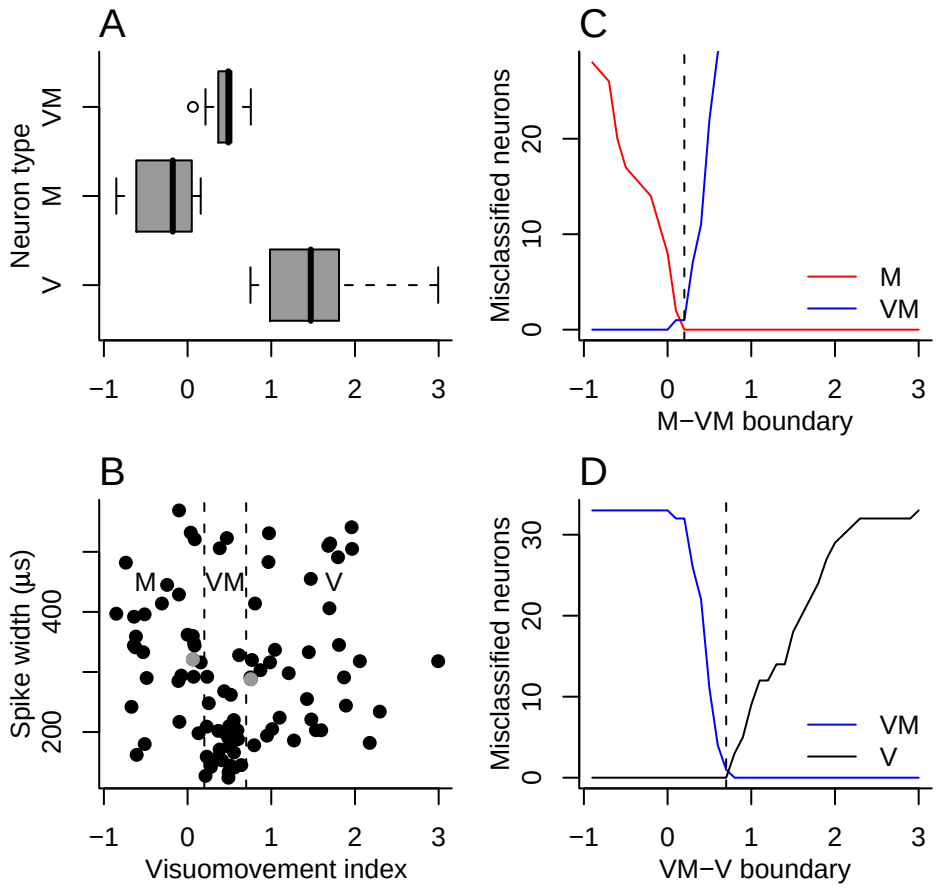

Figure 5.3: *Visuomovement index.* ***A***: boxplot of visuomovement indices derived from activity during the memory-guided saccade task. ***B***: scatter plot of spike width vs. visuomovement index. Neurons were classified into movement (M), visuomovement (VM), and visual (V) groups separated by dashed black lines, and 2 neurons that were classified as visuomovement during the memory-guided task were classified differently using the index; these are shown in gray. ***C***: number of misclassified M and VM neurons as a function of the boundary between M and VM in ***B***. The value minimizing the number of misclassified neurons was 0.2, indicated by the dashed vertical line. ***D***: number of misclassified VM and V neurons as a function of the boundary between VM and V in ***B***. The value minimizing the number of misclassified neurons was 0.7, indicated by the dashed vertical line.

neuron. The boundaries shown in Fig. 5.3*B* (0.2 and 0.7) correspond to the minimum number of misclassified neurons (the 2 visuomovement neurons shown in gray in Fig. 5.3*B*). These boundaries are indicated by dashed vertical lines in Fig. 5.3, *C* and *D*.

5.4.3 Spiking variability

To obtain another measure useful for distinguishing neuron types, we measured the coefficient of variation of spiking (CV) in bins of 100 interspike intervals. Figure 5.4 shows cumulative distributions of CV for the three classes of neurons. CV was significantly larger for visuomovement neurons than for visual neurons (Wilcoxon rank sum test, $p < 0.001$) and for movement neurons ($p < 0.001$). CV was not significantly different between visual and movement neurons (Wilcoxon rank sum test, $p > 0.5$).

5.5 Discussion

We have shown that three functional types of FEF neurons have different spike waveforms. This suggests that distinct types of neurons defined functionally may constitute different types of neurons defined morphologically. It is tempting to classify visuomovement neurons, those neurons with the thinnest spikes, as local inhibitory interneurons. We cannot, however, say that all neurons with short spike durations are inhibitory. Some studies suggest only particular subclasses of GABAergic neurons display short spike durations (McCormick et al., 1985; Naegele and Katz, 1990). Some or all may be small neurons with local excitatory connections (Gur et al., 1999). Likewise, we cannot say that all visual and movement neurons are pyramidal neurons

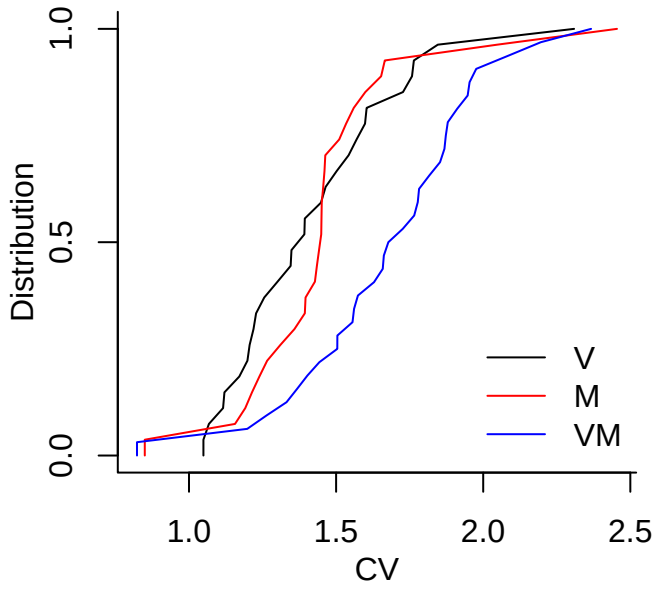

Figure 5.4: Cumulative distributions of CV in bins of 100 ISIs for visual (V), movement (M), and visuomovement (VM) neurons.

because they have wider spikes than visuomovement neurons although data from anatomical and physiological studies are in agreement with such a claim (Fries, 1984; Segraves and Goldberg, 1987; Sommer and Wurtz, 1998, 2001).

Are there really three categories of neurons in FEF? Although there appears to be a continuum of responses from visual related to movement related (see Fig. 5.3), our results reveal a significant difference in spike width related to functional neuron classification. This is important for exposing the possibility that visuomovement neurons may constitute a different morphological type of neuron than visual or movement neurons. While further research is needed to verify or refute this hypothesis, the current results add to a growing literature providing evidence for the heterogeneity of neurons in FEF. The ability to distinguish types of neurons in FEF is necessary

to understand whether the visual to motor transformation occurs within or across distinct neuron types.

CHAPTER VI

ON THE ORIGIN OF EVENT-RELATED POTENTIALS INDEXING COVERT ATTENTIONAL SELECTION DURING VISUAL SEARCH

6.1 Abstract

Despite nearly a century of electrophysiological studies recording extracranially from humans and intracranially from monkeys, the neural generators of nearly all human event-related potentials (ERPs) have not been definitively localized. We recorded an attention-related ERP component, known as the N2pc, simultaneously with intracranial spikes and local field potentials (LFPs) in macaques to test the hypothesis that an attentional-control structure, the frontal eye field (FEF), contributed to the generation of the macaque homologue of the N2pc (m-N2pc). While macaques performed a difficult visual search task, the search target was selected earliest by spikes from single FEF neurons, later by FEF LFPs, and latest by the m-N2pc. This neurochronometric comparison provides an empirical bridge connecting macaque and human experiments and a step toward localizing the neural generator of this important attention-related ERP component.[1]

[1]This chapter was published as Cohen JY, Heitz RP, Schall JD, Woodman GF. On the origin of event-related potentials indexing covert attentional selection during visual search. *J Neurophysiol* 102: 2375-2386, 2009.

6.2 Introduction

The electroencephalogram (EEG) has long been used as an electrophysiological measure of human brain activity (Berger, 1929). Time-averaged event-related potentials (ERPs) derived from the EEG map onto diverse perceptual and cognitive states and processes (Rugg and Coles, 1995). However, definitively identifying the neural generators of ERP components measuring specific cognitive operations has been intractable because the number of source configurations that can produce a given EEG voltage distribution on the scalp is infinite (Hillyard and Anllo-Vento, 1998; Luck, 2006; Nunez and Srinivasan, 2006). Helmholtz (1853) proved that when the number of electrical generators is unknown, an infinite number of inverse solutions can account for any pattern of voltages across a sphere (like the head). Since the dawn of human electrophysiology, investigators have sought solutions to this inverse problem (Adrian and Matthews, 1934; Walter, 1938). Modern approaches infer the neural generators of human ERP components using source estimation algorithms (Nunez and Srinivasan, 2006) or additional information from brain imaging (e.g., Heinze et al., 1994). However, this basic problem will remain underdetermined without constraints from intracranial recordings.

Intracranial recordings from epilepsy patients have provided useful information (Lachaux et al., 2003; Michel et al., 2004), but clinical and ethical constraints limit the general utility of this approach. Intracranial recordings can be carried out systematically and thoroughly in nonhuman primates. However, this is predicated on the homology of specific ERP components in humans and nonhuman primates. Several

studies have identified ERP components in monkeys that are homologous to those in humans (Arthur and Starr, 1984; Glover et al., 1991; Javitt et al., 1992; Lamme et al., 1992; Mehta et al., 2000a,b; Paller et al., 1992; Schroeder et al., 1991, 1992). Recently, we described a macaque homologue of the N2pc (an abbreviation of N2-posterior-contralateral, hereafter referred to as *m-N2pc*) (Woodman et al., 2007), an ERP component that measures the allocation of covert visual attention (Luck and Hillyard, 1994a,b). We determined that the m-N2pc is maximal over extrastriate visual cortex and that the time and magnitude of the m-N2pc vary with visual search array set size. These properties parallel observations in humans.

The N2pc has been critical in distinguishing between models of attentional deployment during visual search because it provides a millisecond-by-millisecond measure of the focusing of attention in the left or right visual field (Woodman and Luck, 1999, 2003b). The N2pc indexes a covert visual attention mechanism that is sensitive to the degree of distractor suppression required during visual search (Luck and Hillyard, 1994a,b; Luck et al., 1997) and a perceptual selection mechanism that operates independent of later stages of processing (Woodman and Luck, 2003a). When the N2pc was discovered, it was hypothesized to result from feedback from an attentional-control structure because this index of covert attention occurred after the earliest evidence for attentional selection found using spatial cuing paradigms (Heinze et al., 1994; Hopf et al., 2004; Luck and Hillyard, 1994a). By establishing the homology between the N2pc in human and monkey, we can now test hypotheses about the origin of the N2pc.

To understand the dynamics of this component, we collected three measures of

neural activity while macaque monkeys performed a difficult visual search task. We recorded intracranially from microelectrodes in the frontal eye field (FEF), an area in prefrontal cortex involved in covert visual selection hypothesized to represent a saliency map used to guide attention (Cohen et al., 2009a; Sato and Schall, 2003; Sato et al., 2001; Schall, 2004b; Schall and Hanes, 1993; Thompson and Bichot, 2005; Thompson et al., 1997, 2005b). The first neural measure was from the spike times of single neurons in FEF that discriminate between target and distractors during visual search. The second measure was from local field potentials (LFPs) recorded simultaneously with the single neurons that exhibit polarization differences for the target compared with distractors (Monosov et al., 2008). The LFP is believed to be a weighted average of dendrosomatic activity of about 10^5 neurons in approximately $1\,\mathrm{mm}^2$ of cerebral cortex (Braitenberg and Schüz, 1991; Katzner et al., 2009; Logothetis and Wandell, 2004; Rockel et al., 1980). The third measure was the m-N2pc component, which is maximal over extrastriate visual cortex. ERP components have been estimated to arise from a weighted average of the LFPs summating from the synchronous activity of around 10^7 neurons in about $6\,\mathrm{cm}^2$ of cortex (Cooper et al., 1965; Ebersole, 1997; Nunez and Srinivasan, 2006). These electrophysiological signals provide millisecond resolution of attention-related activity at multiple spatial scales.

By measuring these three signals we addressed a simple question: when the brain selects a target on which to allocate attention, does it happen all at once or through some sequence of processes at different scales in different places? The answer provides insight into the origin of the m-N2pc. If, under the conditions tested, the m-N2pc is driven by feedback from the selection process in FEF, then we should find that 1)

target selection in FEF precedes the m-N2pc and 2) the amplitude of FEF activity correlates with the amplitude of the m-N2pc trial by trial.

6.3 Methods

6.3.1 Behavioral task and recording

We recorded spikes from FEF neurons and LFPs from the same microelectrodes in both hemispheres of two male macaque monkeys (*Macaca radiata*, identified as Q and S). Simultaneously, we recorded ERPs from skull electrodes located at approximately OL/OR and T5/T6 in the human 1020 system scaled to the macaque skull. In monkey S, we also recorded from anterior and middle electrodes corresponding to F3/F4 and C1/C2 in the human 1020 system. The monkeys performed a memory-guided saccade task and a visual search task. In the search task, monkeys searched for a target (**T** or **L** in one of four orientations) among distractors (**L** or **T**). Distractors could be homogeneous (oriented uniformly) or heterogeneous (oriented randomly). Each trial began with the monkey fixating a central spot for about 600 ms. A target was then presented at one of eight isoeccentric locations equally spaced around the fixation spot (Fig. 6.1*A*). The other seven locations contained one, three, or seven distractor stimuli (set sizes 2, 4, and 8). The monkey was given a liquid reward for making a single saccade to the target location and fixating it for 1000 ms. This single-saccadic-response criterion was used to ensure that the animals would process the search array prior to their response, enabling us to observe the deployment of covert attention to the target. Within sessions, trials with different set sizes were randomly interleaved.

Across sessions the monkeys alternated between searching for **T**s with **L**s as distractors or **L**s with **T**s as distractors.

Activity from each neuron was recorded during a memory-guided saccade task to distinguish visual- from movement-related activity (Bruce and Goldberg, 1985; Hikosaka and Wurtz, 1983). The target was flashed alone for 80 ms. Monkeys were required to maintain fixation for 400-1000 ms after the target onset. When the fixation spot disappeared, the monkey was rewarded for a saccade to the remembered location of the target.

Our data set consisted of 57 neurons from monkey Q and 23 neurons from monkey S, with simultaneously recorded LFPs and ERPs. Spikes were sorted on-line and off-line using principal-components analysis and template matching (Plexon). FEF LFPs were recorded from the same electrodes (2- to 5-MΩ impedance) as the single neurons, sampled at 1 kHz, and filtered at 0.7170 Hz, using Plexon head-stage HST/8 050-G20 with an input impedance of 38 MΩ. EEG signals were sampled at 1 kHz and filtered between 0.7 and 170 Hz. A guide tube used with the microelectrodes, in contact with the surface of the dura, was used as reference for the LFP signal. The frontal EEG electrode (approximating human Fz) was used as reference for the EEG signal (Woodman et al., 2007).

Monkeys were surgically implanted with a head post, a subconjunctival scleral eye coil, EEG electrodes, and recording chambers under aseptic conditions with isoflurane anesthesia. Antibiotics and analgesics were administered postoperatively. All surgical and experimental procedures were in accordance with the Guide for the Care and Use of Laboratory Animals and approved by the Vanderbilt Institutional Animal Care and

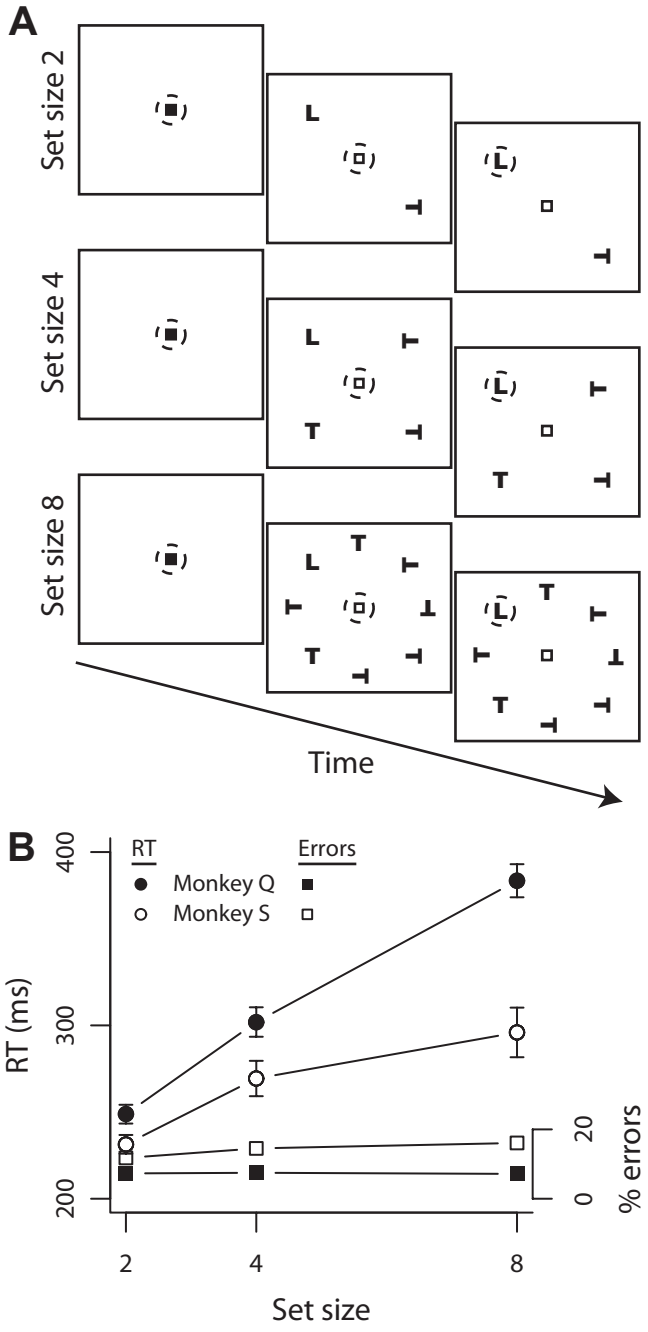

Figure 6.1: *Visual search task.* ***A***: monkeys made saccades to a target (here, an upright **L**; not to scale) presented with 1, 3, or 7 distractors. The monkey's eye position is represented by the dashed circle, which is invisible to the monkey. ***B***: saccade response time (circles) and percentage error (squares) vs. set size for each monkey. Error bars represent SE around the mean of the session means. Filled symbols: monkey Q; open symbols: monkey S. Error bars for percentage error are smaller than plotted points.

Use Committee.

6.3.2 Data analysis

To measure the firing rate of each neuron, we used a spike density function, convolving each spike with a kernel resembling a postsynaptic potential (Thompson et al., 1996). We used a memory-guided saccade task to classify neurons (Cohen et al., 2009b). Visual neurons had significantly greater activity in the 100 ms after the target flash than in the 100 ms before the target flash. Movement neurons had greater responses in the 100 ms leading up to the saccade than in the 100 ms before the target flash. Visuomovement neurons had greater responses in the 100 ms after the target flash and in the 100 ms leading up to the saccade than in the 100 ms before the target flash. Neurons analyzed in this study exhibited tonic visual and visuomovement activity with firing rates above baseline during the memory delay in the memory-guided task.

To measure the time of target selection, we used millisecond-by-millisecond Wilcoxon rank-sum tests. Selection time is defined as the time at which the distribution of activity when the search target was inside a neuron's receptive field (RF) was significantly greater than the distribution of activity when the target was opposite the RF for 10 consecutive milliseconds with $p < 0.01$. This "neuronantineuron" approach (Britten et al., 1992; Thompson et al., 1996) presumes that a population of neurons in the brain representing the location of the target competes with a population of neurons representing the location of distractors opposite the target. No difference in target selection time was seen between visual neurons and visuomovement neurons.

We measured target selection time in LFPs and ERPs similarly. The beginning of the m-N2pc is simply the target selection time in ERPs as defined earlier. Because ERPs do not have RFs per se, we did two kinds of comparisons. The first comparison was based on the RF of the neuron recorded simultaneously with the ERP; we measured the difference between the ERPs on trials when the search array target was inside the single neuron's RF and the ERPs on trials when the target fell at the location(s) opposite the neuron's RF. The second comparison was the more typical approach used in ERP research: we measured the difference between the ERPs on trials when the target was in the hemifield contralateral to the EEG electrode and the ERPs on trials when the target was in the hemifield ipsilateral to the EEG electrode. Of the 80 recording sessions, each neuron selected the target of search, 56 LFPs selected the target, and 77 ERPs selected the target. Thus for the paired comparisons of simultaneously recorded neurons and LFPs (and LFPs and ERPs) the sample size was 56.

We also measured the trial-by-trial correlation in the amplitude of modulation of spike rate, LFP polarization, and ERP polarization in the 56 spikeLFPERP triplets in which all three signals selected the target. We computed a Pearson correlation coefficient for each simultaneously recorded spikesERP (and spikesLFP) pair using the trial-by-trial spike rate and integral of ERP (or LFP) amplitude in a window from 150 ms after the search array appeared until saccade initiation (to exclude the initial nonselective visual response), divided by the length of the time window. Similarly, we computed the correlation for each LFP-ERP pair using the trial-by-trial integral of the amplitude in the same time window, divided by the length of the window.

To measure the onset time of visual activity in each signal, we compared baseline activity in the 100 ms before search array onset to each millisecond of activity after array onset. We used millisecond-by-millisecond Wilcoxon rank-sum tests to compare the two distributions. To ensure that our measurements of covert attentional selection were not an artifact of the overt response required to perform the task we also analyzed the signals truncated 20 ms prior to the saccade response. These analyses yielded the same pattern of results. Visual onset time was defined as the first time when activity after array onset exceeded baseline activity for 10 consecutive milliseconds with $p < 0.01$. All statistical tests were done with Bonferroni corrections for multiple comparisons. All analyses were done with R (`http://www.r-project.org/`) (Cohen and Cohen, 2008).

6.4 Results

6.4.1 Behavior

Two monkeys searched for a target stimulus among one, three, or seven distractor stimuli (set sizes 2, 4, and 8) composed of the same basic features in a **T**/**L** search display (Fig. 6.1*A*). Both monkeys responded to larger set sizes with longer saccade response times (Fig. 6.1*B*, Table 6.1), demonstrating the attentional demands of the task (Cohen et al., 2009a; Duncan and Humphreys, 1989; Treisman and Gelade, 1980).

	Monkey Q	Monkey S
Target selection time mean ± s.e.m. (ms)		
Neuron	163 ± 4.2	156 ± 5.7
LFP	191 ± 3.9	169 ± 7.7
ERP	213 ± 4.6	191 ± 4.5
Visual onset time mean ± s.e.m. (ms)		
Neuron	72 ± 3.0	62 ± 4.0
LFP	54 ± 2.2	59 ± 4.3
ERP	67 ± 1.8	77 ± 1.8
RT mean ± s.e.m. (ms)		
Set size 2	249 ± 5.4	231 ± 5.4
Set size 4	302 ± 8.5	269 ± 10.2
Set size 8	383 ± 9.5	296 ± 14.3
Slope of linear regression	22.1 ± 1.9	10.2 ± 2.5
Target selection time mean ± s.e.m. (ms)		
Neuron set size 2	177 ± 6.1	168 ± 8.4
Neuron set size 4	179 ± 5.7	189 ± 8.8
Neuron set size 8	194 ± 6.0	191 ± 9.2
LFP set size 2	203 ± 4.9	208 ± 14.3
LFP set size 4	221 ± 6.6	213 ± 15.7
LFP set size 8	234 ± 7.1	226 ± 16.1
ERP set size 2	206 ± 4.3	197 ± 7.1
ERP set size 4	235 ± 6.2	215 ± 8.2
ERP set size 8	266 ± 6.3	239 ± 8.6

Table 6.1: Comparisons of RT, target selection time and visual onset time. Values are means and standard errors of the mean.

6.4.2 Target selection time

We recorded spiking activity from 57 neurons in monkey Q and 23 neurons in monkey S, simultaneously with LFPs in FEF and the m-N2pc from EEG electrodes over extrastriate visual cortex. Each neuron exhibited visual responses and sustained activity during a memory-guided saccade task. We compared target selection time in each of the three measures of neural activity, defined as the time at which each signal

discriminated between the target and distractors.

Figure 6.2 shows representative simultaneous recordings of spikes and LFPs in FEF and the m-N2pc in the ERP over extrastriate visual cortex. The FEF neuron initially responded at the same rate when the target or only distractors appeared in its RF but then evolved to select the target of search by increasing discharge rate when the target was in its RF relative to when a distractor was in its RF. The concurrently recorded LFP exhibited an equivalent early polarization when the target was in the neuron's RF relative to when only distractors were in the neuron's RF followed by a greater negativity for the target relative to distractors. Likewise, the simultaneously recorded visual ERP over extrastriate visual cortex exhibited an initial period of unselective polarization in response to the search array, but eventually showed a more positive polarization when the target appeared inside the simultaneously recorded neuron's RF relative to when a distractor appeared in the neuron's RF (the m-N2pc). Thus qualitatively, each level and location of electrophysiological signal underwent the same state change from nonselective to a selective representation. However, this state change occurred at different times for each level of electrophysiological signal. A differential signal sufficient to locate the target occurred earliest in the spikes of the FEF neuron (113 ms after search array onset), later in the FEF LFP (163 ms), and latest in the visual ERP (183 ms). This was also observed in comparisons of all trials with the target contralateral compared with those with the target ipsilateral to the EEG electrode (Fig. 6.3).

Figure 6.4*A* demonstrates that this sequence of target selection was a common observation across the sample of sessions with different neurons recorded with LFPs

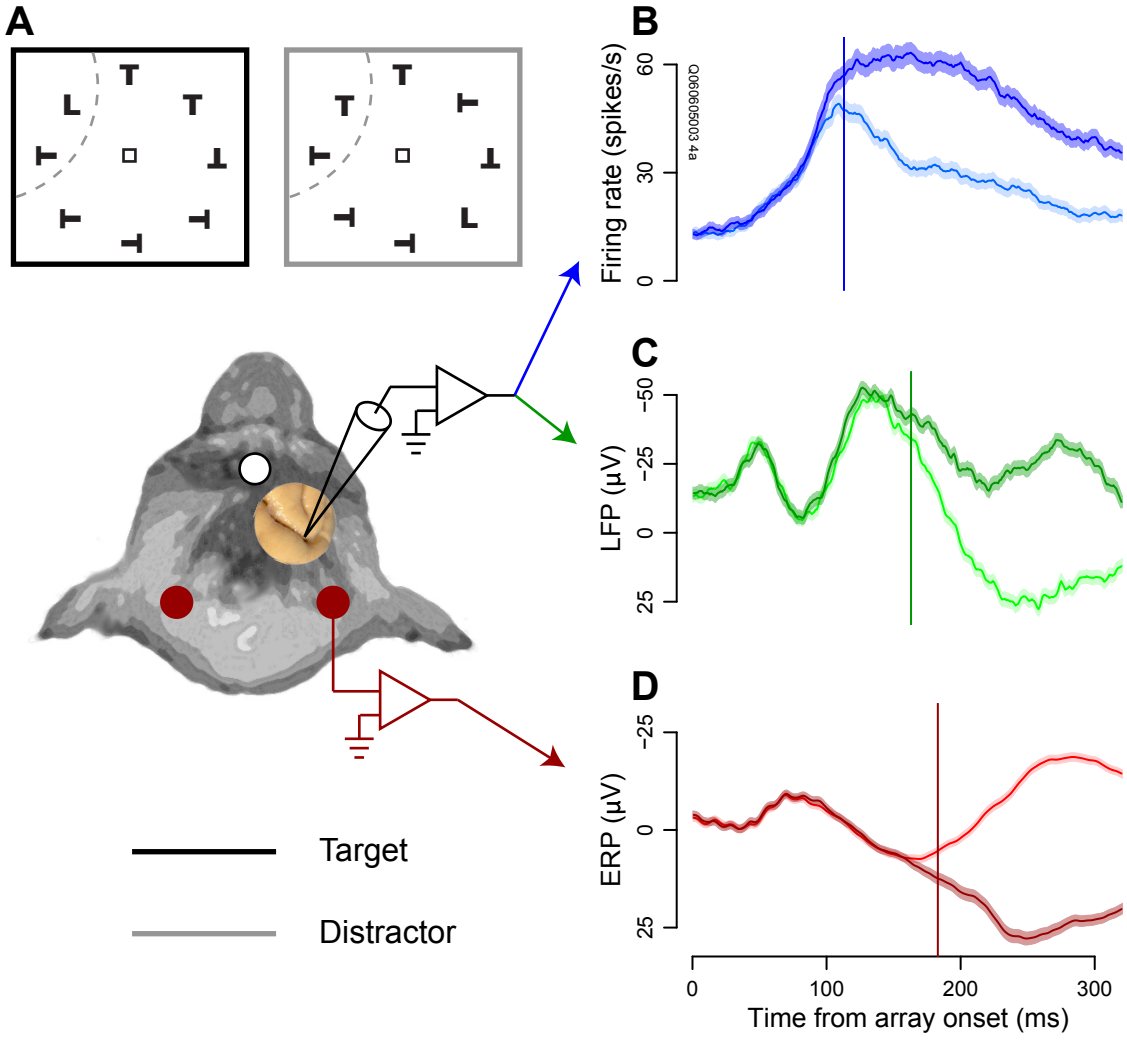

Figure 6.2: *Target selection during a representative session.* ***A***, top: visual search display (shown here with a set size of 8) with the target (**L**) inside the neuron's receptive field (indicated by the dashed arc) (left) and opposite the receptive field (right). Bottom: schematic of recording sites and signals. Single-unit discharges (blue) and local field potentials (green) were recorded intracranially from frontal eye field (FEF). Event-related potentials (ERPs) were recorded from electrodes over extrastriate visual cortex (red). ***B***: average activity of one neuron when the search target was inside (dark) and opposite (light) its receptive field. Bands around average firing rates show time-varying SE. Vertical line indicates target selection time when the 2 curves became statistically significantly different. ***C***: FEF local field potential (LFP) with the target inside (dark) and opposite (light) the simultaneously recorded neuron's receptive field (RF). ***D***: ERP over extrastriate visual cortex from trials with the target inside (dark) and opposite (light) the receptive field of the concomitantly recorded FEF neuron. This component is the macaque homologue of the human N2pc (m-N2pc).

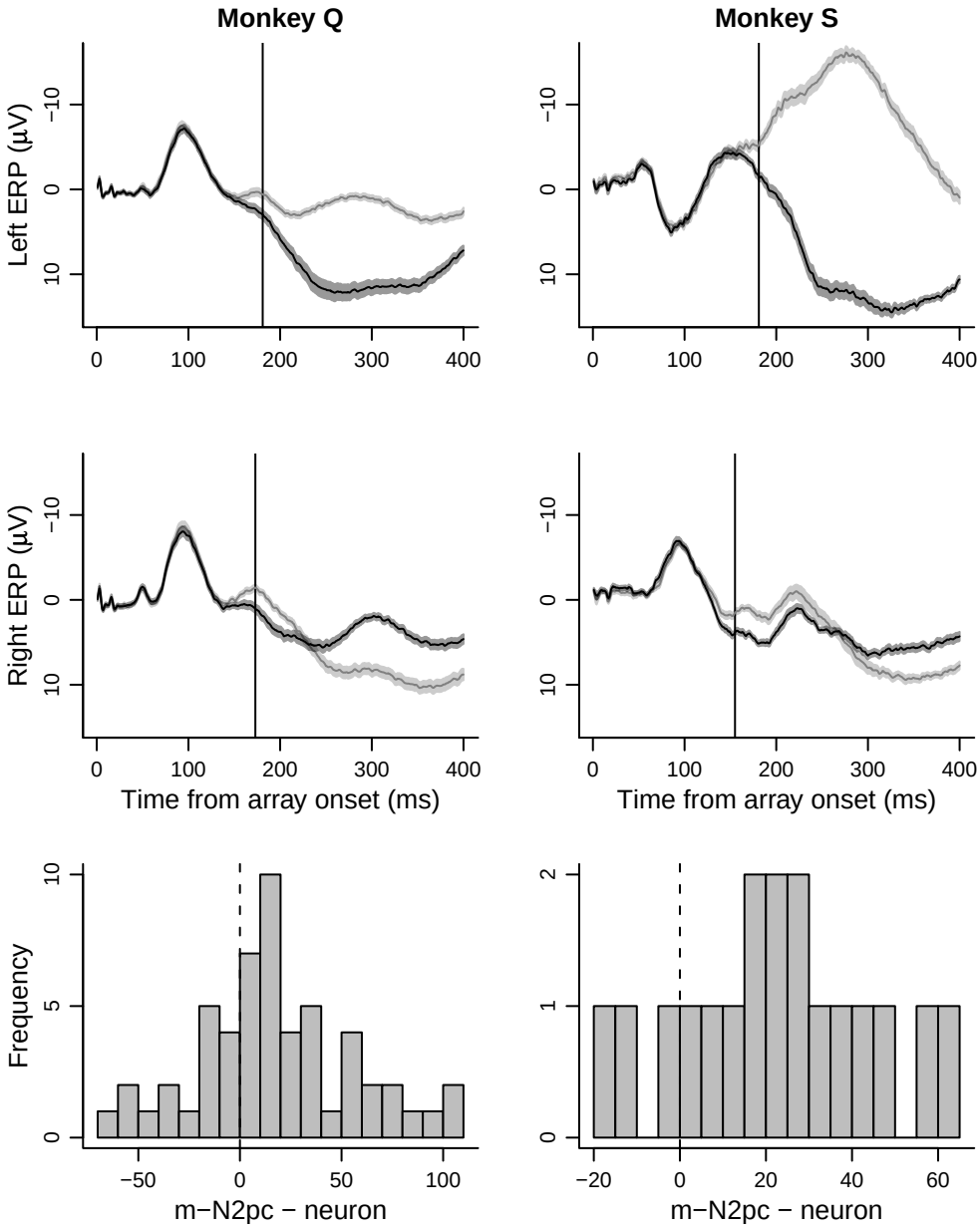

Figure 6.3: Average left (*1st row*) and right (*2nd row*) hemisphere ERPs with the search target in the hemifield contralateral (dark curves) and ipsilateral (light curves) to the recording site. Bands around activity curves indicate SE. Solid vertical lines indicate onset of the m-N2pc. The bottom row shows histograms of m-N2pc minus single-neuron selection times for each monkey, in which m-N2pc was computed using contralateral vs. ipsilateral target responses. Despite the increased number of trials associated with the m-N2pc, single-neuron spikes selected targets earlier than the hemisphere-based m-N2pc (Wilcoxon signed-rank test, $p < 0.001$ for each monkey). Dashed vertical lines indicate zero difference between m-N2pc and neuron.

at different sites in FEF and with the same posterior EEG electrodes. Overall, the target was selected significantly earlier by FEF single-neuron spikes (mean ± SE, 161±3.4 ms) than by FEF LFPs (184±3.7 ms) (Wilcoxon signed-rank test, $p < 0.001$), as observed previously (Monosov et al., 2008). Moreover, single neurons in FEF selected the target before the m-N2pc (207 ± 3.7 ms) ($p < 0.001$). Likewise, the target was selected significantly earlier by FEF LFPs than by the ERPs, as reflected by the m-N2pc ($p < 0.001$; Table 6.1). This sequence of target selection timing was highly reliable within recording sessions for both monkeys (Figs. 6.4 and 6.5; Table 6.1). The average difference between FEF single-neuron selection time and LFP selection time was 31 ± 5.4 ms for monkey Q and 13 ± 5.9 ms for monkey S. The average difference between LFP selection time and the m-N2pc was 18 ± 4.3 ms for monkey Q and 22 ± 8.6 ms for monkey S, and the average difference between neuron selection time and the m-N2pc was 49 ± 5.6 ms for monkey Q and 37 ± 6.3 ms for monkey S.

To ensure that the delay of LFP and ERP signals relative to the spike rate modulation was not an artifact of the recording procedures, we measured the latency of the earliest visual response in each neural signal. The earliest visual response was observed in FEF LFPs (Table 6.1), in agreement with a recent study of the relationship between visually responsive neurons and concurrently recorded LFPs (Monosov et al., 2008). The latencies of the initial nonselective visual ERP component were similar to those observed in extrastriate areas such as V4 (Schmolesky et al., 1998). Across monkeys, the onset of the earliest visual response was 57 ms for the FEF LFPs, 67 ms for FEF neurons, and 72 ms for the posterior visual ERPs. Thus the differences we

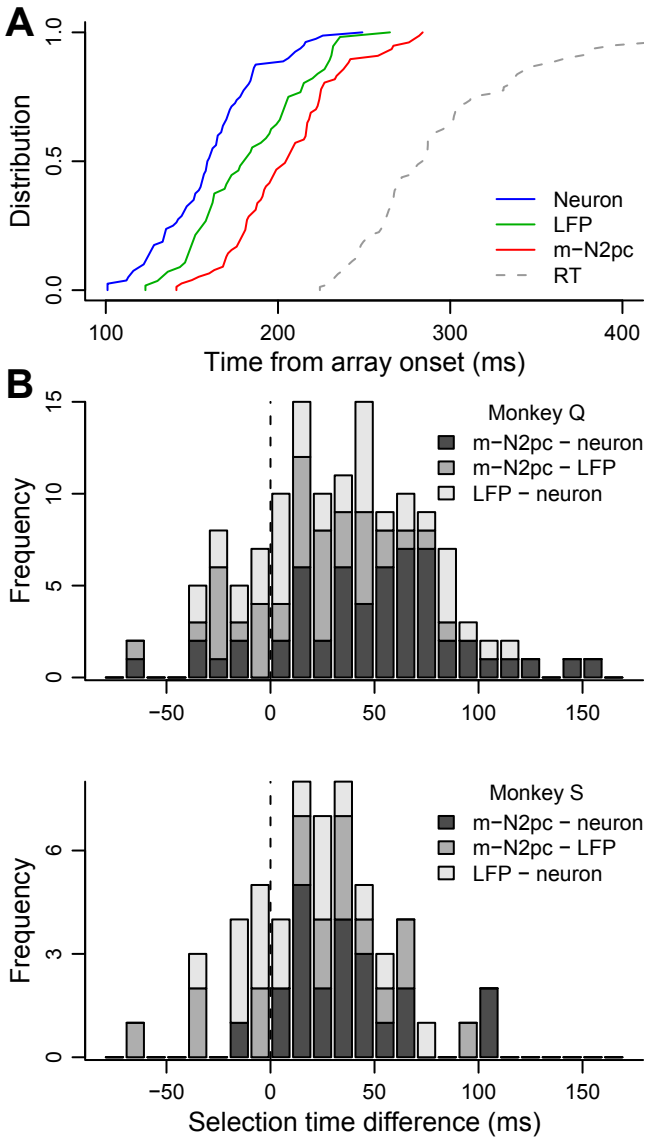

Figure 6.4: *Target selection time differences.* ***A***: cumulative distributions of target selection times measured from simultaneously recorded intracranial FEF neuron spike times (blue) and FEF LFPs (green) with extracranial m-N2pc (red). These events precede the saccade response times (RTs, dashed gray curve). ***B***: stacked histograms showing differences between target selection time measured from simultaneously recorded m-N2pc and single-neuron spikes (dark gray), m-N2pc and LFPs (gray), and LFPs and single-neuron spikes (light gray) for each monkey. Most of the values exceed zero, indicated by the dashed vertical line.

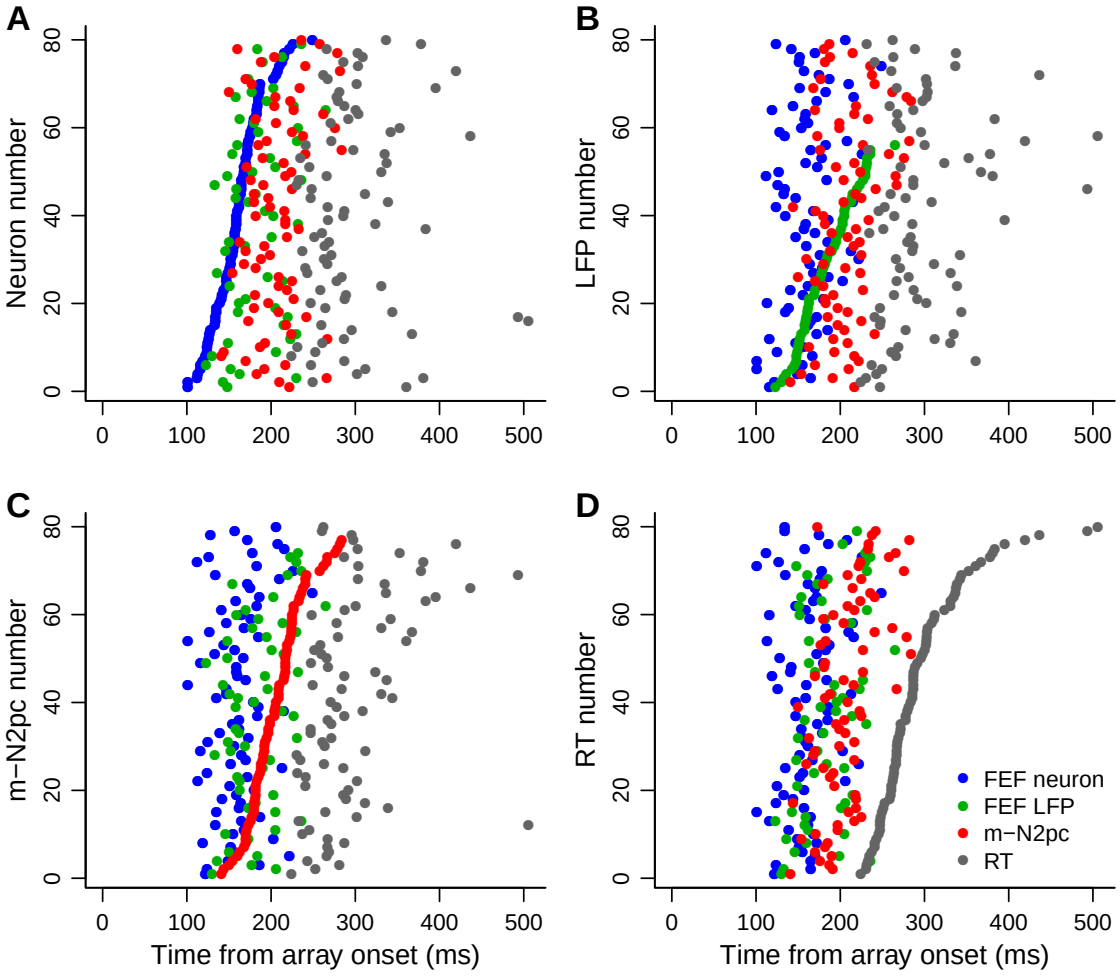

Figure 6.5: Target selection time within sessions sorted by neuron selection time (***A***), LFP selection time (***B***), m-N2pc (***C***), and saccade RT (***D***). Each row corresponds to one recording session, with FEF single-neuron selection time in blue, FEF LFP selection time in green, visual cortex ERP selection time (m-N2pc) in red, and mean saccade RT in that session in gray.

observed in the timing of attentional selection signals cannot be explained by inherent differences in when the first visual activity was observed across the different signals.

Results of these analyses are consistent with the hypothesis that feedback from FEF contributes to the generation of the m-N2pc component. This was tested further by assessing whether the target selection time in FEF and the m-N2pc varied in parallel with search array set size and saccade response time.

6.4.3 Set-size effects

As noted earlier, both monkeys produced longer saccade response times with larger set sizes (Fig. 6.1*B*, Table 6.1). The single-unit recordings show that a delay in the time for FEF neurons to locate the target predicted the increase of saccade response time with set size (Cohen et al., 2009a) (Fig. 6.6). Next, we determined the extent to which delays of target selection by LFPs and the m-N2pc predicted the delay of saccade response time. Figure 6.6 shows that the time of target selection was delayed with increasing set size measured through single FEF neurons (linear regression slope 3.0 ± 1.4 SE ms/item for monkey Q, 2.7 ± 2.3 ms/item for monkey S), FEF LFPs (5.0 ± 1.9 Q, 3.0 ± 4.0 S), and the m-N2pc (9.6 ± 1.4 Q, 6.8 ± 1.8 S). Thus increasing the set size led to delayed target selection for the FEF activity and the m-N2pc. Note that this delay was significantly greater for the m-N2pc than that for FEF LFPs or single neurons.

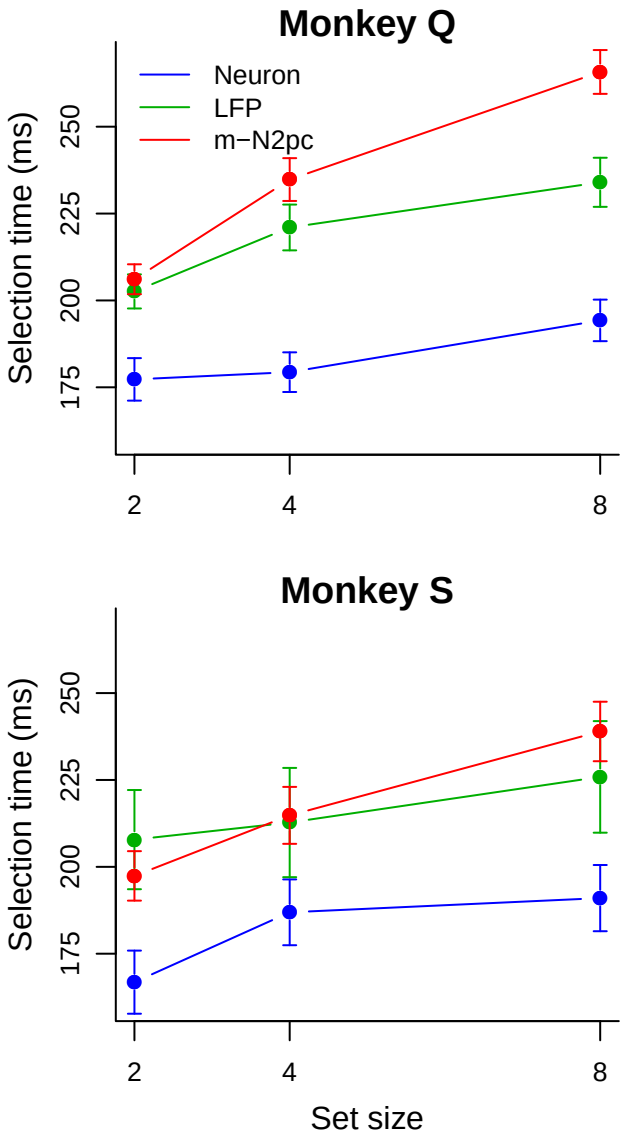

Figure 6.6: Target selection time mean and SE for FEF single-neuron spikes (blue), FEF LFPs (green) and m-N2pc (red) for each set size for each monkey.

6.4.4 Trial-by-trial correlation of spike rate, LFP, and ERP amplitude

If FEF contributes to the generation of the m-N2pc measured over extrastriate visual cortex, then the amplitude of FEF activity and posterior ERPs should covary across trials. We used FEF single-neuron spikes, FEF LFPs, and the extrastriate ERPs that selected the target from distractors and computed the correlation coefficients from trials in which the target was inside the neuronal RFs. The trial-by-trial correlation between the spike rate of individual neurons in FEF and the integral of ERP amplitude was significant in just 4 of the 56 pairs (Fisher's z test, $p < 0.05$; Fig. 6.7A). In contrast, the trial-by-trial correlation between the integral of FEF LFP and extrastriate ERP amplitude was significant in 34 of the 56 pairs (Fisher's z test, $p < 0.05$; Fig. 6.7B). In addition, the LFPERP correlation coefficients were significantly larger when the target fell within the RFs (mean $r\pm$ SE, 0.26 ± 0.02), compared with when only distractors fell within the RFs (0.19 ± 0.02) (Wilcoxon signed-rank test, $p < 0.05$). The lack of correlation between spikes and ERPs was not a result of comparing different signal types. The trial-by-trial correlation between spikes and LFPs was significant in 32 of the 56 pairs (Fisher's z test, $p < 0.05$; Fig. 6.7C). These amplitude correlations between FEF LFPs and posterior ERPs support the hypothesis that FEF contributes to the generation of the m-N2pc.

6.4.5 Signal and noise in each measure of neural activity

Although the timing of target selection by FEF neurons and LFP relative to the extrastriate ERPs is consistent with the hypothesis that the m-N2pc is driven by

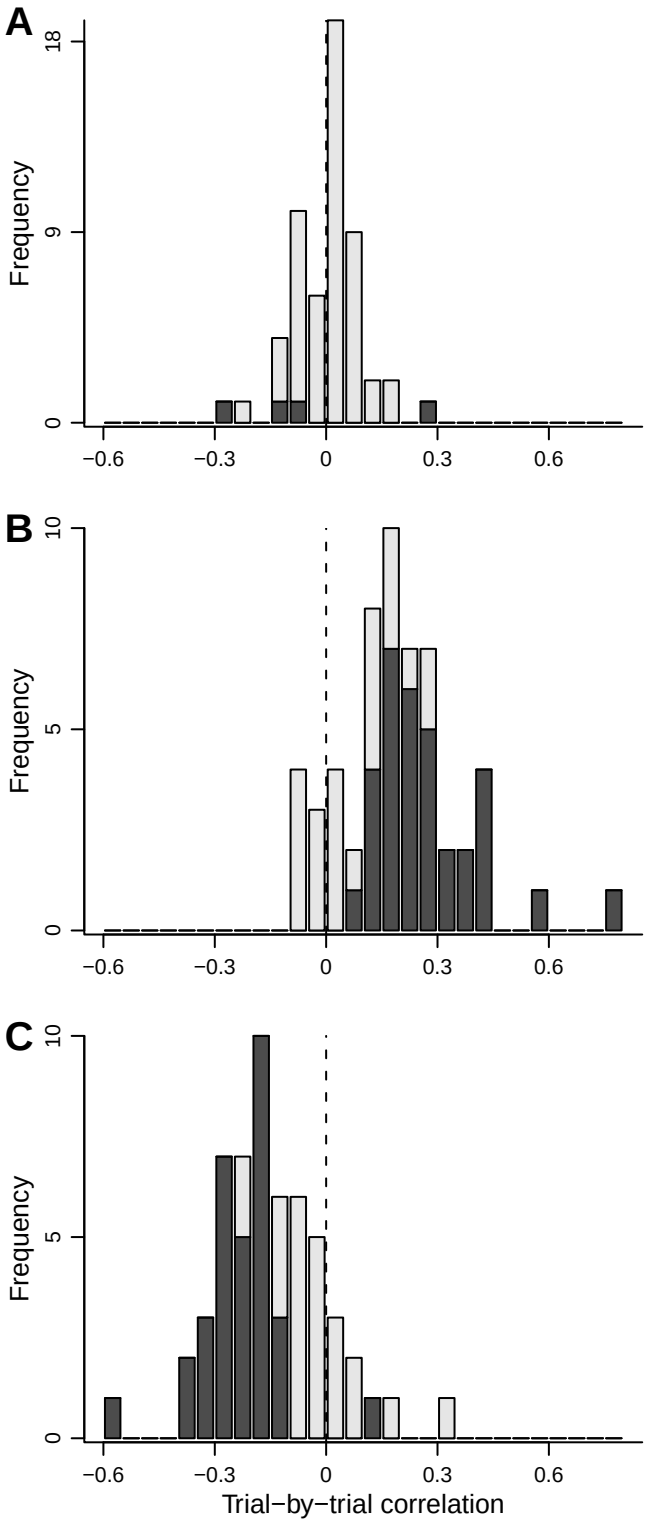

Figure 6.7: Trial-by-trial correlation between spike rates and ERP amplitude (***A***), between LFP and ERP amplitude (***B***), and between spike rates and LFP amplitude (***C***). Significant correlation coefficients are shown in dark bars (Fishers z test, $p < 0.05$). Dashed vertical lines indicate a correlation of zero.

feedback from the selection process in FEF, we wanted to rule out a simple alternative explanation. The pattern of target selection times could just be a difference inherent in the neural measures at different spatial scales. In particular, the signal-to-noise characteristics of the spike times of single neurons may be different from the signal-to-noise characteristics of an LFP (derived from $\sim 10^5$ neurons) and from the signal-to-noise characteristics of an ERP component (derived from $\sim 10^7$ neurons). It may be that through summation the LFP and ERP become more reliable measures. Alternatively, the summation may introduce more noise into the LFP and ERP. To quantify the reliability of the signals at each spatial scale, we computed target selection time for each signal as a function of number of trials (Fig. 6.8, *A* and *B*). The estimate of target selection time tends to decrease with the number of trials contributing to the calculation until an asymptote is reached (Bichot et al., 2001b). We reasoned that target selection time would vary with trial number according to the signal-to-noise characteristics of the signals at different spatial scales. We fit an exponential function to the average curves of FEF single-neuron selection time, FEF LFP selection time, and the m-N2pc,

$$\mathrm{TST} = \mathrm{TST}_{\mathrm{max+min}} e^{-n/\tau} + \mathrm{TST}_{\mathrm{min}},$$

where TST is target selection time; n is the number of trials; and τ, $\mathrm{TST}_{\mathrm{max+min}}$, and $\mathrm{TST}_{\mathrm{min}}$ are the decay (in units of trials), baseline (ms), and asymptote (ms) parameters that were free to vary. The mean decay parameter $\tau \pm$ SE was 336 ± 96

trials for neurons, 308 ± 75 trials for LFPs, and 432 ± 125 trials for the m-N2pc for monkey Q, and 423 ± 224 trials for neurons, 209 ± 39 trials for LFPs, and 358 ± 245 trials for the m-N2pc for monkey S (Fig. 6.8*C*). These values were not significantly different from one another (Wilcoxon rank-sum test, $p > 0.1$). The mean $\mathrm{TST_{min}} \pm$ SE was 139 ± 12 ms for neurons, 156 ± 6 ms for LFPs, and 157 ± 14 ms for the m-N2pc for monkey Q, and 134 ± 12 ms for neurons, 131 ± 80 ms for LFPs, and 164 ± 26 ms for the m-N2pc for monkey S (Fig. 6.8*D*). For monkey Q, $\mathrm{TST_{min}}$ was significantly smaller for neurons than for LFPs and ERPs (Wilcoxon rank-sum test, $p < 0.01$). For monkey S, $\mathrm{TST_{min}}$ was significantly smaller for neurons than for ERPs and for LFPs than for ERPs (Wilcoxon rank-sum test, $p < 0.01$), corresponding to the differences in target selection time reported earlier (Fig. 6.4; Table 6.1).

These fits show that the asymptote of target selection time was reached with fewer trials than the number of trials sampled in our data set (indicated by the black point and horizontal error bars in Fig. 6.8*B*). We next compared selection times across the three measures for varying numbers of sampled trials. When the number of trials exceeded 400, FEF single-neuron selection time was significantly earlier than FEF LFP selection time and FEF LFP selection time was significantly earlier than the m-N2pc (Wilcoxon signed-rank tests, $p < 0.05$). These findings are consistent with the observation that the SEs of the means for the signals at each spatial scale were comparable (Fig. 6.2). Therefore the timing differences across the electrophysiological indices of attentional selection seem not to be an artifact of different signal-to-noise characteristics of the signals at different spatial scales.

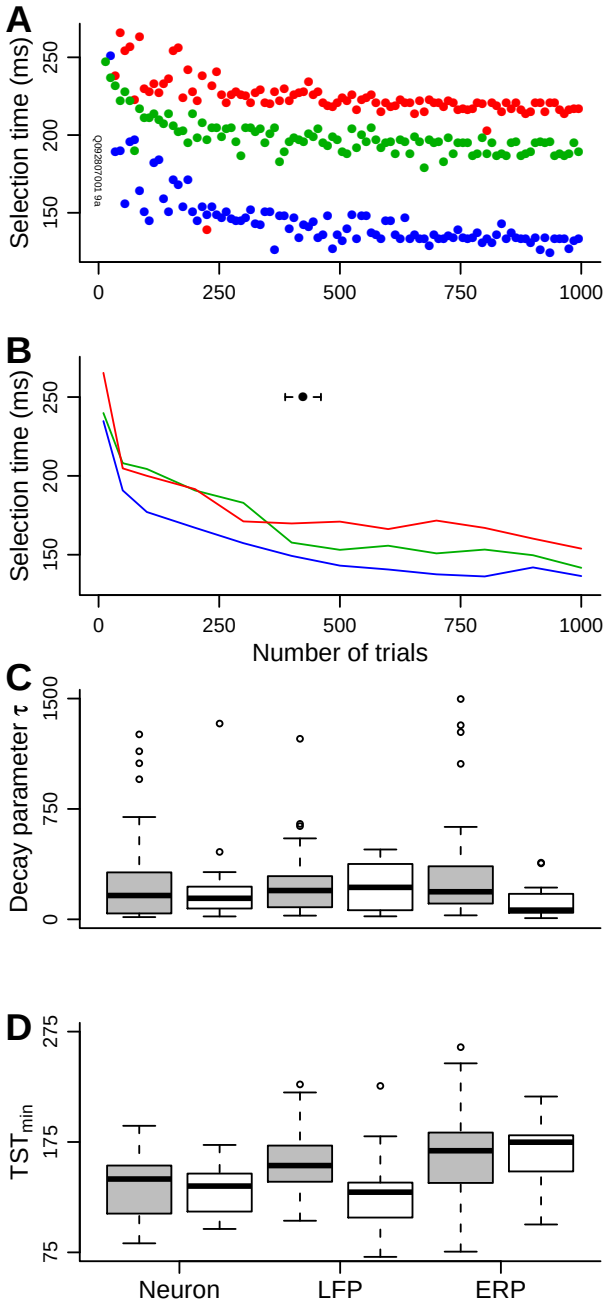

Figure 6.8: *Target selection time as a function of number of trials.* ***A***: target selection time estimates as a function of randomly sampled (without replacement) trials from an example recording of an FEF single neuron (blue), FEF LFP (green), and extrastriate visual cortex ERP (m-N2pc; red). ***B***: average target selection time estimates as a function of randomly sampled (with replacement) trials across recordings for FEF neurons (blue), FEF LFPs (green) and m-N2pc (red). The black point with SE bars indicates the number of trials sampled in our data set. ***C***: decay parameter estimates from exponential fits to the selection time × number of trials curve for each session. Gray boxes are from monkey Q, white boxes from monkey S. ***D***: asymptote parameter estimates from the same exponential fits as in ***C***.

6.4.6 Spatial distribution of the m-N2pc

To evaluate the possibility that dipoles in FEF contributed to the posterior ERPs, we measured ERPs from anterior, middle, and posterior pairs of lateralized electrode sites. As shown previously, the m-N2pc is not observed on anterior electrodes (Woodman et al., 2007). This is so despite the clear evidence of a target-selection process in LFPs recorded in FEF beneath these anterior surface electrode pairs (Fig. 6.9). Apparently, the LFPs in FEF do not create a dipole with the proper geometry to be observed on EEG electrodes over frontal cortex. This is not surprising, given the anatomical location of FEF in the rostral bank of the arcuate sulcus with pyramidal neurons oriented close to parallel to the surface of the skull.

If the LFPs generated in FEF create an electrical dipole oriented perpendicular to the pial surface of the frontal lobe, then this would result in a rostrocaudally oriented electrical field. Such an electric field could produce surface voltage density gradients over the parietal or occipital lobe. Thus it is possible that the m-N2pc is really a manifestation of the volume conduction of the FEF dipole. However, if this were the case, then because electrical signal conduction is essentially instantaneous in the conductive medium of the brain (Nunez and Srinivasan, 2006), the m-N2pc should occur instantaneously with the FEF LFPs. This was not the case under the conditions of this experiment.

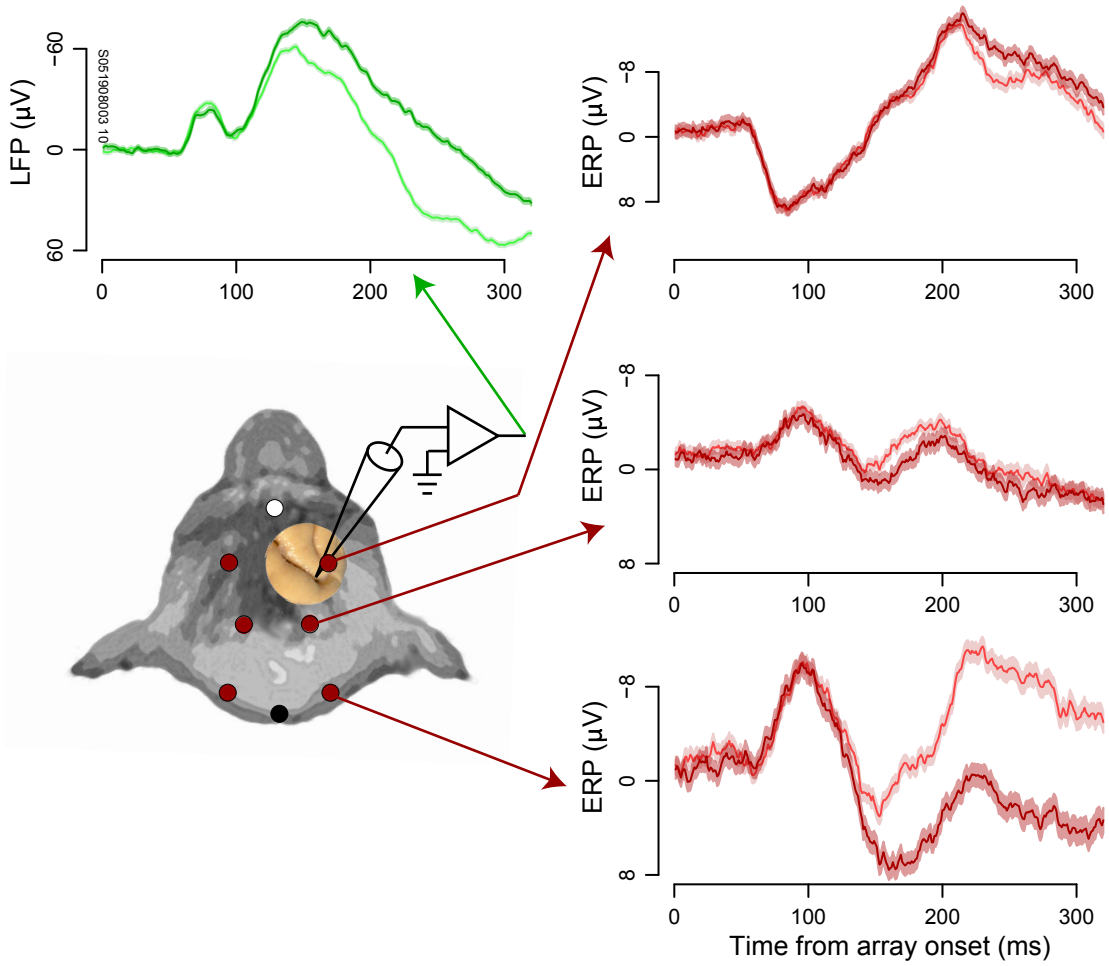

Figure 6.9: Spatial distribution of ERPs shown with FEF LFP from an example recording session in monkey S. Dark curves represent potentials when the target was contralateral to the recording site (i.e., left visual field), light curves represent potentials when the target was ipsilateral to the recording site (i.e., right visual field). Bands around activity curves indicate SE. The anterior electroencephalographic (EEG) electrode was embedded in the skull, but is displayed here on top of the exposed cortical surface for purposes of illustration.

6.4.7 Shape of the ERP

ERPs over posterior cortex show a transient negative polarization in response to a visual stimulus in humans and monkeys known as the N1 component (Woodman et al., 2007). Curiously, a craniotomy over FEF in monkey S inverted the N1 to a positive polarization in the left hemisphere but not the right (Fig. 6.3). Note that the m-N2pc was not inverted; it remained a positive polarization. Importantly, the m-N2pc timing was not significantly different between left and right hemispheres for either monkey (Wilcoxon rank-sum test, $p > 0.2$ for each monkey), although the shape of the target-selection signal was different between left and right hemispheres for each monkey (Fig. 6.3).

6.4.8 Signal distortion by the recording circuit

Recent work has shown that LFPs are distorted by the intrinsic filtering characteristics of high-impedance microelectrode recording circuits (Nelson et al., 2008). This distortion is systematic and can be corrected. An example corrected LFP is shown in Fig. 6.10. Target selection time was not significantly different between corrected and uncorrected LFPs. Because of this lack of difference in selection times, we report values drawn from the raw, uncorrected LFPs, to compare directly to a previous study (Monosov et al., 2008). The impedance of the EEG electrodes, 25 kΩ measured at 30 kHz, was sufficiently low that it caused minimal signal distortion; indeed, when we applied the correction to ERPs, we saw no difference in target selection time between uncorrected and corrected signals.

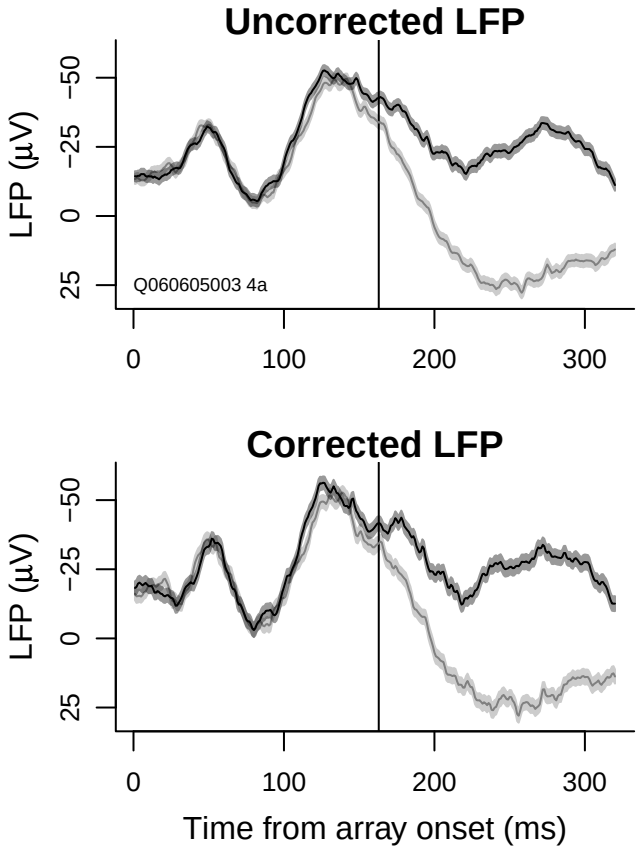

Figure 6.10: *Signal distortion by the recording circuit.* The top panel shows the raw LFP with the target inside (dark) and opposite (light) the simultaneously recorded neuron's RF; this is from the example session in Fig. 6.2. The bottom panel shows the corrected LFP using an empirical estimate of the recording circuit's transfer function obtained from a procedure described in Nelson et al. (2008). Target selection time was not significantly different between corrected and uncorrected LFPs. Vertical lines indicate target selection time measured using the uncorrected LFPs. Bands around activity curves indicate SE.

6.5 Discussion

To create a bridge between research investigating attentional selection using human ERPs and research using macaque intracranial electrophysiology, we recorded the putative macaque homologue of the N2pc component indexing covert selection simultaneously with spikes from single neurons and LFPs in FEF. We show that visual targets are selected by FEF spikes and LFPs earlier than the ERP component that is maximal over extrastriate visual cortex. Thus our findings support the hypothesis that the N2pc is generated due to feedback from an attentional-control structure (such as FEF) because in this visual search task the target is located by FEF before it is located by the m-N2pc. Before accepting this conclusion, we discuss three alternative explanations that can be ruled out.

First, the signal-to-noise characteristics of the spike times of single neurons may be different from the signal-to-noise characteristics of the ensemble activity measured with LFPs and ERPs. However, as shown earlier (Fig. 6.8), the three electrophysiological measures of target selection time exhibited similar reliability as a function of the number of trials sampled. If one of the signals were more reliable across trials, then the estimate of target selection time would have reached asymptote with fewer trials sampled. Not observing any difference is consistent with the basic observation of similar variability in the different signals (Fig. 6.2, Table 6.1) and rules out the possibility that the differences in timing were simply due to greater intrinsic signal-to-noise differences in the ERPs or LFPs relative to the neurons. This finding has implications for neural prosthetics. If the signal-to-noise ratio of spikes, LFPs, and

ERPs are similar, then the ability to decode an appropriately chosen ERP will be similar to that of spikes.

Second, the difference in voltage polarity between human N2pc (negative) and macaque m-N2pc (positive) could mean that these potentials are measuring different underlying ERP components. However, this proposition would need to explain why the m-N2pc and the human N2pc have such similar timing (Figs. 6.26.5), task dependence (Fig. 6.6), and spatial distribution (Fig. 6.9). On the other hand, the difference in polarity can be explained by the difference in anatomy. The neural generator of the human N2pc is thought to include area V4 (Hopf et al., 2000; Luck et al., 1997). Macaque V4 is located partially on the surface of the prelunate gyrus (Gattass et al., 1988; Zeki, 1971), whereas the human homologue of V4 is buried in a region containing multiple sulci and gyri (Orban et al., 2004; Sereno et al., 1995; Tootell and Hadjikhani, 2001). Thus it is plausible that the m-N2pc has the opposite polarity of the human N2pc because of the differences in cortical folding between species. Indeed, similar reasoning about the contribution of cortical folding to the polarity of ERPs applies to at least two other ERP components. The human C1 has a negative polarity when a visual stimulus is presented above the horizontal meridian and a positive polarity when a stimulus is presented below the horizontal meridian, consistent with the shape of the calcarine sulcus (Clark et al., 1995). The lateralized readiness potential has a negative polarity preceding hand movements and a positive polarity preceding foot movements, consistent with the opposing locations of the hand (lateral) and foot (medial) representations in primary motor cortex (Brunia and Vingerhoets, 1980; Leuthold and Jentzsch, 2002). Thus based on differences in

cortical folding between macaques and humans, we believe that the m-N2pc is homologous to the human N2pc. We also considered the possibility that the m-N2pc could be generated from a rostrocaudally oriented dipole in the macaque FEF. However, the timing differences between target selection in the FEF LFP and the m-N2pc are inconsistent with this hypothesis. It is likely that the FEF dipole is actively cancelled out by electrical fields with similar timing and of opposite polarity generated in neighboring cortical areas or in brain areas that lie between FEF and the posterior electrodes above extrastriate visual cortex (e.g., the lateral intraparietal area). This latter source of active cancellation of the FEF dipole would be consistent with a magnetoencephalography study of the N2pc component in humans, showing that the N2pc over ventral visual cortex is preceded by an activation in posterior parietal cortex (Hopf et al., 2000).

Third, one might hypothesize that an ERP component recorded outside the brain arises with some delay after the synaptic events in the dipole source producing that ERP component. We can reject this hypothesis because, whereas EEG is subject to spatial distortion, it is not delayed relative to synaptic activity (Nunez and Srinivasan, 2006). Thus the remaining and most plausible hypothesis is that, under the conditions tested, target selection in FEF precedes that of the m-N2pc.

Our results demonstrate that the brain selects a target during visual search through a sequence of processes manifesting in the frontal lobe before posterior visual areas. This attentional cascade occurs in the spike rates of single neurons in FEF before the selective polarization of intracranial LFPs and the ERPs recorded through the skull, which represent a summation of field potentials in the brain. This shows

that the N2pc component in primates does not index the earliest time that the brain selects a visual search target to receive the benefit of attention. This is consistent with evidence suggesting that areas that perform spatial visual selection lead those that perform detailed processing of object identity (Hopf et al., 2000).

These findings bear on hypotheses about the functional architecture of attention and visual search. The larger increase in m-N2pc onset than target selection time in FEF as a function of set size (Fig. 6.6) is consistent with the hypothesis that the selection process in a putative saliency map (such as FEF) takes less time than the focusing of visual attention performed in the areas generating the m-N2pc (Luck and Hillyard, 1994b). Attentional models of visual search such as Guided Search (Wolfe, 2007) propose that increased activity in the saliency map precedes the effects of focusing visual attention on the target representation in extrastriate visual cortex, resulting in the binding of target features.

We also rule out a simple feedforward architecture, in which visual signals propagate only from visual cortex to frontal cortex. The data support theories of attention that propose that top-down input from frontal cortex guides attentional selection in visual cortical areas (Bundesen et al., 2005; Desimone and Duncan, 1995; Lamme and Roelfsema, 2000). FEF is situated chronometrically and anatomically to influence areas such as V4 and IT (Barone et al., 2000; Gregoriou et al., 2009; Schmolesky et al., 1998) and it appears that target-selecting neurons in FEF may be a major source of signals to extrastriate visual cortex (Pouget et al., 2009). The potency of this signal has been demonstrated in humans and macaques. Transcranial magnetic stimulation over human FEF biases attention in the corresponding part of space and

visual ERPs (Juan et al., 2008; Taylor et al., 2007) and microstimulation of macaque FEF biases attention and activity in extrastriate visual cortex (Armstrong et al., 2006). Finally, our results provide the first direct test of the hypothesis that the N2pc is due to feedback from an area that controls the focus of visuospatial attention (Luck and Hillyard, 1994b). The timing of this feedback may depend strongly on task demands. A recent study reported that attentional modulation occurred on average 8 ms earlier in FEF neurons than in V4 neurons (Gregoriou et al., 2009), although this measurement had a large amount of variability. Our results indicate nearly an order-of-magnitude greater time difference (ranging from $\sim$ 30 to 70 ms depending on set size). This difference may have arisen from a difference in the attentional demands of the task or the contribution of other areas in extrastriate or parietal cortex to the m-N2pc. Gregoriou et al. (2009) suggested that the 8-ms delay corresponded to the axonal transmission time between FEF and V4. However, the reliability of axonal conduction cannot explain the degree of variability in their estimate. The time differences we measured are long enough to permit axonal conduction plus synaptic integration, which seems more plausible for an interaction of the sort described by models of top-down processing.

In addition to our conclusions about the relationship between FEF and the m-N2pc, we also replicated a recent finding in FEF: LFPs select visual targets later than the simultaneously recorded spikes (Monosov et al., 2008). This may seem counterintuitive; if the LFP represents synaptic potentials that lead to spikes, then one might expect them to show target selection before spikes. Indeed, the initial visual responses were earlier in the LFPs than in the spikes (Table 6.1). However,

the later target selection times in LFPs than those in spikes suggests that FEF LFPs reflect nonselective visual inputs to FEF neurons, whereas FEF spikes reflect the outcome of target selection that is computed in FEF itself.

Despite this seemingly clear dissociation between FEF inputs and outputs, our results also challenge the view that LFPs represent only the synaptic input to a region of cortex. We observed a strong trial-by-trial correlation between FEF LFPs and posterior ERPs, but not between FEF spikes and posterior ERPs (Fig. 6.7). If spikes represent output from a cortical area and LFPs represent strictly input, then these correlations could reflect that the neural generator of the m-N2pc also projected to FEF but that FEF did not project directly to the neural generator of the m-N2pc. Because the projection from FEF to extrastriate cortex is strong (Barone et al., 2000; Pouget et al., 2009) and it is likely that many of the neurons we recorded projected to extrastriate cortex (see Fig. 5 in Thompson et al., 1996), this explanation seems unlikely. Thus we propose that the weak correlations between spikes and ERPs reflect the weak relationships between these signals. Indeed, several studies have shown weak relationships between spikes and slow-wave EEG (Buchwald et al., 1965; Fromm and Bond, 1964, 1967; Marsan, 1965) (but see Baker et al., 2003; Foote et al., 1980). We also propose that the strong correlations between LFPs and ERPs represent the strong relationship between aggregate local synaptic processing of target selection in FEF and the neural generator of the m-N2pc, suggesting that LFPs do not reflect only input to a cortical area.

The findings from this combination of techniques provide a step toward understanding the neural basis of selective visual processing across spatial scales and brain

areas. Recording ERP components simultaneously with LFPs and single-neuron activity achieves two goals of cognitive neuroscience. First, recording ERPs from macaques performing the same tasks used in studies of humans allows us to bridge the gap between human and nonhuman primate electrophysiology. Second, this combination of methods yields data with excellent spatial and temporal resolution. This has been the goal of combining ERP and imaging methods, although this marriage of neuroscientific techniques uses source estimation procedures that are themselves suggestive, not definitive, due to a number of factors (e.g., Hillyard and Anllo-Vento, 1998; Nunez and Srinivasan, 2006). Our study shows how hypotheses about the generation of human ERP components can be tested by recording multiple electrophysiological measures from primates exhibiting homologous ERP components. Understanding the neural substrates of noninvasive electrophysiological measures of human cognition is vital for progress in testing psychological theories, treating disorders, and creating braincomputer interfaces.

CHAPTER VII

NEURAL BASIS OF THE SET-SIZE EFFECT IN FRONTAL EYE FIELD: TIMING OF ATTENTION DURING VISUAL SEARCH

7.1 Abstract

Visual search for a target object among distractors often takes longer when more distractors are present. To understand the neural basis of this capacity limitation, we recorded activity from visually responsive neurons in the frontal eye field (FEF) of macaque monkeys searching for a target among distractors defined by form (randomly oriented **T** or **L**). To test the hypothesis that the delay of response time with increasing number of distractors originates in the delay of attention allocation by FEF neurons, we manipulated the number of distractors presented with the search target. When monkeys were presented with more distractors, visual target selection was delayed and neuronal activity was reduced in proportion to longer response time. These findings indicate that the time taken by FEF neurons to select the target contributes to the variation in visual search efficiency.[1]

7.2 Introduction

Because only some of all the information entering the visual system is relevant for acting in a given environment, attention must be allocated to selectively process

[1]This chapter was published as Cohen JY, Heitz RP, Woodman GF, Schall JD. Neural basis of the set-size effect in frontal eye field: timing of attention during visual search. *J Neurophysiol* 101: 1699-1704, 2009.

one among many alternatives, especially when those alternatives are difficult to distinguish. This has been investigated using visual search for a target stimulus in an array of distractor stimuli (Bergen and Julesz, 1983; Carrasco and Yeshurun, 1998; Duncan and Humphreys, 1989; Palmer, 1994; Treisman and Gelade, 1980; Wolfe, 2007). The observation that visual search response time (RT) often increases with the number of distractors has been central in theories of attention (Bundesen, 1990; Bundesen et al., 2005; Desimone and Duncan, 1995; Duncan and Humphreys, 1989; Treisman and Gelade, 1980; Wolfe, 2007). Previous work has shown that brain areas in the macaque visuomotor system have distinct classes of neurons involved in different stages of visual search. Visual and visuomovement neurons in the frontal eye field (FEF) (Schall and Hanes, 1993; Thompson et al., 1996), lateral intraparietal area (LIP) (Bisley and Goldberg, 2003; Ipata et al., 2006; Thomas and Paré, 2007), and superior colliculus (SC) (McPeek and Keller, 2002) participate in the visual selection of target objects by increasing activity when the target is inside the neurons receptive field (RF) relative to when a distractor is in the RF. Other neurons in these areas participate in preparing eye movement responses (Bruce and Goldberg, 1985; Hanes and Schall, 1996; Segraves and Goldberg, 1987; Sommer and Wurtz, 1998; Sparks et al., 1976; Wurtz and Goldberg, 1971). Neurophysiological recordings from nonhuman primates can distinguish between competing accounts of the locus of increases in RT with increased set size because the activity of different types of neurons reveals the timing of different stages of processing (Sato et al., 2001; Sternberg, 2001; Woodman et al., 2008).

To determine the neural locus of processing delays with increasing search set sizes,

we measured the activity of visually responsive neurons in FEF during a demanding visual search task. The activity of these neurons discriminates between target and distractor, thus measuring the time of target selection, which corresponds to attention allocation (Bichot and Schall, 1999b; Juan et al., 2004; Murthy et al., 2001; Schall, 2004b; Thompson et al., 1997, 2005b). We trained two monkeys to search for a target stimulus among one, three, or seven distractor stimuli (set sizes 2, 4, and 8) in a **T**/**L** search display (Fig. 7.1*A*). Monkeys fixated a spot at the center of the display and received a liquid reward for producing a single saccadic eye movement to the target (in Fig. 7.11*A*, the **L**). Across experimental sessions, the monkeys alternated between searching for **T**s or **L**s among randomly rotated distractors. This visual search task results in longer RT with larger set size in human observers (Bergen and Julesz, 1983; Carrasco and Yeshurun, 1998; Duncan and Humphreys, 1989; Palmer, 1994; Treisman and Gelade, 1980; Wolfe, 2007). We found that neurons selected search targets later and discharged fewer spikes when presented with more distractors.

7.3 Methods

7.3.1 Behavioral task and recording

Activity of FEF neurons was recorded in both hemispheres of two male macaques (*Macaca radiata*) performing memory-guided saccade and visual search tasks. Recordings were acquired from the rostral bank of the arcuate sulcus using tungsten microelectrodes (FHC). In the search task, monkeys searched for a target (**T** or **L**) among distractors (**L** or **T**) (Woodman et al. 2007). Distractors could be homogeneous (e.g.,

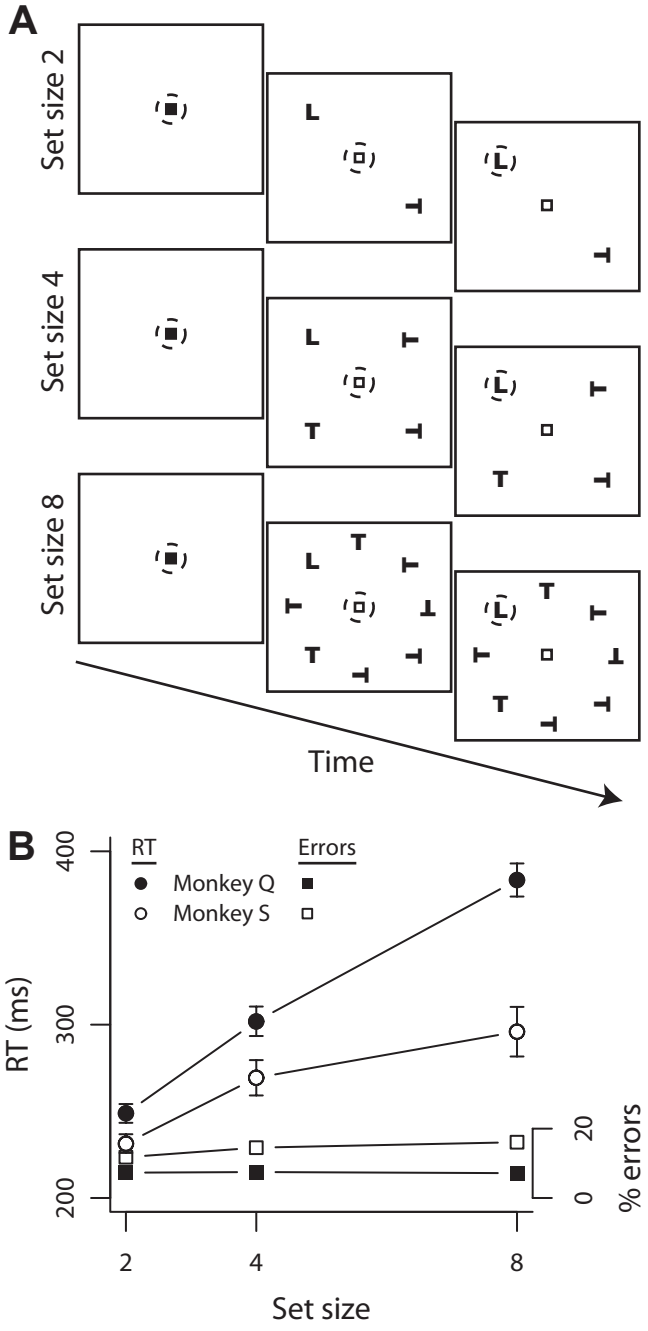

Figure 7.1: *Visual search task.* ***A***: monkeys made saccades to a target (here, an upright **L**; not to scale) presented with 1, 3, or 7 distractors. The monkeys eye position is represented by the dashed circle, which is invisible to the monkey. ***B***: response time (RT, circles) and percentage error (squares) vs. set size for each monkey. Error bars represent SE around the mean of the session means. Filled symbols: monkey Q. Open symbols: monkey S. Error bars for percentage error are smaller than plotted points.

upright **L**s) or heterogeneous (e.g., **L**s oriented differently). Each trial began with monkeys fixating a central spot for about 600 ms. A target was then presented at one of eight isoeccentric locations equally spaced around the fixation spot (Fig. 7.1*A*). The other seven locations contained seven distractor stimuli, three distractors, or one distractor. During each recording session, the target was a **T** or an **L** rotated by 0, 90, 180, or 270°. Monkeys were given a liquid reward for making a saccade to the target location and fixating it for 1000 ms.

Activity from each neuron was recorded during a memory-guided saccade task to distinguish visual- from movement-related activity (Bruce and Goldberg, 1985; Hikosaka and Wurtz, 1983). The target was flashed alone for 80 ms. Monkeys were required to maintain fixation for 500-1000 ms after the target onset. When the fixation spot disappeared, the monkey was rewarded for a saccade to the remembered location of the target.

Our data set consists of 57 neurons from monkey Q and 26 neurons from monkey S. Spikes were sorted on-line and off-line using principal components analysis and template matching (Plexon, Dallas, TX).

Monkeys were surgically implanted with a head post, a subconjunctival eye coil, and recording chambers. Surgery was conducted under aseptic conditions with animals under isoflurane anesthesia. Antibiotics and analgesics were administered postoperatively. All surgical and experimental procedures were in accordance with the National Institutes of Health Guide for the Care and Use of Laboratory Animals and approved by the Vanderbilt Institutional Animal Care and Use Committee.

7.3.2 Data analysis

To measure the firing rate of each neuron, we used a spike density function, convolving each spike with a kernel resembling a postsynaptic potential (Thompson et al., 1996).

We used a memory-guided saccade task to classify neurons. Visual neurons had significantly greater activity in the 100 ms after the target flash than in the 100 ms before the target flash. Movement neurons had greater responses in the 100 ms leading up to the saccade than in the 100 ms before the target flash. Visuomovement neurons had greater responses in the 100 ms after the target flash and in the 100 ms leading up to the saccade than in the 100 ms before the target flash. Neurons analyzed in this study were visual and visuomovement and had significant above-baseline activity during the memory delay.

To measure the time of target selection we used millisecond-by-millisecond Wilcoxon rank-sum tests. Selection time is defined as the time at which the distribution of activity when the search target was inside a neuron's RF was significantly greater than the distribution of activity when the target was opposite the RF for ten consecutive milliseconds with $p < 0.01$. This "neuron-antineuron" approach presumes that a population of neurons in the brain representing the location of the target competes with a population of neurons representing the location of distractors opposite the target. Measuring selection time with a receiver operating characteristic analysis (Thompson et al., 1996) yielded similar results. There was no difference in target selection time between visual and visuomovement neurons.

All statistical tests were done with Bonferroni corrections for multiple comparisons. All analyses were done with R (`http://www.r-project.org/`).

7.4 Results

7.4.1 Behavior

Both monkeys exhibited a consistent and strong effect of set size on RT (Fig. 7.1*B*). Across sessions RT was significantly longer for set size 8 compared with set size 4 and for set size 4 compared with set size 2 and, within sessions, RT increased significantly with set size in 100% of sessions (Table 7.1). The slopes of RT by set size corresponded to an increase of 22 ms per additional distractor for monkey Q and 10 ms per additional distractor for monkey S. Percentage error (moving the eyes to a distractor) was low for both monkeys and increased with set size only for monkey S (Fig. 7.1*B*; Wilcoxon signed-rank test, $p < 0.001$). These results indicate that the monkeys consistently emphasized accuracy over speed.

	Monkey Q	Monkey S
Target selection time mean ± s.e.m. (ms)		
Neuron	163 ± 4.2	156 ± 5.7
LFP	191 ± 3.9	169 ± 7.7
ERP	213 ± 4.6	191 ± 4.5
Visual onset time mean ± s.e.m. (ms)		
Neuron	72 ± 3.0	62 ± 4.0
LFP	54 ± 2.2	59 ± 4.3
ERP	67 ± 1.8	77 ± 1.8
RT mean ± s.e.m. (ms)		
Set size 2	249 ± 5.4	231 ± 5.4
Set size 4	302 ± 8.5	269 ± 10.2
Set size 8	383 ± 9.5	296 ± 14.3
Slope of linear regression	22.1 ± 1.9	10.2 ± 2.5
Target selection time mean ± s.e.m. (ms)		
Neuron set size 2	177 ± 6.1	168 ± 8.4
Neuron set size 4	179 ± 5.7	189 ± 8.8
Neuron set size 8	194 ± 6.0	191 ± 9.2
LFP set size 2	203 ± 4.9	208 ± 14.3
LFP set size 4	221 ± 6.6	213 ± 15.7
LFP set size 8	234 ± 7.1	226 ± 16.1
ERP set size 2	206 ± 4.3	197 ± 7.1
ERP set size 4	235 ± 6.2	215 ± 8.2
ERP set size 8	266 ± 6.3	239 ± 8.6

Table 7.1: Comparisons of RT, target selection time and visual onset time. Values are means and standard errors of the mean.

7.4.2 Set-size effects on target selection time

We recorded the activity of 57 visually responsive FEF neurons from monkey Q and 26 from monkey S that selected the target in the visual search task. This selection has been identified with the allocation of attention (Bichot et al., 2001b; Schall, 2004b; Thompson and Bichot, 2005; Thompson et al., 2005b). Each neuron exhibited visual responses and sustained activity during the delay period of a memory-guided saccade task. Target selection time measures the time at which a neuron's activity on trials with the search target inside its RF exceeded activity on trials with

a distractor in its RF (and the target opposite its RF). To determine how variation of target selection time related to variation of RT, we aligned neuronal responses to the time of presentation of the search array and measured target selection time for each set size.

Figure 7.2 shows the average response of a neuron when the target versus a distractor appeared in the RF for each set size, aligned to the onset of the search array. The neuron selected the target after 160 ms when one distractor was present (Fig. 7.2*A*, vertical line), after 177 ms when three distractors were present (Fig. 7.2*B*), and after 230 ms when seven distractors were present (Fig. 7.2*C*). The delay of the target selection corresponded with the delay of the RT (set size 2 mean RT $\pm$ SE, 219 ± 4.2 ms; set size 4, 265 ± 7.8 ms; set size 8, 386 ± 12.3 ms). Median RT for each set size is indicated by the black arrowhead in each panel.

Neurons selected the target later when confronted with larger set sizes (Fig. 7.3, Table 7.1). Comparing across neurons, target selection time was significantly later for set size 8 than for set sizes 2 or 4 (KruskalWallis rank-sum test, $p < 0.01$). Comparing within neurons, target selection time was significantly later for set size 4 compared with set size 2 for monkey S and was significantly later for set size 8 than for set size 4 and for set size 8 than for set size 2 for both monkeys.

We measured the relationship between RT and selection time by computing a linear regression for each set size (Table 7.1). The regression for monkey Q was significant for set size 8 (solid gray line in Fig. 7.4*C*). For monkey S, regression was significant for set size 4 (solid line in Fig. 7.4*B*) and set size 8 (solid black line in Fig. 7.4*C*). Combined across monkeys, regression was significant for set size 8, with a

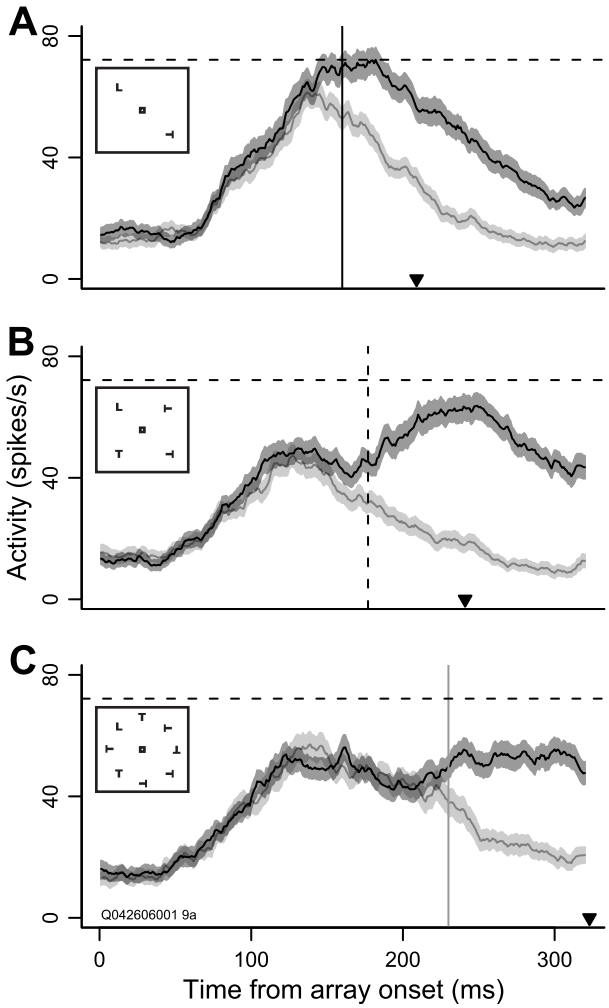

Figure 7.2: *Target selection time by set size for an example neuron.* ***A***: average firing rate when the target was inside the neuron's receptive field (RF; dark band around black curve, 102 trials) and opposite the RF (light band around gray curve, 113 trials) for set size 2. Median RT is denoted by the black arrowhead. Filled bands indicate SE around the mean firing rates. The solid vertical line indicates target selection time. The dashed horizontal line indicates the peak firing rate. The inset shows an example search array of set size 2. ***B***: the same as in ***A***, but for set size 4 (dark, 108 trials; light, 105 trials), with the dashed vertical line indicating target selection time. The dashed horizontal line indicates the peak firing rate in ***A***. ***C***: the same as in ***A***, but for set size 8 (dark, 102 trials; light, 92 trials), with the solid gray line indicating selection time and the dashed horizontal line indicating peak firing rate in ***A***.

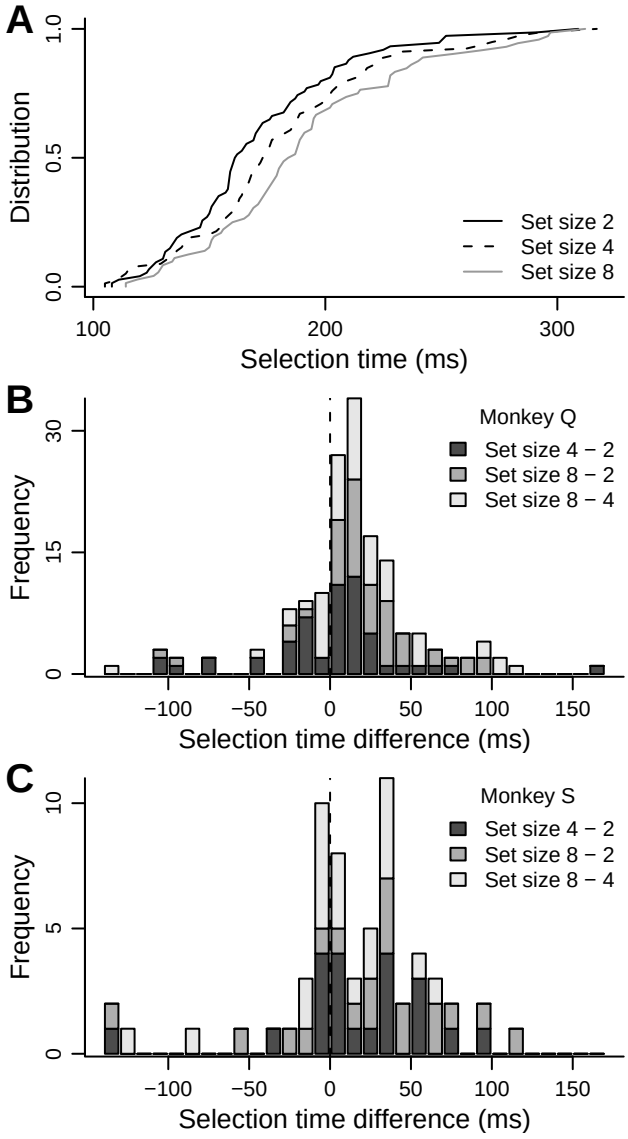

Figure 7.3: *Target selection time by set size.* ***A***: cumulative distributions of selection time across neurons for set sizes 2 (black), 4 (dashed), and 8 (gray). ***B***: stacked histogram of differences in selection time between set sizes 4 and 2 (dark gray), 8 and 2 (gray), and 4 and 2 (light gray), for monkey Q. Most of the histogram falls to the right of zero, indicated by the dashed vertical line. ***C***: the same as in ***B***, but for monkey S.

slope of 0.79 ± 0.16 ($p < 0.001$) and intercept of 189 ± 31 ms ($p < 0.001$). That is, for set size 8, a 10 ms increase in selection time corresponded to an approximately 8 ms increase in RT. Thus target selection time of FEF neurons accounts for a significant amount of variance in RT for large set sizes.

7.4.3 Set-size effects on firing rate

We measured peak mean firing rate for each neuron from search array onset until saccade onset when the search target was inside the neuron's RF. For the example neuron in Fig. 7.2, the dashed horizontal lines indicate peak mean firing rate for set size 2. Peak firing rate decreased from 72 to 64 to 56 spikes/s for set sizes 2, 4, and 8, respectively. Across the population of neurons, peak firing rate decreased with increasing set size (Fig. 7.5, Table 7.1). Firing rate was significantly higher for set size 2 than that for set size 4 for monkey Q. Firing rate was significantly higher for set size 2 than that for set size 8 and for set size 4 than that for set size 8 for both monkeys. Thus increasing set size decreases peak firing rate in FEF.

7.5 Discussion

We discovered that neurons in FEF that select the location of the target in a visual search array do so later with fewer spikes when presented with progressively more, complex distractors. This result complements earlier observations that the time course of target selection by FEF neurons is related to the visual similarity between targets and distractors in singleton and conjunction search (Bichot and Schall, 1999a; Bichot et al., 2001b; Sato et al., 2001; Thompson et al., 1996). The target selection

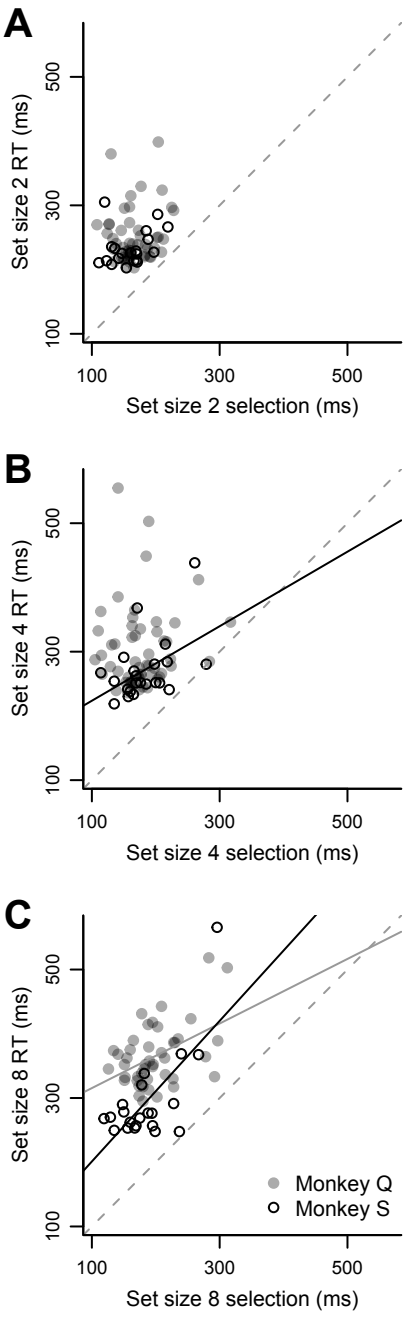

Figure 7.4: RT vs. selection time for set sizes 2 (***A***), 4 (***B***), and 8 (***C***). The solid black lines indicate significant regression lines for monkey S, the gray line for monkey Q. Dashed gray lines indicate unity.

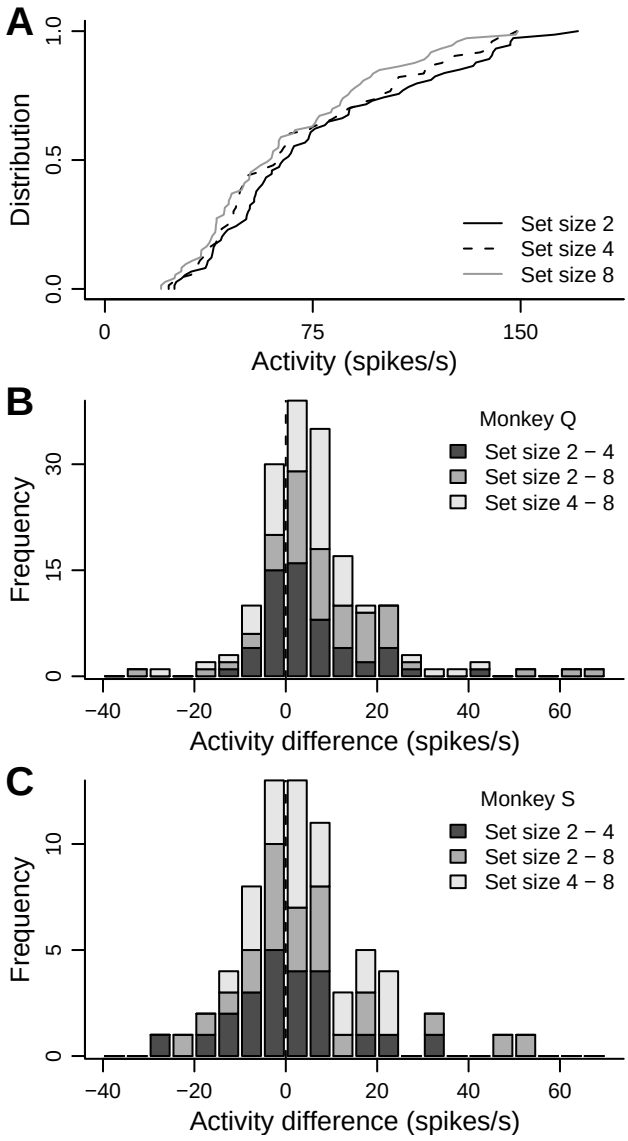

Figure 7.5: *Firing rate by set size.* ***A***: cumulative distributions of firing rate across neurons for set sizes 2 (black), 4 (dashed), and 8 (gray). ***B***: stacked histogram of differences in firing rate between set sizes 2 and 4 (dark gray), 2 and 8 (gray), and 4 and 8 (light gray), for monkey Q. Most of the histogram falls to the right of zero, indicated by the dashed vertical line. ***C***: the same for monkey S.

process first described in FEF (Schall and Hanes, 1993) has now been observed in posterior parietal cortex (Constantinidis and Steinmetz, 2001a; Ipata et al., 2006; Thomas and Paré, 2007) and SC (McPeek and Keller, 2002). These results are consistent with the hypothesis that a population of neurons in FEF, LIP, and SC can be identified with the salience map in models of visual search and attention (Bundesen et al., 2005; Itti and Koch, 2000; Thompson and Bichot, 2005; Wolfe, 2007). These neurons represent the extent to which a stimulus in their RF is the focus of attention. The target selection process marks the outcome of visual processing and the covert allocation of attention to the target that precedes overt responses (Schall, 2004b; Thompson and Bichot, 2005). We found that RT varied with selection time as if the saccade could not be produced until the target was located. This occurs because the onset of activation of presaccadic movement neurons in FEF is delayed when visual search is less efficient, yielding longer RT (Woodman et al., 2008). In other words, under the conditions of our experiments, preparation of the eye-movement response does not begin until perceptual processing of the visual array is completed. Note that although target selection time in FEF accounted for a large amount of variation of RT, other sources also contributed to the variation in RT; the major source is the postselection stochastic process of saccade preparation (Woodman et al., 2008).

Theories of visual attention propose that the cause of longer RT with increased set size arises because of the limited capacity of the visual system to simultaneously analyze all elements in a visual search array (Bundesen, 1990; Bundesen et al., 2005; Desimone and Duncan, 1995; Duncan and Humphreys, 1989; Treisman and Gelade, 1980; Wolfe, 2007). Such theories predict that a neural index of the allocation of at-

tention to the target is delayed when more nontarget stimuli must be processed. The time at which visually responsive neurons in FEF signal the location of the target provides a neurochronometric measure of the conclusion of perceptual analysis (Juan et al., 2004; Murthy et al., 2001; Schall, 2004b; Thompson et al., 1997, 2005b) and Wolfe's Guided Search (Wolfe, 2007), target selection maps onto a mechanism directing attention in the visual field. Our measure of selection time indicates when, on average, attention is reliably focused on the target. This time is later with larger set sizes because attention shifts more often to one or more distractors before focusing on the target. According to other theories of attention, such as Bundesen's Theory of Visual Attention (TVA) (Bundesen, 1990; Bundesen et al., 2005), attention is deployed to all of the possible targets simultaneously and eventually selects an object when it enters short-term memory. According to TVA, the neurochronometric measure of target selection would mark the time at which perceptual processing is completed and the target representation is transferred into memory. Because FEF activity has been associated with attention and working memory (Funahashi et al., 1989) both of these theoretical explanations of our findings are tenable and distinguishing between them is a goal for future research.

The reduced discharge rate with larger stimulus arrays has been observed previously (Balan et al., 2008) and described in terms of increased uncertainty (Basso and Wurtz, 1998), number of alternatives (Lee and Keller, 2008), or RF surround suppression (Schall et al., 1995a). This may underlie the capacity limitation of visual search with increasing number of distractors (Desimone and Duncan, 1995; Palmer, 1994; Treisman and Gelade, 1980). Lower discharge rates among the neurons representing

the target and distractors result in less dynamic range for discriminating between the alternative representations. Thus more time is taken to achieve a given signal-to-noise ratio (Bichot et al., 2001b; Shadlen et al., 1996). This is consistent with accounts of variation of search efficiency in terms of signal detection theory (Palmer et al., 2000). Confronted with stimulus ambiguity and armed with a target template, a top-down influence can bias processing of stimuli that resemble the target (Bundesen et al., 2005; Desimone and Duncan, 1995; Sato et al., 2003). The dense reciprocity of connectivity between FEF and extrastriate visual cortex (Schall et al., 1995b) makes it difficult to distinguish the respective contributions of activity in areas like V4 and MT signaling the features of search items (Ogawa and Komatsu, 2004) and activation in FEF feeding back to influence extrastriate areas (Hamker, 2005; Moore and Armstrong, 2003). This basic question may be resolved in future studies that directly compare the timing of signals across areas.

In contrast to what we found in FEF, a recent study of area LIP in macaques performing a different visual search task reported that the time for target selection did not vary with set size (Balan et al., 2008). We believe that these contradictory findings are unlikely to be due to differences between LIP and FEF and instead can be attributed to differences in performance. The effect of set size on RT was larger in our study of FEF than it was in the study of LIP. For example, we obtained a significant increase of RT with set size in 100% of the experimental sessions, compared with roughly 70% of the sessions reported in the LIP study. Also, we obtained a variation of RT relative to the overall mean RT from the largest (8) to the smallest (2) set size of 2543%; the study of LIP found a ratio from the largest (6) to the smallest

(2) set size of around 10%. Finally, the error rates in our experiment did not vary substantially with set size; the error rates in the LIP study increased with set size. Consequently, it seems most plausible that we observed the variation of RT with neural selection time because we obtained a larger variation of RT against which to perform the regression.

In summary, when presented with complex search arrays containing more distractors, FEF neurons, as part of a distributed network, take longer to locate the target because the representations of both target and distractors are weaker. This provides a mechanistic basis for the capacity limitation that is expressed when visual inputs compete for representation.

CHAPTER VIII

GENERAL DISCUSSION

> In proportion to the development of the faculty of attention are the intellectual and reflective powers manifested. This is in accordance with the anatomical development of the frontal lobes of the brain, and we have various experimental and pathological data for localizing in these centers of inhibition, the physiological substrata of this psychological faculty.
>
> —Ferrier (1876)

8.1 Summary of results

How does the brain select visual targets for eye movements? Chapters 2-7 describe studies of the neural coding and timing of visual target selection. We recorded neural activity while macaques performed visual search in which they were trained to move their eyes to a target stimulus among an array of distractor stimuli for a reward. Three signals were used to measure the relationship between the decision to move the eyes to a target and neural activity: spike rates from neurons in FEF, LFPs from FEF, and ERPs recorded from the skull. We found that (1) FEF neurons cooperated and competed to select visual targets, measured using correlations between spike times of simultaneously recorded neurons, (2) FEF neurons interacted more when the visual search task was easier (i.e., the target and distractors were easily discriminable), measured using a multivariate analysis and decreased firing variability before eye movements, (3) FEF neurons decreased firing variability around the time of target selection by the mean firing rate, (4) FEF neurons were distinguished both

functionally and biophysically, on the basis of action potential width, (5) FEF may be a source of a human cognitive event-related potential (the N2pc) that marks the allocation of attention, and (6) the time between visual search array presentation and the time that FEF neurons discriminated between target and distractors was later when there were more stimuli the animal needed to choose from.

8.2 Decision making in other tasks and sensory systems

The neural basis and circuits of decision making nonhuman primates (Gold and Shadlen, 2007; Schall, 2003a) and invertebrates (Kristan, 2008) has received much attention in the last two decades. Is our work limited to visual target selection and attention or does it generalize to other tasks and sensory systems? Put another way, does the brain use different perceptual decision making processes for different contexts and sensory modalities, or is there a general (or "central") mechanism for perceptual decision making? A few studies have examined perceptual decision making in other sensory modalities across species. In monkeys making somatosensory decisions, neurons in parietal cortex reflect the outcome of the decision (Romo et al., 2002). Microstimulation of primary somatosensory cortex biases somatosensory discrimination decisions (Romo et al., 1998, 2000), analogous to similar work in MT and LIP.

Several studies have examined perceptual decision making in the auditory system (e.g., Binder et al., 2004), olfactory system (e.g., Uchida and Mainen, 2003) and gustatory system (e.g., Padoa-Schioppa and Assad, 2006, 2008). In humans, there may be a general circuit involved in perceptual decision making irrespective of response

modality (Heekeren et al., 2004, 2006).

8.3 Neural integration in perceptual decision making

A common theme of perceptual decision-making studies across sensory modalities is the integration of sensory information over time. It is well known that neural integration exists in, for example, eye movement generation in the brainstem (Aksay et al., 2001; Cannon et al., 1983; Cannon and Robinson, 1987; Koulakov et al., 2002). Recent studies have described neural activity that resembles activation functions in mathematical models of decision making. For example, FEF movement neurons increase firing rates before saccades in a manner similar to diffusion models (Hanes and Schall, 1996); this increase may reflect integration of visual inputs from visual and visuomovement neurons in FEF (Purcell et al., 2008) or, similarly, in SC (Schiller and Koerner, 1971). A random-dot motion task has been used in monkeys to show that LIP neurons appear to integrate inputs from MT (Mazurek et al., 2003).

Not all models of decision making assume integration of sensory input by a different population of neurons, however (Ghose, 2006; Ghose and Harrison, 2009; Ludwig et al., 2005; Nienborg and Cumming, 2009). In a recent study, observers made saccades to a target stimulus that had, on average over time, higher luminance than the distractor, but at any given moment could have lower luminance than the distractor stimulus (Ludwig et al., 2005). Observers did not use the optimal strategy of integrating luminance over time. Instead, they appeared to use a temporal impulse response

8.4 Learning

The animals in our studies were well-trained and performed several thousand trials of visual search each session over the course of many months. Although we did not include learning as a variable in our experiments, it is well known that training induces behavioral and neural changes. In humans, training in visual search (e.g., Czerwinski et al., 1992) and other perceptual decision tasks (e.g., Ahissar and Hochstein, 1997) results in faster RT and higher percent correct. Several changes in different brain areas have been reported during learning or as a result of training. In visual search, FEF neurons in monkeys repeatedly exposed to one target have higher firing rates when shown that target than a rare target (Bichot et al., 1996). In monkeys learning a random-dot motion discrimination task, LIP neurons increase their firing rate selectivity for direction of motion, while MT neurons maintain the same magnitude of selectivity for motion (Law and Gold, 2008). In humans, there is evidence for changes in V1 with training on an orientation discrimination task (Schiltz et al., 1999).

Many of these behavioral and neural changes fall under the umbrella of *plasticity*. Despite the wealth of studies reporting these changes, little is known about how they occur. Synaptic long-term potentiation and long-term depression, involving input-dependent changes in pre- and postsynaptic insertion of receptors, are commonly thought to underlie plasticity (Malenka and Bear, 2004), although this has yet to be explored fully *in vivo*.

8.5 A preview of things to come

Neuroscience, like most of science, has developed in parallel with technological advances. The discovery of electricity in the 19$^{\text{th}}$ century led to early recordings of neural activity (Caton, 1875) and early observations of the effects of electrical stimulation on brain function and behavior (Ferrier, 1876; Fritsch and Hitzig, 1870). Similarly, 20$^{\text{th}}$-century revolutions in genetics, molecular biology and physics have led to advances in genetic manipulations and functional brain imaging. By the end of 21$^{\text{st}}$ century we may be able to map poetic statements about the brain onto reality:

> The neural flash swoops relentlessly in its Achillean path, in shapes stranger then [sic] the dash of a gnat-hungry swallow; every twist, every turn fore-ordained by the neural structure in Achilles' brain, until sensory input messages interfere.
>
> —Hofstadter (1979)

REFERENCES

Abeles M. *Corticonics: Neural Circuits of the Cerebral Cortex*. Cambridge: Cambridge University Press, 1991.

Adrian ED, Matthews BH. The interpretation of potential waves in the cortex. *J Physiol* 81: 440–471, 1934.

Aertsen AM, Gerstein GL, Habib MK, Palm G. Dynamics of neuronal firing correlation: modulation of "effective connectivity". *J Neurophysiol* 61: 900–917, 1989.

Ahissar M, Ahissar E, Bergman H, Vaadia E. Encoding of sound-source location and movement: activity of single neurons and interactions between adjacent neurons in the monkey auditory cortex. *J Neurophysiol* 67: 203–215, 1992.

Ahissar M, Hochstein S. Task difficulty and the specificity of perceptual learning. *Nature* 387: 401–406, 1997.

Aksay E, Gamkrelidze G, Seung HS, Baker R, Tank DW. In vivo intracellular recording and perturbation of persistent activity in a neural integrator. *Nat Neurosci* 4: 184–193, 2001.

Allum JH, Hepp-Reymond MC, Gysin R. Cross-correlation analysis of interneuronal connectivity in the motor cortex of the monkey. *Brain Res* 231: 325–334, 1982.

Andersen RA, Buneo CA. Intentional maps in posterior parietal cortex. *Annu Rev Neurosci* 25: 189–220, 2002.

Armstrong KM, Fitzgerald JK, Moore T. Changes in visual receptive fields with microstimulation of frontal cortex. *Neuron* 50: 791–798, 2006.

Armstrong KM, Moore T. Rapid enhancement of visual cortical response discriminability by microstimulation of the frontal eye field. *Proc Natl Acad Sci U S A* 104: 9499–9504, 2007.

Arthur DL, Starr A. Task-relevant late positive component of the auditory event-related potential in monkeys resembles P300 in humans. *Science* 223: 186–188, 1984.

Averbeck BB, Latham PE, Pouget A. Neural correlations, population coding and computation. *Nat Rev Neurosci* 7: 358–366, 2006.

Averbeck BB, Lee D. Neural noise and movement-related codes in the macaque supplementary motor area. *J Neurosci* 23: 7630–7641, 2003.

Averbeck BB, Lee D. Coding and transmission of information by neural ensembles. *Trends Neurosci* 27: 225–230, 2004.

Bair W, Zohary E, Newsome WT. Correlated firing in macaque visual area MT: time scales and relationship to behavior. *J Neurosci* 21: 1676–1697, 2001.

Baker SN, Curio G, Lemon RN. EEG oscillations at 600 Hz are macroscopic markers for cortical spike bursts. *J Physiol* 550: 529–534, 2003.

Balan PF, Oristaglio J, Schneider DM, Gottlieb J. Neuronal correlates of the set-size effect in monkey lateral intraparietal area. *PLoS Biol* 6: e158, 2008.

Barone P, Batardiere A, Knoblauch K, Kennedy H. Laminar distribution of neurons in extrastriate areas projecting to visual areas V1 and V4 correlates with the hierarchical rank and indicates the operation of a distance rule. *J Neurosci* 20: 3263–3281, 2000.

Barthó P, Hirase H, Monconduit L, Zugaro M, Harris KD, Buzsáki G. Characterization of neocortical principal cells and interneurons by network interactions and extracellular features. *J Neurophysiol* 92: 600–608, 2004.

Basso MA, Wurtz RH. Modulation of neuronal activity in superior colliculus by changes in target probability. *J Neurosci* 18: 7519–7534, 1998.

Becker W, Jürgens R. An analysis of the saccadic system by means of double step stimuli. *Vision Res* 19: 967–983, 1979.

Behrmann M, Geng JJ, Shomstein S. Parietal cortex and attention. *Curr Opin Neurobiol* 14: 212–217, 2004.

Bergen JR, Julesz B. Parallel versus serial processing in rapid pattern discrimination. *Nature* 303: 696–698, 1983.

Berger H. Über das elektrenkephalogramm des menschen. *Arch Psychiat Nervenkr* 87: 527–570, 1929.

Bichot NP, Chenchal Rao S, Schall JD. Continuous processing in macaque frontal cortex during visual search. *Neuropsychologia* 39: 972–982, 2001a.

Bichot NP, Desimone R. Finding a face in the crowd: parallel and serial neural mechanisms of visual selection. *Prog Brain Res* 155: 147–156, 2006.

Bichot NP, Rossi AF, Desimone R. Parallel and serial neural mechanisms for visual search in macaque area V4. *Science* 308: 529–534, 2005.

Bichot NP, Schall JD. Effects of similarity and history on neural mechanisms of visual selection. *Nat Neurosci* 2: 549–554, 1999a.

Bichot NP, Schall JD. Saccade target selection in macaque during feature and conjunction visual search. *Vis Neurosci* 16: 81–89, 1999b.

Bichot NP, Schall JD, Thompson KG. Visual feature selectivity in frontal eye fields induced by experience in mature macaques. *Nature* 381: 697–699, 1996.

Bichot NP, Thompson KG, Chenchal Rao S, Schall JD. Reliability of macaque frontal eye field neurons signaling saccade targets during visual search. *J Neurosci* 21: 713–725, 2001b.

Binder JR, Liebenthal E, Possing ET, Medler DA, Ward BD. Neural correlates of sensory and decision processes in auditory object identification. *Nat Neurosci* 7: 295–301, 2004.

Bisley JW, Goldberg ME. Neuronal activity in the lateral intraparietal area and spatial attention. *Science* 299: 81–86, 2003.

Boussaoud D, Wise SP. Primate frontal cortex: neuronal activity following attentional versus intentional cues. *Exp Brain Res* 95: 15–27, 1993.

Braitenberg V, Schüz A. *Anatomy of the Cortex: Statistics and Geometry.* Berlin: Springer-Verlag, 1991.

Britten KH, Shadlen MN, Newsome WT, Movshon JA. The analysis of visual motion: a comparison of neuronal and psychophysical performance. *J Neurosci* 12: 4745–4765, 1992.

Brody CD. Correlations without synchrony. *Neural Comput* 11: 1537–1551, 1999a.

Brody CD. Disambiguating different covariation types. *Neural Comput* 11: 1527–1535, 1999b.

Brown EN, Barbieri R, Ventura V, Kass RE, Frank LM. The time-rescaling theorem and its application to neural spike train data analysis. *Neural Comput* 14: 325–346, 2002.

Brown SP, Hestrin S. Intracortical circuits of pyramidal neurons reflect their long-range axonal targets. *Nature* 457: 1133–1136, 2009.

Bruce CJ, Goldberg ME. Primate frontal eye fields. I. Single neurons discharging before saccades. *J Neurophysiol* 53: 603–635, 1985.

Bruce CJ, Goldberg ME, Bushnell MC, Stanton GB. Primate frontal eye fields. II. Physiological and anatomical correlates of electrically evoked eye movements. *J Neurophysiol* 54: 714–734, 1985.

Brunia CH, Vingerhoets AJ. CNV and EMG preceding a plantar flexion of the foot. *Biol Psychol* 11: 181–191, 1980.

Buchwald JS, Hala ES, Schramm S. Comparison of multiple-unit and electroencephalogram activity recorded from the same brain sites during behavioural conditioning. *Nature* 205: 1012–1014, 1965.

Bullier J, Henry GH. Laminar distribution of first-order neurons and afferent terminals in cat striate cortex. *J Neurophysiol* 42: 1271–1281, 1979.

Bundesen C. A theory of visual attention. *Psychol Rev* 97: 523–547, 1990.

Bundesen C, Habekost T, Kyllingsbæk S. A neural theory of visual attention: bridging cognition and neurophysiology. *Psychol Rev* 112: 291–328, 2005.

Buschman TJ, Miller EK. Top-down versus bottom-up control of attention in the prefrontal and posterior parietal cortices. *Science* 315: 1860–1862, 2007.

Bushnell MC, Goldberg ME, Robinson DL. Behavioral enhancement of visual responses in monkey cerebral cortex. I. Modulation in posterior parietal cortex related to selective visual attention. *J Neurophysiol* 46: 755–772, 1981.

Camalier CR, Gotler A, Murthy A, Thompson KG, Logan GD, Palmeri TJ, Schall JD. Dynamics of saccade target selection: race model analysis of double step and search step saccade production in human and macaque. *Vision Res* 47: 2187–2211, 2007.

Cannon SC, Robinson DA. Loss of the neural integrator of the oculomotor system from brain stem lesions in monkey. *J Neurophysiol* 57: 1383–1409, 1987.

Cannon SC, Robinson DA, Shamma S. A proposed neural network for the integrator of the oculomotor system. *Biol Cybern* 49: 127–136, 1983.

Carello CD, Krauzlis RJ. Manipulating intent: evidence for a causal role of the superior colliculus in target selection. *Neuron* 43: 575–583, 2004.

Carpenter RH, Williams ML. Neural computation of log likelihood in control of saccadic eye movements. *Nature* 377: 59–62, 1995.

Carrasco M, Yeshurun Y. The contribution of covert attention to the set-size and eccentricity effects in visual search. *J Exp Psychol Hum Percept Perform* 24: 673–692, 1998.

Caspi A, Beutter BR, Eckstein MP. The time course of visual information accrual guiding eye movement decisions. *Proc Natl Acad Sci U S A* 101: 13086–13090, 2004.

Caton R. The electric currents of the brain. *Br Med J* 2: 278, 1875.

Cauli B, Audinat E, Lambolez B, Angulo MC, Ropert N, Tsuzuki K, Hestrin S, Rossier J. Molecular and physiological diversity of cortical nonpyramidal cells. *J Neurosci* 17: 3894–3906, 1997.

Celikel T, Szostak VA, Feldman DE. Modulation of spike timing by sensory deprivation during induction of cortical map plasticity. *Nat Neurosci* 7: 534–541, 2004.

Chelazzi L. Neural mechanisms for stimulus selection in cortical areas of the macaque subserving object vision. *Behav Brain Res* 71: 125–134, 1995.

Chelazzi L, Duncan J, Miller EK, Desimone R. Responses of neurons in inferior temporal cortex during memory-guided visual search. *J Neurophysiol* 80: 2918–2940, 1998.

Chelazzi L, Miller EK, Duncan J, Desimone R. Responses of neurons in macaque area V4 during memory-guided visual search. *Cereb Cortex* 11: 761–772, 2001.

Chen Y, Martinez-Conde S, Macknik SL, Bereshpolova Y, Swadlow HA, Alonso JM. Task difficulty modulates the activity of specific neuronal populations in primary visual cortex. *Nat Neurosci* 11: 974–982, 2008.

Churchland MM, Yu BM, Ryu SI, Santhanam G, Shenoy KV. Neural variability in premotor cortex provides a signature of motor preparation. *J Neurosci* 26: 3697–3712, 2006.

Clark VP, Fan S, Hillyard SA. Identification of early visual evoked potential generators by retinotopic and topographic analyses. *Hum Brain Mapp* 2: 170–187, 1995.

Clarke E, Jacyna LS. *Nineteenth-Century Origins of Neuroscientific Concepts*. Berkeley: University of California Press, 1987.

Cohen JY, Heitz RP, Woodman GF, Schall JD. Neural basis of the set-size effect in frontal eye field: timing of attention during visual search. *J Neurophysiol* 101: 1699–1704, 2009a.

Cohen JY, Pouget P, Heitz RP, Woodman GF, Schall JD. Biophysical support for functionally distinct cell types in the frontal eye field. *J Neurophysiol* 101: 912–916, 2009b.

Cohen JY, Pouget P, Woodman GF, Subraveti CR, Schall JD, Rossi AF. Difficulty of visual search modulates neuronal interactions and response variability in the frontal eye field. *J Neurophysiol* 98: 2580–2587, 2007.

Cohen MR, Newsome WT. Context-dependent changes in functional circuitry in visual area MT. *Neuron* 60: 162–173, 2008.

Cohen MR, Newsome WT. Estimates of the contribution of single neurons to perception depend on timescale and noise correlation. *J Neurosci* 29: 6635–6648, 2009.

Cohen Y, Cohen JY. *Statistics and Data with R: An Applied Approach Through Examples*. London: Wiley, 2008.

Condé F, Lund JS, Jacobowitz DM, Baimbridge KG, Lewis DA. Local circuit neurons immunoreactive for calretinin, calbindin D-28k or parvalbumin in monkey prefrontal cortex: distribution and morphology. *J Comp Neurol* 341: 95–116, 1994.

Connor CE, Preddie DC, Gallant JL, Van Essen DC. Spatial attention effects in macaque area V4. *J Neurosci* 17: 3201–3214, 1997.

Connors BW, Gutnick MJ. Intrinsic firing patterns of diverse neocortical neurons. *Trends Neurosci* 13: 99–104, 1990.

Constantinidis C. Posterior parietal mechanisms of visual attention. *Rev Neurosci* 17: 415–427, 2006.

Constantinidis C, Franowicz MN, Goldman-Rakic PS. Coding specificity in cortical microcircuits: a multiple-electrode analysis of primate prefrontal cortex. *J Neurosci* 21: 3646–3655, 2001a.

Constantinidis C, Franowicz MN, Goldman-Rakic PS. The sensory nature of mnemonic representation in the primate prefrontal cortex. *Nat Neurosci* 4: 311–316, 2001b.

Constantinidis C, Goldman-Rakic PS. Correlated discharges among putative pyramidal neurons and interneurons in the primate prefrontal cortex. *J Neurophysiol* 88: 3487–3497, 2002.

Constantinidis C, Steinmetz MA. Neuronal responses in area 7a to multiple-stimulus displays: I. neurons encode the location of the salient stimulus. *Cereb Cortex* 11: 581–591, 2001a.

Constantinidis C, Steinmetz MA. Neuronal responses in area 7a to multiple stimulus displays: II. responses are suppressed at the cued location. *Cereb Cortex* 11: 592–597, 2001b.

Cooper R, Winter AL, Crow HJ, Walter WG. Comparison of subcortical, cortical and scalp activity using chronically indwelling electrodes in man. *Electroencephalogr Clin Neurophysiol* 18: 217–228, 1965.

Couzin ID. Collective cognition in animal groups. *Trends Cogn Sci* 13: 36–43, 2009.

Crawford TJ, Muller HJ. Spatial and temporal effects of spatial attention on human saccadic eye movements. *Vision Res* 32: 293–304, 1992.

Csicsvari J, Hirase H, Czurkó A, Mamiya A, Buzsáki G. Oscillatory coupling of hippocampal pyramidal cells and interneurons in the behaving Rat. *J Neurosci* 19: 274–287, 1999.

Czerwinski M, Lightfoot N, Shiffrin RM. Automatization and training in visual search. *Am J Psychol* 105: 271–315, 1992.

Das A, Gilbert CD. Topography of contextual modulations mediated by short-range interactions in primary visual cortex. *Nature* 399: 655–661, 1999.

David SV, Hayden BY, Mazer JA, Gallant JL. Attention to stimulus features shifts spectral tuning of V4 neurons during natural vision. *Neuron* 59: 509–521, 2008.

de la Rocha J, Doiron B, Shea-Brown E, Josić K, Reyes A. Correlation between neural spike trains increases with firing rate. *Nature* 448: 802–806, 2007.

De Monte S, d'Ovidio F, Danø S, Sørensen PG. Dynamical quorum sensing: Population density encoded in cellular dynamics. *Proc Natl Acad Sci U S A* 104: 18377–18381, 2007.

de Ruyter van Steveninck RR, Lewen GD, Strong SP, Koberle R, Bialek W. Reproducibility and variability in neural spike trains. *Science* 275: 1805–1808, 1997.

DeAngelis GC, Ghose GM, Ohzawa I, Freeman RD. Functional micro-organization of primary visual cortex: receptive field analysis of nearby neurons. *J Neurosci* 19: 4046–4064, 1999.

deCharms RC, Merzenich MM. Primary cortical representation of sounds by the coordination of action-potential timing. *Nature* 381: 610–613, 1996.

Desimone R, Duncan J. Neural mechanisms of selective visual attention. *Annu Rev Neurosci* 18: 193–222, 1995.

Desimone R, Schein SJ. Visual properties of neurons in area V4 of the macaque: sensitivity to stimulus form. *J Neurophysiol* 57: 835–868, 1987.

Deubel H. The time course of presaccadic attention shifts. *Psychol Res* 72: 630–640, 2008.

Deubel H, Schneider WX. Saccade target selection and object recognition: evidence for a common attentional mechanism. *Vision Res* 36: 1827–1837, 1996.

DiCarlo JJ, Maunsell JH. Form representation in monkey inferotemporal cortex is virtually unaltered by free viewing. *Nat Neurosci* 3: 814–821, 2000.

DiCarlo JJ, Maunsell JH. Using neuronal latency to determine sensory-motor processing pathways in reaction time tasks. *J Neurophysiol* 93: 2974–2986, 2005.

Donders FC. On the speed of mental processes. *Acta Psychol (Amst)* 30: 412–431, 1868/1969.

Dorris MC, Paré M, Munoz DP. Neuronal activity in monkey superior colliculus related to the initiation of saccadic eye movements. *J Neurosci* 17: 8566–8579, 1997.

Dow BM. Functional classes of cells and their laminar distribution in monkey visual cortex. *J Neurophysiol* 37: 927–946, 1974.

Duncan J, Humphreys GW. Visual search and stimulus similarity. *Psychol Rev* 96: 433–458, 1989.

Ebersole JS. Defining epileptogenic foci: past, present, future. *J Clin Neurophysiol* 14: 470–483, 1997.

Eckstein MP, Beutter BR, Stone LS. Quantifying the performance limits of human saccadic targeting during visual search. *Perception* 30: 1389–1401, 2001.

Engel AK, König P, Singer W. Direct physiological evidence for scene segmentation by temporal coding. *Proc Natl Acad Sci U S A* 88: 9136–9140, 1991a.

Engel AK, Kreiter AK, König P, Singer W. Synchronization of oscillatory neuronal responses between striate and extrastriate visual cortical areas of the cat. *Proc Natl Acad Sci U S A* 88: 6048–6052, 1991b.

Eriksen CW, Hoffman JE. Temporal and spatial characteristics of selective encoding from visual displays. *Percept Psychophys* 12: 201–204, 1972.

Everling S, Dorris MC, Klein RM, Munoz DP. Role of primate superior colliculus in preparation and execution of anti-saccades and pro-saccades. *J Neurosci* 19: 2740–2754, 1999.

Everling S, Munoz DP. Neuronal correlates for preparatory set associated with pro-saccades and anti-saccades in the primate frontal eye field. *J Neurosci* 20: 387–400, 2000.

Everling S, Tinsley CJ, Gaffan D, Duncan J. Selective representation of task-relevant objects and locations in the monkey prefrontal cortex. *Eur J Neurosci* 23: 2197–2214, 2006.

Fecteau JH, Munoz DP. Salience, relevance, and firing: a priority map for target selection. *Trends Cogn Sci* 10: 382–390, 2006.

Fecteau JH, Munoz DP. Warning signals influence motor processing. *J Neurophysiol* 97: 1600–1609, 2007.

Feng JF, Brown D. Coefficient of variation of interspike intervals greater than 0.5. How and when? *Biol Cybern* 80: 291–297, 1999.

Ferrera VP, Cohen JK, Lee BB. Activity of prefrontal neurons during location and color delayed matching tasks. *Neuroreport* 10: 1315–1322, 1999.

Ferrera VP, Lisberger SG. Attention and target selection for smooth pursuit eye movements. *J Neurosci* 15: 7472–7484, 1995.

Ferrera VP, Lisberger SG. Neuronal responses in visual areas MT and MST during smooth pursuit target selection. *J Neurophysiol* 78: 1433–1446, 1997.

Ferrier D. Experiments on the brains of monkeys. *Proc R Soc Lond* 23: 409–430, 1874-1875.

Ferrier D. *The Functions of the Brain.* London: Smith, Elder and Company, 1876.

Findlay JM. Saccade target selection during visual search. *Vision Res* 37: 617–631, 1997.

Fischer B, Boch R. Enhanced activation of neurons in prelunate cortex before visually guided saccades of trained rhesus monkeys. *Exp Brain Res* 44: 129–137, 1981.

Foote SL, Aston-Jones G, Bloom FE. Impulse activity of locus coeruleus neurons in awake rats and monkeys is a function of sensory stimulation and arousal. *Proc Natl Acad Sci U S A* 77: 3033–3037, 1980.

Fries W. Cortical projections to the superior colliculus in the macaque monkey: a retrograde study using horseradish peroxidase. *J Comp Neurol* 230: 55–76, 1984.

Fritsch G, Hitzig E. Uber die elektrische Erregbarkeit des Grosshirns. *Arch Anat Physiol Wiss Med* 37: 300–332, 1870.

Fromm GH, Bond HW. Slow changes in the electrocorticogram and the activity of cortical neurons. *Electroencephalogr Clin Neurophysiol* 17: 520–523, 1964.

Fromm GH, Bond HW. The relationship between neuron activity and cortical steady potentials. *Electroencephalogr Clin Neurophysiol* 22: 159–166, 1967.

Funahashi S, Bruce CJ, Goldman-Rakic PS. Mnemonic coding of visual space in the monkey's dorsolateral prefrontal cortex. *J Neurophysiol* 61: 331–349, 1989.

Funahashi S, Inoue M. Neuronal interactions related to working memory processes in the primate prefrontal cortex revealed by cross-correlation analysis. *Cereb Cortex* 10: 535–551, 2000.

Fuster J. *The Prefrontal Cortex*. London: Academic Press, 2008, 4th edn.

Gallant JL, Connor CE, Van Essen DC. Neural activity in areas V1, V2 and V4 during free viewing of natural scenes compared to controlled viewing. *Neuroreport* 9: 2153–2158, 1998.

Gardner JL, Lisberger SG. Linked target selection for saccadic and smooth pursuit eye movements. *J Neurosci* 21: 2075–2084, 2001.

Gattass R, Sousa APB, Gross CG. Visuotopic organization and extent of V3 and V4 of the macaque. *J Neurosci* 8: 1831–1845, 1988.

Ghose GM. Strategies optimize the detection of motion transients. *J Vis* 6: 429–440, 2006.

Ghose GM, Harrison IT. Temporal precision of neuronal information in a rapid perceptual judgment. *J Neurophysiol* 101: 1480–1493, 2009.

Glimcher PW, Sparks DL. Movement selection in advance of action in the superior colliculus. *Nature* 355: 542–545, 1992.

Glover A, Ghilardi MF, Bodis-Wollner I, Onofrj M, Mylin LH. Visual 'cognitive' evoked potentials in the behaving monkey. *Electroencephalogr Clin Neurophysiol* 80: 65–72, 1991.

Gochin PM, Miller EK, Gross CG, Gerstein GL. Functional interactions among neurons in inferior temporal cortex of the awake macaque. *Exp Brain Res* 84: 505–516, 1991.

Gold JI, Shadlen MN. The neural basis of decision making. *Annu Rev Neurosci* 30: 535–574, 2007.

Goldberg ME, Bushnell MC. Behavioral enhancement of visual responses in monkey cerebral cortex. II. Modulation in frontal eye fields specifically related to saccades. *J Neurophysiol* 46: 773–787, 1981.

Goldberg ME, Wurtz RH. Activity of superior colliculus in behaving monkey. II. Effect of attention on neuronal responses. *J Neurophysiol* 35: 560–574, 1972.

González-Burgos G, Krimer LS, Povysheva NV, Barrionuevo G, Lewis DA. Functional properties of fast spiking interneurons and their synaptic connections with pyramidal cells in primate dorsolateral prefrontal cortex. *J Neurophysiol* 93: 942–953, 2005.

Gottlieb J. From thought to action: the parietal cortex as a bridge between perception, action, and cognition. *Neuron* 53: 9–16, 2007.

Gottlieb JP, Kusunoki M, Goldberg ME. The representation of visual salience in monkey parietal cortex. *Nature* 391: 481–484, 1998.

Gregoriou GG, Gotts SJ, Zhou H, Desimone R. High-frequency, long-range coupling between prefrontal and visual cortex during attention. *Science* 324: 1207–1210, 2009.

Gur M, Beylin A, Snodderly DM. Physiological properties of macaque V1 neurons are correlated with extracellular spike amplitude, duration, and polarity. *J Neurophysiol* 82: 1451–1464, 1999.

Hamker FH. The reentry hypothesis: the putative interaction of the frontal eye field, ventrolateral prefrontal cortex, and areas V4, IT for attention and eye movement. *Cereb Cortex* 15: 431–447, 2005.

Hamker FH, Zirnsak M. V4 receptive field dynamics as predicted by a systems-level model of visual attention using feedback from the frontal eye field. *Neural Netw* 19: 1371–1382, 2006.

Hanes DP, Patterson WF, Schall JD. Role of frontal eye fields in countermanding saccades: visual, movement, and fixation activity. *J Neurophysiol* 79: 817–834, 1998.

Hanes DP, Schall JD. Neural control of voluntary movement initiation. *Science* 274: 427–430, 1996.

Hasegawa RP, Matsumoto M, Mikami A. Search target selection in monkey prefrontal cortex. *J Neurophysiol* 84: 1692–1696, 2000.

Hayden BY, Gallant JL. Time course of attention reveals different mechanisms for spatial and feature-based attention in area V4. *Neuron* 47: 637–643, 2005.

Hayhoe M, Ballard D. Eye movements in natural behavior. *Trends Cogn Sci* 9: 188–194, 2005.

Heekeren HR, Marrett S, Bandettini PA, Ungerleider LG. A general mechanism for perceptual decision-making in the human brain. *Nature* 431: 859–862, 2004.

Heekeren HR, Marrett S, Ruff DA, Bandettini PA, Ungerleider LG. Involvement of human left dorsolateral prefrontal cortex in perceptual decision making is independent of response modality. *Proc Natl Acad Sci U S A* 103: 10023–10028, 2006.

Heinze HJ, Mangun GR, Burchert W, Hinrichs H, Scholz M, Münte TF, Gös A, Scherg M, Johannes S, Hundeshagen H, Gazzaniga MS, Hillyard SA. Combined spatial and temporal imaging of brain activity during visual selective attention in humans. *Nature* 372: 543–546, 1994.

Helmholtz H. Ueber einige Gesetze der Vertheilung elektrischer Ströme in körperlichen Leitern mit Anwendung auf die thierisch-elektrischen Versuche. *Ann Physik Chem* 89: 211–233, 354–377, 1853.

Helminski JO, Segraves MA. Macaque frontal eye field input to saccade-related neurons in the superior colliculus. *J Neurophysiol* 90: 1046–1062, 2003.

Henderson JM. Stimulus discrimination following covert attentional orienting to an exogenous cue. *J Exp Psychol Hum Percept Perform* 17: 91–106, 1991.

Henderson JM, Pierce GL. Eye movements during scene viewing: evidence for mixed control of fixation durations. *Psychon Bull Rev* 15: 566–573, 2008.

Henze DA, Borhegyi Z, Csicsvari J, Mamiya A, Harris KD, Buzsáki G. Intracellular features predicted by extracellular recordings in the hippocampus in vivo. *J Neurophysiol* 84: 390–400, 2000.

Hikosaka O, Wurtz RH. Visual and oculomotor functions of monkey substantia nigra pars reticulata. III. Memory-contingent visual and saccade responses. *J Neurophysiol* 49: 1268–1284, 1983.

Hillyard SA, Anllo-Vento L. Event-related brain potentials in the study of visual selective attention. *Proc Natl Acad Sci U S A* 95: 781–787, 1998.

Hoffman JE, Subramaniam B. The role of visual attention in saccadic eye movements. *Percept Psychophys* 57: 787–795, 1995.

Hofstadter DR. *Gödel, Escher, Bach: an Eternal Golden Braid*. New York: Basic Books, 1979.

Hooge IT, Erkelens CJ. Control of fixation duration in a simple search task. *Percept Psychophys* 58: 969–976, 1996.

Hooge IT, Erkelens CJ. Adjustment of fixation duration in visual search. *Vision Res* 38: 1295–1302, 1998.

Hooge IT, Erkelens CJ. Peripheral vision and oculomotor control during visual search. *Vision Res* 39: 1567–1575, 1999.

Hopf JM, Boelmans K, Schoenfeld MA, Luck SJ, Heinze HJ. Attention to features precedes attention to locations in visual search: evidence from electromagnetic brain responses in humans. *J Neurosci* 24: 1822–1832, 2004.

Hopf JM, Luck SJ, Girelli M, Hagner T, Mangun GR, Scheich H, Heinze HJ. Neural sources of focused attention in visual search. *Cereb Cortex* 10: 1233–1241, 2000.

Horwitz GD, Newsome WT. Separate signals for target selection and movement specification in the superior colliculus. *Science* 284: 1158–1161, 1999.

Horwitz GD, Newsome WT. Target selection for saccadic eye movements: prelude activity in the superior colliculus during a direction-discrimination task. *J Neurophysiol* 86: 2543–2558, 2001.

Huerta MF, Krubitzer LA, Kaas JH. Frontal eye field as defined by intracortical microstimulation in squirrel monkeys, owl monkeys, and macaque monkeys: I. Subcortical connections. *J Comp Neurol* 253: 415–439, 1986.

Hunt AR, Kingstone A. Covert and overt voluntary attention: linked or independent? *Brain Res Cogn Brain Res* 18: 102–105, 2003.

Ignashchenkova A, Dicke PW, Haarmeier T, Thier P. Neuron-specific contribution of the superior colliculus to overt and covert shifts of attention. *Nat Neurosci* 7: 56–64, 2004.

Ipata AE, Gee AL, Goldberg ME, Bisley JW. Activity in the lateral intraparietal area predicts the goal and latency of saccades in a free-viewing visual search task. *J Neurosci* 26: 3656–3661, 2006.

Itti L, Koch C. A saliency-based search mechanism for overt and covert shifts of visual attention. *Vision Res* 40: 1489–1506, 2000.

Itti L, Koch C. Computational modelling of visual attention. *Nat Rev Neurosci* 2: 194–203, 2001.

Jackson A, Gee VJ, Baker SN, Lemon RN. Synchrony between neurons with similar muscle fields in monkey motor cortex. *Neuron* 38: 115–125, 2003.

Jacobs AM. *Eye Movements: From Physiology to Cognition*, chap. Toward a model of eye movement control in visual search, pp. 275–284. Elsevier (North Holland), 1987.

Javitt DC, Schroeder CE, Steinschneider M, Arezzo JC, Vaughan HG. Demonstration of mismatch negativity in the monkey. *Electroencephalogr Clin Neurophysiol* 83: 87–90, 1992.

Jonides J. Towards a model of the mind's eye's movement. *Can J Psychol* 34: 103–112, 1980.

Jouve B, Rosenstiehl P, Imbert M. A mathematical approach to the connectivity between the cortical visual areas of the macaque monkey. *Cereb Cortex* 8: 28–39, 1998.

Jovancevic-Misic J, Hayhoe M. Adaptive gaze control in natural environments. *J Neurosci* 29: 6234–6238, 2009.

Juan CH, Muggleton NG, Tzeng OJ, Hung DL, Cowey A, Walsh V. Segregation of visual selection and saccades in human frontal eye fields. *Cereb Cortex* 18: 2410–2415, 2008.

Juan CH, Shorter-Jacobi SM, Schall JD. Dissociation of spatial attention and saccade preparation. *Proc Natl Acad Sci* 101: 15541–15544, 2004.

Katzner S, Nauhaus I, Benucci A, Bonin V, Ringach DL, Carandini M. Local origin of field potentials in visual cortex. *Neuron* 61: 35–41, 2009.

Kawaguchi Y. Physiological subgroups of nonpyramidal cells with specific morphological characteristics in layer II/III of rat frontal cortex. *J Neurosci* 15: 2638–2655, 1995.

Kim B, Basso MA. Saccade target selection in the superior colliculus: a signal detection theory approach. *J Neurosci* 28: 2991–3007, 2008.

Kim JN, Shadlen MN. Neural correlates of a decision in the dorsolateral prefrontal cortex of the macaque. *Nat Neurosci* 2: 176–185, 1999.

Kim MS, Cave KR. Spatial attention in visual search for features and feature conjunctions. *Psychol Sci* 6: 376–380, 1995.

Klein R. *Attention and Performance VIII*, chap. Does oculomotor readiness mediate cognitive control of visual attention?, pp. 259–276. Erlbaum (Hillsdale, NJ), 1980.

Klein R, Kingstone A, Pontefract A. *Eye Movements and Visual Cognition*, chap. Orienting of visual attention, pp. 46–65. Springer-Verlag (New York), 1992.

Klein RM, Pontefract A. *Attention and Performance XV*, chap. Does oculomotor readiness mediate cognitive control of visual attention? Revisited!, pp. 333–350. MIT Press (Cambridge, MA), 1994.

Knierim JJ, van Essen DC. Neuronal responses to static texture patterns in area V1 of the alert macaque monkey. *J Neurophysiol* 67: 961–980, 1992.

Kodaka Y, Mikami A, Kubota K. Neuronal activity in the frontal eye field of the monkey is modulated while attention is focused on to a stimulus in the peripheral visual field, irrespective of eye movement. *Neurosci Res* 28: 291–298, 1997.

König P, Engel AK. Correlated firing in sensory-motor systems. *Curr Opin Neurobiol* 5: 511–519, 1995.

Koulakov AA, Raghavachari S, Kepecs A, Lisman JE. Model for a robust neural integrator. *Nat Neurosci* 5: 775–782, 2002.

Kowler E, Anderson E, Dosher B, Blaser E. The role of attention in the programming of saccades. *Vision Res* 35: 1897–1916, 1995.

Krauzlis R, Dill N. Neural correlates of target choice for pursuit and saccades in the primate superior colliculus. *Neuron* 35: 355–363, 2002.

Krauzlis RJ, Zivotofsky AZ, Miles FA. Target selection for pursuit and saccadic eye movements in humans. *J Cogn Neurosci* 11: 641–649, 1999.

Krimer LS, Zaitsev AV, Czanner G, Kröner S, González-Burgos G, Povysheva NV, Iyengar S, Barrionuevo G, Lewis DA. Cluster analysis-based physiological classification and morphological properties of inhibitory neurons in layers 2-3 of monkey dorsolateral prefrontal cortex. *J Neurophysiol* 94: 3009–3022, 2005.

Kristan WB. Neuronal decision-making circuits. *Curr Biol* 18: 928–932, 2008.

Kustov AA, Robinson DL. Shared neural control of attentional shifts and eye movements. *Nature* 384: 74–77, 1996.

Kusunoki M, Gottlieb J, Goldberg ME. The lateral intraparietal area as a salience map: the representation of abrupt onset, stimulus motion, and task relevance. *Vision Res* 40: 1459–1468, 2000.

Lachaux JP, Rudrauf D, Kahane P. Intracranial EEG and human brain mapping. *J Physiol Paris* 97: 613–628, 2003.

Lamme VA, Roelfsema PR. The distinct modes of vision offered by feedforward and recurrent processing. *Trends Neurosci* 23: 571–579, 2000.

Lamme VA, Van Dijk BW, Spekreijse H. Texture segregation is processed by primary visual cortex in man and monkey. Evidence from VEP experiments. *Vision Res* 32: 797–807, 1992.

Law CT, Gold JI. Neural correlates of perceptual learning in a sensory-motor, but not a sensory, cortical area. *Nat Neurosci* 11: 505–513, 2008.

Lee KM, Keller EL. Neural activity in the frontal eye fields modulated by the number of alternatives in target choice. *J Neurosci* 28: 2242–2251, 2008.

Letinic K, Zoncu R, Rakic P. Origin of GABAergic neurons in the human neocortex. *Nature* 417: 645–649, 2002.

Leuthold H, Jentzsch I. Distinguishing neural sources of movement preparation and execution. An electrophysiological analysis. *Biol Psychol* 60: 173–198, 2002.

Li X, Basso MA. Competitive stimulus interactions within single response fields of superior colliculus neurons. *J Neurosci* 25: 11357–11373, 2005.

Logothetis NK, Wandell BA. Interpreting the BOLD signal. *Annu Rev Physiol* 66: 735–769, 2004.

Luck SJ. *An Introduction to the Event-Related Potential Technique*. Cambridge, MA: MIT Press, 2006.

Luck SJ, Girelli M, McDermott MT, Ford MA. Bridging the gap between monkey neurophysiology and human perception: an ambiguity resolution theory of visual selective attention. *Cogn Psychol* 33: 64–87, 1997.

Luck SJ, Hillyard SA. Electrophysiological correlates of feature analysis during visual search. *Psychophysiology* 31: 291–308, 1994a.

Luck SJ, Hillyard SA. Spatial filtering during visual search: evidence from human electrophysiology. *J Exp Psychol Hum Percept Perform* 20: 1000–1014, 1994b.

Ludwig CJ, Gilchrist ID, McSorley E, Baddeley RJ. The temporal impulse response underlying saccadic decisions. *J Neurosci* 25: 9907–9912, 2005.

Malenka RC, Bear MF. LTP and LTD: an embarrassment of riches. *Neuron* 44: 5–21, 2004.

Maljkovic V, Nakayama K. Priming of pop-out: I. Role of features. *Mem Cognit* 22: 657–672, 1994.

Maljkovic V, Nakayama K. Priming of pop-out: II. The role of position. *Percept Psychophys* 58: 977–991, 1996.

Marsan CA. Electrical activity of the brain: slow waves and neuronal activity. *Isr J Med Sci* 1: 104–117, 1965.

Martina M, Schultz JH, Ehmke H, Monyer H, Jonas P. Functional and molecular differences between voltage-gated K+ channels of fast-spiking interneurons and pyramidal neurons of rat hippocampus. *J Neurosci* 18: 8111–8125, 1998.

Mazer JA, Gallant JL. Goal-related activity in V4 during free viewing visual search. Evidence for a ventral stream visual salience map. *Neuron* 40: 1241–1250, 2003.

Mazurek ME, Roitman JD, Ditterich J, Shadlen MN. A role for neural integrators in perceptual decision making. *Cereb Cortex* 13: 1257–1269, 2003.

McCormick DA, Connors BW, Lighthall JW, Prince DA. Comparative electrophysiology of pyramidal and sparsely spiny stellate neurons of the neocortex. *J Neurophysiol* 54: 782–806, 1985.

McCullagh P, Nelder JA. *Generalized Linear Models*. Boca Raton, FL: Chapman & Hall/CRC, 1989, 2nd edn.

McPeek RM. Incomplete suppression of distractor-related activity in the frontal eye field results in curved saccades. *J Neurophysiol* 96: 2699–2711, 2006.

McPeek RM. Reversal of a distractor effect on saccade target selection after superior colliculus inactivation. *J Neurophysiol* 99: 2694–2702, 2008.

McPeek RM, Han JH, Keller EL. Competition between saccade goals in the superior colliculus produces saccade curvature. *J Neurophysiol* 89: 2577–2590, 2003.

McPeek RM, Keller EL. Saccade target selection in the superior colliculus during a visual search task. *J Neurophysiol* 88: 2019–2034, 2002.

McPeek RM, Keller EL. Deficits in saccade target selection after inactivation of superior colliculus. *Nat Neurosci* 7: 757–763, 2004.

McPeek RM, Maljkovic V, Nakayama K. Saccades require focal attention and are facilitated by a short-term memory system. *Vision Res* 39: 1555–1566, 1999.

Mehta AD, Ulbert I, Schroeder CE. Intermodal selective attention in monkeys. I: distribution and timing of effects across visual areas. *Cereb Cortex* 10: 343–358, 2000a.

Mehta AD, Ulbert I, Schroeder CE. Intermodal selective attention in monkeys. II: physiological mechanisms of modulation. *Cereb Cortex* 10: 359–370, 2000b.

Michel CM, Murray MM, Lantz G, Gonzalez S, Spinelli L, Grave de Peralta R. EEG source imaging. *Clin Neurophysiol* 115: 2195–2222, 2004.

Miller J. Discrete and continuous models of human information processing: theoretical distinctions and empirical results. *Acta Psychol (Amst)* 67: 191–257, 1988.

Mirabella G, Bertini G, Samengo I, Kilavik BE, Frilli D, Della Libera C, Chelazzi L. Neurons in area V4 of the macaque translate attended visual features into behaviorally relevant categories. *Neuron* 54: 303–318, 2007.

Mitchell JF, Sundberg KA, Reynolds JH. Differential attention-dependent response modulation across cell classes in macaque visual area V4. *Neuron* 55: 131–141, 2007.

Mohler CW, Goldberg ME, Wurtz RH. Visual receptive fields of frontal eye field neurons. *Brain Res* 61: 385–389, 1973.

Monosov IE, Trageser JC, Thompson KG. Measurements of simultaneously recorded spiking activity and local field potentials suggest that spatial selection emerges in the frontal eye field. *Neuron* 57: 614–625, 2008.

Moore T. Shape representations and visual guidance of saccadic eye movements. *Science* 285: 1914–1917, 1999.

Moore T, Armstrong KM. Selective gating of visual signals by microstimulation of frontal cortex. *Nature* 421: 370–373, 2003.

Moore T, Chang MH. Presaccadic discrimination of receptive field stimuli by area V4 neurons. *Vision Res* 49: 1227–1232, 2009.

Moschovakis AK, Scudder CA, Highstein SM. The microscopic anatomy and physiology of the mammalian saccadic system. *Prog Neurobiol* 50: 133–254, 1996.

Motter BC. Neural correlates of attentive selection for color or luminance in extrastriate area V4. *J Neurosci* 14: 2178–2189, 1994.

Motter BC, Belky EJ. The guidance of eye movements during active visual search. *Vision Res* 38: 1805–1815, 1998.

Mountcastle VB, Andersen RA, Motter BC. The influence of attentive fixation upon the excitability of the light-sensitive neurons of the posterior parietal cortex. *J Neurosci* 1: 1218–1225, 1981.

Mountcastle VB, Talbot WH, Sakata H, Hyvärinen J. Cortical neuronal mechanisms in flutter-vibration studied in unanesthetized monkeys. Neuronal periodicity and frequency discrimination. *J Neurophysiol* 32: 452–484, 1969.

Muggleton NG, Juan CH, Cowey A, Walsh V. Human frontal eye fields and visual search. *J Neurophysiol* 89: 3340–3343, 2003.

Murthy A, Ray S, Shorter SM, Priddy EG, Schall JD, Thompson KG. Frontal eye field contributions to rapid corrective saccades. *J Neurophysiol* 97: 1457–1469, 2007.

Murthy A, Ray S, Shorter SM, Schall JD, Thompson KG. Neural control of visual search by frontal eye field: effects of unexpected target displacement on visual selection and saccade preparation. *J Neurophysiol* 101: 2485–2506, 2009.

Murthy A, Thompson KG, Schall JD. Dynamic dissociation of visual selection from saccade programming in frontal eye field. *J Neurophysiol* 86: 2634–2637, 2001.

Naegele JR, Katz LC. Cell surface molecules containing N-acetylgalactosamine are associated with basket cells and neurogliaform cells in cat visual cortex. *J Neurosci* 10: 540–557, 1990.

Najemnik J, Geisler WS. Simple summation rule for optimal fixation selection in visual search. *Vision Res* 49: 1286–1294, 2009.

Narayanan NS, Laubach M. Top-down control of motor cortex ensembles by dorsomedial prefrontal cortex. *Neuron* 52: 921–931, 2006.

Nelson MJ, Pouget P, Nilsen EA, Patten CD, Schall JD. Review of signal distortion through metal microelectrode recording circuits and filters. *J Neurosci Methods* 169: 141–157, 2008.

Newsome WT, Britten KH, Movshon JA. Neuronal correlates of a perceptual decision. *Nature* 341: 52–54, 1989.

Nienborg H, Cumming BG. Decision-related activity in sensory neurons reflects more than a neuron's causal effect. *Nature* 459: 89–92, 2009.

Nowak LG, Munk MH, Nelson JI, James AC, Bullier J. Structural basis of cortical synchronization. I. Three types of interhemispheric coupling. *J Neurophysiol* 74: 2379–2400, 1995.

Nunez PL, Srinivasan R. *Electric Fields of the Brain.* New York: Oxford University Press, 2006.

Ogawa T, Komatsu H. Target selection in area V4 during a multidimensional visual search task. *J Neurosci* 24: 6371–6382, 2004.

Ogawa T, Komatsu H. Neuronal dynamics of bottom-up and top-down processes in area V4 of macaque monkeys performing a visual search. *Exp Brain Res* 173: 1–13, 2006.

Ogawa T, Komatsu H. Condition-dependent and condition-independent target selection in the macaque posterior parietal cortex. *J Neurophysiol* 101: 721–736, 2009.

Okatan M, Wilson MA, Brown EN. Analyzing functional connectivity using a network likelihood model of ensemble neural spiking activity. *Neural Comput* 17: 1927–1961, 2005.

Olivier E, Dorris MC, Munoz DP. Lateral interactions in the superior colliculus, not an extended fixation zone, can account for the remote distractor effect. *Behav Brain Sci* 22: 694–695, 1999.

Opris I, Barborica A, Ferrera VP. Microstimulation of the dorsolateral prefrontal cortex biases saccade target selection. *J Cogn Neurosci* 17: 893–904, 2005.

Orban GA. Higher order visual processing in macaque extrastriate cortex. *Physiol Rev* 88: 59–89, 2008.

Orban GA, Van Essen D, Vanduffel W. Comparative mapping of higher visual areas in monkeys and humans. *Trends Cogn Sci* 8: 315–324, 2004.

O'Shea J, Muggleton NG, Cowey A, Walsh V. Timing of target discrimination in human frontal eye fields. *J Cogn Neurosci* 16: 1060–1067, 2004.

Ottes FP, Van Gisbergen JA, Eggermont JJ. Collicular involvement in a saccadic colour discrimination task. *Exp Brain Res* 66: 465–478, 1987.

Padoa-Schioppa C, Assad JA. Neurons in the orbitofrontal cortex encode economic value. *Nature* 441: 223–226, 2006.

Padoa-Schioppa C, Assad JA. The representation of economic value in the orbitofrontal cortex is invariant for changes of menu. *Nat Neurosci* 11: 95–102, 2008.

Paller KA, McCarthy G, Roessler E, Allison T, Wood CC. Potentials evoked in human and monkey medial temporal lobe during auditory and visual oddball paradigms. *Electroencephalogr Clin Neurophysiol* 84: 269–279, 1992.

Palmer J. Set-size effects in visual search: the effect of attention is independent of the stimulus for simple tasks. *Vision Res* 34: 1703–1721, 1994.

Palmer J, Verghese P, Pavel M. The psychophysics of visual search. *Vision Res* 40: 1227–1268, 2000.

Panzeri S, Petroni F, Petersen RS, Diamond ME. Decoding neuronal population activity in rat somatosensory cortex: role of columnar organization. *Cereb Cortex* 13: 45–52, 2003.

Panzeri S, Schultz SR, Treves A, Rolls ET. Correlations and the encoding of information in the nervous system. *Proc Biol Sci* 266: 1001–1012, 1999.

Passino KM, Seeley TD, Visscher PK. Swarm cognition in honey bees. *Behav Ecol Sociobiol* 62: 401–414, 2008.

Peterson MS, Kramer AF, Irwin DE. Covert shifts of attention precede involuntary eye movements. *Percept Psychophys* 66: 398–405, 2004.

Platt ML, Glimcher PW. Responses of intraparietal neurons to saccadic targets and visual distractors. *J Neurophysiol* 78: 1574–1589, 1997.

Polyak S. *The Vertebrate Visual System*. Chicago, Illinois: The University of Chicago Press, 1957.

Port NL, Wurtz RH. Target selection and saccade generation in monkey superior colliculus. *Exp Brain Res* 192: 465–477, 2009.

Posner MI. Orienting of attention. *Q J Exp Psychol* 32: 3–25, 1980.

Pouget A, Dayan P, Zemel R. Information processing with population codes. *Nat Rev Neurosci* 1: 125–132, 2000.

Pouget P, Stepniewska I, Crowder EA, Leslie MW, Emeric EE, Nelson MJ, Schall JD. Visual and motor connectivity and the distribution of calcium-binding proteins in macaque frontal eye field: implications for saccade target selection. *Front Neuroanat* 3: 2–2, 2009.

Poulet JF, Petersen CC. Internal brain state regulates membrane potential synchrony in barrel cortex of behaving mice. *Nature* 454: 881–885, 2008.

Powell KD, Goldberg ME. Response of neurons in the lateral intraparietal area to a distractor flashed during the delay period of a memory-guided saccade. *J Neurophysiol* 84: 301–310, 2000.

Pratt SC, Mallon EB, Sumpter DJ, Franks NR. Quorum sensing, recruitment, and collective decision-making during colony emigration by the ant Leptothorax albipennis. *Behav Ecol Sociobiol* 52: 117–127, 2002.

Purcell BA, Heitz RP, Cohen JY, Logan GD, Schall JD, Palmeri TJ. Modeling interactions between visually-responsive and movement-related neurons in FEF during saccade visual search. Vision Sci Soc, 2008.

Rainer G, Asaad WF, Miller EK. Selective representation of relevant information by neurons in the primate prefrontal cortex. *Nature* 393: 577–579, 1998.

Ray S, Schall JD, Murthy A. Programming of double-step saccade sequences: modulation by cognitive control. *Vision Res* 44: 2707–2718, 2004.

Reddi BA, Asrress KN, Carpenter RH. Accuracy, information, and response time in a saccadic decision task. *J Neurophysiol* 90: 3538–3546, 2003.

Reddi BA, Carpenter RH. The influence of urgency on decision time. *Nat Neurosci* 3: 827–830, 2000.

Reich DS, Mechler F, Victor JD. Independent and redundant information in nearby cortical neurons. *Science* 294: 2566–2568, 2001.

Remington RW. Attention and saccadic eye movements. *J Exp Psychol Hum Percept Perform* 6: 726–744, 1980.

Reuter-Lorenz PA, Fendrich R. Oculomotor readiness and covert orienting: differences between central and peripheral precues. *Percept Psychophys* 52: 336–344, 1992.

Reynolds JH, Chelazzi L. Attentional modulation of visual processing. *Annu Rev Neurosci* 27: 611–647, 2004.

Richmond BJ, Sato T. Enhancement of inferior temporal neurons during visual discrimination. *J Neurophysiol* 58: 1292–1306, 1987.

Riehle A, Kornblum S, Requin J. Neuronal correlates of sensorimotor association in stimulus-response compatibility. *J Exp Psychol Hum Percept Perform* 23: 1708–1726, 1997.

Rizzolatti G. *Advances in Vertebrate Neuroethology*, chap. Mechanisms of selective attention in mammals, pp. 261–297. Plenum Press (London), 1983.

Robinson DL, Bowman EM, Kertzman C. Covert orienting of attention in macaques. II. Contributions of parietal cortex. *J Neurophysiol* 74: 698–712, 1995.

Robinson DL, Goldberg ME, Stanton GB. Parietal association cortex in the primate: sensory mechanisms and behavioral modulations. *J Neurophysiol* 41: 910–932, 1978.

Rockel AJ, Hiorns RW, Powell TP. The basic uniformity in structure of the neocortex. *Brain* 103: 221–244, 1980.

Rodriguez-Sanchez AJ, Simine E, Tsotsos JK. Attention and visual search. *Int J Neural Syst* 17: 275–288, 2007.

Rolls ET, Aggelopoulos NC, Zheng F. The receptive fields of inferior temporal cortex neurons in natural scenes. *J Neurosci* 23: 339–348, 2003.

Romo R, Hernández A, Zainos A, Brody CD, Lemus L. Sensing without touching: psychophysical performance based on cortical microstimulation. *Neuron* 26: 273–278, 2000.

Romo R, Hernández A, Zainos A, Lemus L, Brody CD. Neuronal correlates of decision-making in secondary somatosensory cortex. *Nat Neurosci* 5: 1217–1225, 2002.

Romo R, Hernández A, Zainos A, Salinas E. Somatosensory discrimination based on cortical microstimulation. *Nature* 392: 387–390, 1998.

Rossi AF, Bichot NP, Desimone R, Ungerleider LG. Top down attentional deficits in macaques with lesions of lateral prefrontal cortex. *J Neurosci* 27: 11306–11314, 2007.

Rossi AF, Desimone R, Ungerleider LG. Contextual modulation in primary visual cortex of macaques. *J Neurosci* 21: 1698–1709, 2001.

Rugg MD, Coles MGH. *Electrophysiology of Mind: Event-Related Potentials and Cognition*. Oxford, UK: Oxford University Press, 1995.

Saito H, Yukie M, Tanaka K, Hikosaka K, Fukada Y, Iwai E. Integration of direction signals of image motion in the superior temporal sulcus of the macaque monkey. *J Neurosci* 6: 145–157, 1986.

Samonds JM, Zhou Z, Bernard MR, Bonds AB. Synchronous activity in cat visual cortex encodes collinear and cocircular contours. *J Neurophysiol* 95: 2602–2616, 2006.

Sato T. Effects of attention and stimulus interaction on visual responses of inferior temporal neurons in macaque. *J Neurophysiol* 60: 344–364, 1988.

Sato T, Murthy A, Thompson KG, Schall JD. Search efficiency but not response interference affects visual selection in frontal eye field. *Neuron* 30: 583–591, 2001.

Sato TR, Schall JD. Effects of stimulus-response compatibility on neural selection in frontal eye field. *Neuron* 38: 637–648, 2003.

Sato TR, Watanabe K, Thompson KG, Schall JD. Effect of target-distractor similarity on FEF visual selection in the absence of the target. *Exp Brain Res* 151: 356–363, 2003.

Schall JD. Neuronal activity related to visually guided saccades in the frontal eye fields of rhesus monkeys: comparison with supplementary eye fields. *J Neurophysiol* 66: 559–579, 1991.

Schall JD. *Cerebral Cortex: Extrastriate Cortex of Primates*, chap. Visuomotor areas of the frontal lobe, pp. 527–638. Plenum Press (New York), 1997.

Schall JD. Neural correlates of decision processes: neural and mental chronometry. *Curr Opin Neurobiol* 13: 182–186, 2003a.

Schall JD. *The Visual Neurosciences*, chap. Selection of targets for saccadic eye movements, pp. 1369–1390. MIT Press (Cambridge, Massachusetts), 2003b.

Schall JD. On building a bridge between brain and behavior. *Annu Rev Psychol* 55: 23–50, 2004a.

Schall JD. On the role of frontal eye field in guiding attention and saccades. *Vision Res* 44: 1453–1467, 2004b.

Schall JD, Hanes DP. Neural basis of saccade target selection in frontal eye field during visual search. *Nature* 366: 467–469, 1993.

Schall JD, Hanes DP, Thompson KG, King DJ. Saccade target selection in frontal eye field of macaque. I. Visual and premovement activation. *J Neurosci* 15: 6905–6918, 1995a.

Schall JD, Morel A, King DJ, Bullier J. Topography of visual cortex connections with frontal eye field in macaque: convergence and segregation of processing streams. *J Neurosci* 15: 4464–4487, 1995b.

Schall JD, Sato TR, Thompson KG, Vaughn AA, Juan CH. Effects of search efficiency on surround suppression during visual selection in frontal eye field. *J Neurophysiol* 91: 2765–2769, 2004.

Schall JD, Thompson KG. Neural selection and control of visually guided eye movements. *Annu Rev Neurosci* 22: 241–259, 1999.

Schall JD, Thompson KG, Bichot NP, Murthy A, Sato TR. *The Primate Visual System*, chap. Visual processing in the frontal eye field, pp. 205–230. CRC Press (Boca Raton, Florida), 2003.

Schiller PH, Chou I. The effects of anterior arcuate and dorsomedial frontal cortex lesions on visually guided eye movements: 2. Paired and multiple targets. *Vision Res* 40: 1627–1638, 2000.

Schiller PH, Koerner F. Discharge characteristics of single units in superior colliculus of the alert rhesus monkey. *J Neurophysiol* 34: 920–936, 1971.

Schiller PH, Tehovnik EJ. Neural mechanisms underlying target selection with saccadic eye movements. *Prog Brain Res* 149: 157–171, 2005.

Schiltz C, Bodart JM, Dubois S, Dejardin S, Michel C, Roucoux A, Crommelinck M, Orban GA. Neuronal mechanisms of perceptual learning: changes in human brain activity with training in orientation discrimination. *Neuroimage* 9: 46–62, 1999.

Schmolesky MT, Wang Y, Hanes DP, Thompson KG, Leutgeb S, Schall JD, Leventhal AG. Signal timing across the macaque visual system. *J Neurophysiol* 79: 3272–3278, 1998.

Schneidman E, Berry MJ, Segev R, Bialek W. Weak pairwise correlations imply strongly correlated network states in a neural population. *Nature* 440: 1007–1012, 2006.

Schoppik D, Nagel KI, Lisberger SG. Cortical mechanisms of smooth eye movements revealed by dynamic covariations of neural and behavioral responses. *Neuron* 58: 248–260, 2008.

Schroeder CE, Tenke CE, Givre SJ. Subcortical contributions to the surface-recorded flash-VEP in the awake macaque. *Electroencephalogr Clin Neurophysiol* 84: 219–231, 1992.

Schroeder CE, Tenke CE, Givre SJ, Arezzo JC, Vaughan HG. Striate cortical contribution to the surface-recorded pattern-reversal VEP in the alert monkey. *Vision Res* 31: 1143–1157, 1991.

Seeley TD, Visscher PK. Quorum sensing during nest-site selection by honeybee swarms. *Behav Ecol Sociobiol* 56: 594–601, 2004.

Segraves MA. Activity of monkey frontal eye field neurons projecting to oculomotor regions of the pons. *J Neurophysiol* 68: 1967–1985, 1992.

Segraves MA, Goldberg ME. Functional properties of corticotectal neurons in the monkey's frontal eye field. *J Neurophysiol* 58: 1387–1419, 1987.

Sereno MI, Dale AM, Reppas JB, Kwong KK, Belliveau JW, Brady TJ, Rosen BR, Tootell RB. Borders of multiple visual areas in humans revealed by functional magnetic resonance imaging. *Science* 268: 889–893, 1995.

Shadlen MN, Britten KH, Newsome WT, Movshon JA. A computational analysis of the relationship between neuronal and behavioral responses to visual motion. *J Neurosci* 16: 1486–1510, 1996.

Shadlen MN, Newsome WT. The variable discharge of cortical neurons: implications for connectivity, computation, and information coding. *J Neurosci* 18: 3870–3896, 1998.

Sharika KM, Ramakrishnan A, Murthy A. Control of predictive error correction during a saccadic double-step task. *J Neurophysiol* 100: 2757–2770, 2008.

Sheinberg DL, Logothetis NK. Noticing familiar objects in real world scenes: the role of temporal cortical neurons in natural vision. *J Neurosci* 21: 1340–1350, 2001.

Sheliga BM, Riggio L, Rizzolatti G. Orienting of attention and eye movements. *Exp Brain Res* 98: 507–522, 1994.

Sheliga BM, Riggio L, Rizzolatti G. Spatial attention and eye movements. *Exp Brain Res* 105: 261–275, 1995.

Shen K, Paré M. Neuronal activity in superior colliculus signals both stimulus identity and saccade goals during visual conjunction search. *J Vis* 7: 1–13, 2007.

Shepherd M, Findlay JM, Hockey RJ. The relationship between eye movements and spatial attention. *Q J Exp Psychol A* 38: 475–491, 1986.

Smith DT, Schenk T. Enhanced probe discrimination at the location of a colour singleton. *Exp Brain Res* 181: 367–375, 2007.

Smith PL, Ratcliff R. Psychology and neurobiology of simple decisions. *Trends Neurosci* 27: 161–168, 2004.

Snider RK, Kabara JF, Roig BR, Bonds AB. Burst firing and modulation of functional connectivity in cat striate cortex. *J Neurophysiol* 80: 730–744, 1998.

Softky WR, Koch C. The highly irregular firing of cortical cells is inconsistent with temporal integration of random EPSPs. *J Neurosci* 13: 334–350, 1993.

Sommer MA, Wurtz RH. Frontal eye field neurons orthodromically activated from the superior colliculus. *J Neurophysiol* 80: 3331–3335, 1998.

Sommer MA, Wurtz RH. Composition and topographic organization of signals sent from the frontal eye field to the superior colliculus. *J Neurophysiol* 83: 1979–2001, 2000.

Sommer MA, Wurtz RH. Frontal eye field sends delay activity related to movement, memory, and vision to the superior colliculus. *J Neurophysiol* 85: 1673–1685, 2001.

Sparks DL, Hartwich-Young R. The deep layers of the superior colliculus. *Rev Oculomot Res* 3: 213–255, 1989.

Sparks DL, Holland R, Guthrie BL. Size and distribution of movement fields in the monkey superior colliculus. *Brain Res* 113: 21–34, 1976.

Stanton GB, Goldberg ME, Bruce CJ. Frontal eye field efferents in the macaque monkey: I. Subcortical pathways and topography of striatal and thalamic terminal fields. *J Comp Neurol* 271: 473–492, 1988.

Stark E, Globerson A, Asher I, Abeles M. Correlations between groups of premotor neurons carry information about prehension. *J Neurosci* 28: 10618–10630, 2008.

Stein RB, Matthews PBC. Differences in variability of discharge frequency between primary and secondary muscle spindle afferent endings of the cat. *Nature* 208: 1217–1218, 1965.

Steinmetz MA, Connor CE, Constantinidis C, McLaughlin JR. Covert attention suppresses neuronal responses in area 7a of the posterior parietal cortex. *J Neurophysiol* 72: 1020–1023, 1994.

Steinmetz MA, Constantinidis C. Neurophysiological evidence for a role of posterior parietal cortex in redirecting visual attention. *Cereb Cortex* 5: 448–456, 1995.

Sternberg S. The discovery of processing stages: Extensions of Donders' method. *Acta Psychol* 30: 276–315, 1969.

Sternberg S. Separate modifiability, mental modules, and the use of pure and composite measures to reveal them. *Acta Psychol* 106: 147–246, 2001.

Stevens CF, Zador AM. Input synchrony and the irregular firing of cortical neurons. *Nat Neurosci* 1: 210–217, 1998.

Taylor AF, Tinsley MR, Wang F, Huang Z, Showalter K. Dynamical quorum sensing and synchronization in large populations of chemical oscillators. *Science* 323: 614–617, 2009.

Taylor PC, Nobre AC, Rushworth MF. FEF TMS affects visual cortical activity. *Cereb Cortex* 17: 391–399, 2007.

Theeuwes J. Cross-dimensional perceptual selectivity. *Percept Psychophys* 50: 184–193, 1991.

Theeuwes J, Kramer AF, Hahn S, Irwin DE. Our eye do not always go where we want them to go: capture of the eyes by new objects. *Psychol Sci* 9: 379–385, 1998.

Thomas NW, Paré M. Temporal processing of saccade targets in parietal cortex area LIP during visual search. *J Neurophysiol* 97: 942–947, 2007.

Thompson KG, Bichot NP. A visual salience map in the primate frontal eye field. *Prog Brain Res* 147: 251–262, 2005.

Thompson KG, Bichot NP, Sato TR. Frontal eye field activity before visual search errors reveals the integration of bottom-up and top-down salience. *J Neurophysiol* 93: 337–351, 2005a.

Thompson KG, Bichot NP, Schall JD. Dissociation of visual discrimination from saccade programming in macaque frontal eye field. *J Neurophysiol* 77: 1046–1050, 1997.

Thompson KG, Bichot NP, Schall JD. *Visual Attention and Cortical Circuits*, chap. From attention to action in frontal cortex, pp. 137–157. MIT Press (Cambridge, Massachusetts), 2001.

Thompson KG, Biscoe KL, Sato TR. Neuronal basis of covert spatial attention in the frontal eye field. *J Neurosci* 25: 9479–9487, 2005b.

Thompson KG, Hanes DP, Bichot NP, Schall JD. Perceptual and motor processing stages identified in the activity of macaque frontal eye field neurons during visual search. *J Neurophysiol* 76: 4040–4055, 1996.

Tolias AS, Moore T, Smirnakis SM, Tehovnik EJ, Siapas AG, Schiller PH. Eye movements modulate visual receptive fields of V4 neurons. *Neuron* 29: 757–767, 2001.

Tomita M, Eggermont JJ. Cross-correlation and joint spectro-temporal receptive field properties in auditory cortex. *J Neurophysiol* 93: 378–392, 2005.

Tootell RB, Hadjikhani N. Where is 'dorsal V4' in human visual cortex? Retinotopic, topographic and functional evidence. *Cereb Cortex* 11: 298–311, 2001.

Toyama K, Kimura M, Tanaka K. Organization of cat visual cortex as investigated by cross-correlation technique. *J Neurophysiol* 46: 202–214, 1981.

Trageser JC, Monosov IE, Zhou Y, Thompson KG. A perceptual representation in the frontal eye field during covert visual search that is more reliable than the behavioral report. *Eur J Neurosci* 28: 2542–2549, 2008.

Treisman A, Sato S. Conjunction search revisited. *J Exp Psychol Hum Percept Perform* 16: 459–478, 1990.

Treisman AM, Gelade G. A feature-integration theory of attention. *Cognit Psychol* 12: 97–136, 1980.

Triesch J, Ballard DH, Hayhoe MM, Sullivan BT. What you see is what you need. *J Vis* 3: 86–94, 2003.

Truccolo W, Eden UT, Fellows MR, Donoghue JP, Brown EN. A point process framework for relating neural spiking activity to spiking history, neural ensemble, and extrinsic covariate effects. *J Neurophysiol* 93: 1074–1089, 2005.

Ts'o DY, Gilbert CD, Wiesel TN. Relationships between horizontal interactions and functional architecture in cat striate cortex as revealed by cross-correlation analysis. *J Neurosci* 6: 1160–1170, 1986.

Tsujimoto S, Genovesio A, Wise SP. Transient neuronal correlations underlying goal selection and maintenance in prefrontal cortex. *Cereb Cortex* 18: 2748–2761, 2008.

Uchida N, Mainen ZF. Speed and accuracy of olfactory discrimination in the rat. *Nat Neurosci* 6: 1224–1229, 2003.

Umeno MM, Goldberg ME. Spatial processing in the monkey frontal eye field. I. Predictive visual responses. *J Neurophysiol* 78: 1373–1383, 1997.

Vaadia E, Haalman I, Abeles M, Bergman H, Prut Y, Slovin H, Aertsen A. Dynamics of neuronal interactions in monkey cortex in relation to behavioural events. *Nature* 373: 515–518, 1995.

Van Loon EM, Hooge IT, Van den Berg AV. The timing of sequences of saccades in visual search. *Proc Biol Sci* 269: 1571–1579, 2002.

Vicente R, Gollo LL, Mirasso CR, Fischer I, Pipa G. Dynamical relaying can yield zero time lag neuronal synchrony despite long conduction delays. *Proc Natl Acad Sci U S A* 105: 17157–17162, 2008.

Wade NJ, Brožek J. *Purkinje's Vision: The Dawning of Neuroscience*. Mahwah, New Jersey: Lawrence Erlbaum Associates, 2001.

Walter WG. Critical review: the technique and application of electro-encephalography. *J Neurol Psychiatry* 1: 359–385, 1938.

Wardak C, Ibos G, Duhamel JR, Olivier E. Contribution of the monkey frontal eye field to covert visual attention. *J Neurosci* 26: 4228–4235, 2006.

Wardak C, Olivier E, Duhamel JR. Saccadic target selection deficits after lateral intraparietal area inactivation in monkeys. *J Neurosci* 22: 9877–9884, 2002.

Wardak C, Olivier E, Duhamel JR. A deficit in covert attention after parietal cortex inactivation in the monkey. *Neuron* 42: 501–508, 2004.

Waters CM, Bassler BL. Quorum sensing: cell-to-cell communication in bacteria. *Annu Rev Cell Dev Biol* 21: 319–346, 2005.

Wolfe JM. *Attention*, chap. Visual search, pp. 99–119. Psychological Press (East Sussex, UK), 1998.

Wolfe JM. *Integrated Models of Cognitive Systems*, chap. Guided search 4.0: current progress with a model of visual search, pp. 99–119. Oxford (New York), 2007.

Wolfe JM, Horowitz TS. What attributes guide the deployment of visual attention and how do they do it? *Nat Rev Neurosci* 5: 495–501, 2004.

Woodman GF, Kang MS, Rossi AF, Schall JD. Nonhuman primate event-related potentials indexing covert shifts of attention. *Proc Natl Acad Sci* 104: 15111–15116, 2007.

Woodman GF, Kang MS, Thompson K, Schall JD. The effect of visual search efficiency on response preparation: neurophysiological evidence for discrete flow. *Psychol Sci* 19: 128–136, 2008.

Woodman GF, Luck SJ. Electrophysiological measurement of rapid shifts of attention during visual search. *Nature* 400: 867–869, 1999.

Woodman GF, Luck SJ. Dissociations among attention, perception, and awareness during object-substitution masking. *Psychol Sci* 14: 605–611, 2003a.

Woodman GF, Luck SJ. Serial deployment of attention during visual search. *J Exp Psychol Hum Percept Perform* 29: 121–138, 2003b.

Wurtz RH, Albano JE. Visual-motor function of the primate superior colliculus. *Annu Rev Neurosci* 3: 189–226, 1980.

Wurtz RH, Goldberg ME. Superior colliculus cell responses related to eye movements in awake monkeys. *Science* 171: 82–84, 1971.

Wurtz RH, Mohler CW. Organization of monkey superior colliculus: enhanced visual response of superficial layer cells. *J Neurophysiol* 39: 745–765, 1976.

Yokota T, Satoh T. Three-dimensional estimation of the distribution and size of putative functional units in rat gustatory cortex as assessed from the inter-neuronal distance between two neurons with correlative activity. *Brain Res Bull* 54: 575–584, 2001.

Zeki SM. Cortical projections from two prestriate areas in the monkey. *Brain Res* 34: 19–35, 1971.

Zelinsky GJ, Sheinberg DL. Eye movements during parallel-serial visual search. *J Exp Psychol Hum Percept Perform* 23: 244–262, 1997.

Zhou HH, Thompson KG. Cognitively directed spatial selection in the frontal eye field in anticipation of visual stimuli to be discriminated. *Vision Res* 49: 1205–1215, 2009.

Zipser K, Lamme VA, Schiller PH. Contextual modulation in primary visual cortex. *J Neurosci* 16: 7376–7389, 1996.

Zohary E, Shadlen MN, Newsome WT. Correlated neuronal discharge rate and its implications for psychophysical performance. *Nature* 370: 140–143, 1994.